SORPTION AND ITS EFFECTS ON TRANSPORT OF ORGANIC DYES AND CESIUM IN SOILS

By

JARAI MON

A dissertation submitted in partial fulfillment of
the requirements for the degree of

DOCTOR OF PHILOSOPHY

WASHINGTON STATE UNIVERSITY
Department of Crop and Soil Sciences

December 2004

To the Faculty of Washington State University:

The members of the Committee appointed to examine the dissertation of JARAI MON find it satisfactory and recommend that it be accepted.

_____

Chair

_____

_____

Acknowledgements

I would like to extend my gratitude and appreciation to several individuals. First, I would like to thank my major advisor, Dr. Markus Flury for his guidance, support, encouragement, and great patience during the course of my studies. Without his assistance and supervision, this research would not have been possible. I would like to thank my academic committee members, Dr. James B. Harsh and Dr. C. Kent Keller for their valuable advice, guidance, and consistent encouragement. I am very fortunate to have them on my academic committee. I would like to express my sincere appreciation to Jon Mathison and Jeffery Boyle for their technical assistance that substantially helps to complete this study. My special thanks to Youjun Deng and Gang Chen, postdoctoral scientists in our lab, who spent time and made efforts to answer all the questions I have for them during my studies. Many thanks also go to Mary Bodley for her friendship and for the time she spent helping me improve my English. I thank my fellow labmates and graduate students for their warm friendships.

I gratefully acknowledge the financial supports from the Water Research Center of the State of Washington, the US Department of Energy's Environmental Science Management Program, the Department of Crop and Soil Sciences and the College of Agricultural, Human and Natural Resource Sciences, Washington State University.

I would like to extend my deepest gratitude to my parents, who have sacrificed towards my eduction. Finally, I would like to thank my husband for his love, moral support, and understanding while I completed this dissertation.

SORPTION AND ITS EFFECTS ON TRANSPORT OF ORGANIC DYES AND CESIUM IN SOILS

Abstract

by Jarai Mon, Ph.D.

Washington State University

December 2004

Chair: Markus Flury

The mobility, fate, and transport of various solutes in the subsurface is influenced by sorption, i.e., association of solutes to solid phases. The goals of this research were to study the sorption of selected organic dyes and cesium and to provide further information on the effects of sorption on the transport and mobility of these solutes in soils. The specific objectives are as follows:

1. To provide a historical sketch and review on the application of dye tracers.
2. To evaluate the sorption of four triarylmethane dyes and test the suitability of column experiments for measuring sorption isotherms.
3. To identify and recommend dyes that are potentially suitable as vadose zone tracers.

4. To investigate the incorporation and desorption of cesium in secondary mineral phases formed in Hanford tank waste simulants.

We conducted a literature review on dyes as hydrological tracers and studied the sorption of four triarylmethane dyes, C.I. Food Blue 2, C.I. Food Green 3, C.I. Acid Blue 7, and C.I. Acid Green 9, in a sandy soil. The results showed that dyes with more SO_3 groups sorbed less than dyes contained fewer SO_3 groups. C.I. Food Green 3 sorbed similarly to C.I. Food Blue 2, a well-known vadose zone tracer, and is likely to be a useful tracer candidate. Sorption isotherms obtained by the column technique were similar to those measured by batch studies. The quantitative structure activity relationship (QSAR) modeling revealed that a number of hypothetical dyes sorb considerably less than currently known vadose zone dye tracers.

Studies on the amount, the exchangeability, and desorption kinetics of Cs associated to feldspathoids, LTA zeolite, and allophane showed that only a small fraction of Cs (1-57%) in cancrinite and sodalite was exchangeable with Ca, K, or Na. K or Na effectively replaced most Cs (94-99%) in LTA zeolite and allophane, but Ca could replace a smaller percentage (65-85%) of Cs. The ability of ions to exchange with Cs appears to be related to their hydrated diameters and hydration energies. Cesium in LTA zeolite was quickly desorbed by Na. However, Cs desorbed slowly from feldspathoids and allophane. Cesium may be trapped in the cages and channels of these minerals.

Table of Contents

List of Tables

List of Figures

Dedication

To the Mon people, who have lost the right and freedom to decide their own future,

And

To my late grandfather and those who made the ultimate sacrifice during the long struggle for peace, justice, and freedom in Burma.

Chapter 1

Introduction

1.1 Background

Sorption generally describes the process of association of solutes to solid phases. Solutes may be attached to surfaces of the solid and/or may penetrate into the solid matrix. The former is named adsorption, while the later is absorption. Usually, the term sorption is used when we cannot distinguish between adsorption and absorption. Concerning the fate and transport of solute in porous media, sorption refers to the immobilization of solutes as a result of their interactions with solid surfaces.

Sorption is an important phenomenon that can dramatically affect the mobility, fate, and transport behavior of various chemicals, including contaminants. Sorption slows down the mobilities of chemicals in the subsurface environment. Therefore, sorption of chemicals to subsurface materials is of particular interest from the viewpoint to retard the spreading of contaminants. On the other hand, retardation is not desirable from the standpoint of tracer applications because retardation does not allow tracers

to move in the same speed as the substance being traced. Sorption and transport behavior of contaminants in the subsurface should be investigated in order to understand potential problems and risks of environmental pollution. Similarly, sorption characteristics tracer of substances should be studied in order to accurately assess the conditions being investigated.

Sorption occurs due to different types of interactions between the sorbate (solutes) and sorbent (surfaces). A few examples are Coulombic electrostatic, London-van der Waals, and hydrophobic interactions [*Hassett and Banwart,* 1989]. Sorption of a solute in the subsurface environment is influenced by three major aspects: the properties of solute, the composition of solid surfaces, and the chemistry of solution interacting with the solid phase [*Schwarzenbach et al.,* 2003].

Sorption characteristics are often determined by measuring adsorption isotherms. Sorption parameters such as sorption coefficients and the maximum adsorption capacity are quantified to compare the sorption of various chemicals in response to different types solid properties and solution chemistry. Often, desorption characteristics are also measured; especially, for investigations of potential redistributions of sorbed contaminants. Traditionally, batch studies are used to measure adsorption isotherms. However, the batch technique has several shortcomings that may introduce errors in measurement of sorption isotherms [*Griffioen et al.,* 1992*; Bürgisser et al.,* 1993]. Column transport experiments have been proposed as an alternative to batch studies.

The focus of this dissertation lies in the soil sorption and how it affects the trans-

port characteristics of selected organic dyes and cesium. The studies covered the effects of sorption on the transport of organic and inorganic solutes in the vadose zone. Dyes were studied for the purpose of tracer applications and cesium was viewed as a contaminant.

The studies of dye sorption to subsurface materials such as soils and sediments are important because sorption to those materials is a major limiting factor to the usefulness dyes as hydrological tracers. Dyes have been used in a variety of hydrological investigations for more than a century and still remain as one of the most important hydrological tracers [*Flury and Wai*, 2003]. Thousand of dyes are commercially available [*Colour Index*, 2001]; however, the 'best' hydrological dye tracer has not yet been found. By understanding the sorption behavior of dyes, we may be able to select or design the best possible dye tracers for specific uses.

The fate and mobility of radioactive cesium in the subsurface is a major environmental concern at the Department Energy's Hanford site. More than one million gallons of cesium containing high level nuclear waste liquid have known to be leaked into the sediments from underground storage tanks. Further knowledge and understanding of cesium sorption and potential redistribution in Hanford sediments can help accelerate the remediation efforts to reduce the environmental damages at the Hanford site.

1.2 Scope and Objectives

The ultimate goals of this dissertation are to provide recommendations on potential new dye tracers and to provide further information on the fate of radioactive cesium in contaminated Hanford sediments. To achieve the first objective, we conducted literature reviews and compiled the information on dyes commonly used as tracers and limitations and problems in dye tracing. We evaluated the sorption characteristics of four triarylmethane dyes using column techniques and the results were compared with those obtained by traditional batch studies. We examined the quantitative structure activity relationships (QSAR) approach as a tool for estimation of dye sorption parameters and for designing potential dyes, which possess the best tracer characteristics. To reach our second objective, we measured cesium incorporation and desorption in secondary alluminosilicate minerals, feldspathoids, zeolite, and allophane, formed in Hanford tank waste simulants. The specific objectives of these studies are as follows:

1. To provide a brief review of literature on the use of dyes as hydrological tracers. We compiled information on historical and present dye tracing applications in hydrology, dyes commonly used as tracers, tracer characteristics, and limitations of dyes as tracers. We also presented a case study on screening and selection of dyes for specific uses.

2. To evaluate the sorption characteristics of four triarylmethane dyes and to test the column technique as an alternative to traditional batch studies. We mea-

sured sorption isotherms of the dyes in a sandy soil and compared the sorption isotherms determined by batch and column methods. We calculated sorption parameters for the four dyes to determine their suitability as hydrological tracers.

3. To identify the dyes that are potentially most suitable for tracing water flow. We examined the sorption properties of dyes consisting of the same molecular template as Brilliant Blue FCF, a common hydrological tracer, but with different numbers and positions of sulfonic acid groups. We established QSAR models that allowed the prediction of sorption characteristics of a sereies of hypothetical dyes.

4. To investigate the sorption and desorption behavior of cesium in feldspathoids, zeolite, and allophane. These minerals were found when simulated Hanford tank wastes were contacted with silica rich solution, similar to the composition in Hanford sediments. We synthesized the minerals and quantified the amount of cesium sorbed or incorporated. We determined desorption kinetics and diffusion coefficients of cesium in each type of the minerals.

1.3 Thesis Outline

This dissertation includes four major chapters that have been prepared as four technical papers to be submitted for publications. In Chapter 2, a literature review on

the use of dyes as hydrological tracers and a case study on the screening and selection of dye tracers are presented. Chapter 3 reports on the sorption characteristics of four triarylmethane dyes and the application of column experiments for measurement of adsorption isotherms. In Chapter 4, the establishment of Quantitative Structure-Activity Relationship (QSAR) models for estimation of dye sorption parameters is described and chemical structures of potential dye tracers are suggested. In Chapter 5, the incorporation and desorption of cesium in feldspathoids and zeolite formed in Hanford tank-waste simulants were reported. Finally, Chapter 6 provides a summary and conclusion of this dissertation. Tables and figures are included at the end of each chapter in conformity with the manuscript format of a journal. Details on basic theory, additional information on experimental procedures, and supportive data and figures, which are not included in the papers, are presented as comments in the respective chapters. For clarity, comments are placed between two horizontal lines. References are listed together at the end of the dissertation.

Chapter 2

Dyes As Hydrological Tracers

2.1 Abstract

Dyes have been used in hydrological investigations for more than a century. Dye tracers are versatile tools to study flow connections, residence times, hydrodynamic dispersion, flow patterns, and chemical leaching. The major advantage of dyes compared with other tracers is that dyes are readily detected at low concentrations, simple to quantify, and inexpensive. The visualization of dyes is often a powerful tool to demonstrate flow pathways. As most dyes are organic molecules, they tend to sorb to solid surfaces and can be photo- and bio-chemically degraded. For water tracing, dyes should therefore be tested under the specific conditions under which dye tracing is to be conducted.

This chapter has been accepted for publication: Jarai Mon and Markus Flury, Dyes as Hydrological Tracers, The Encyclopedia of Water, John Wiley & Sons Inc., Hoboken, NJ.

We present a brief overview on the use of dyes as hydrological tracers, and propose a cost-effective screening technique for selection of optimal dye tracers. This technique is based upon quantitative structure-activity relationships (QSAR). We conducted a case study on the application of QSAR for screening and selection of dye tracers. The QSAR modeling revealed many hypothetical dyes that show potential to be good tracers.

Keywords: dyes, tracers, hydrology, QSAR,

2.2 Introduction

Dye tracers have been used in hydrological investigations for more than a century. In 1877, Uranine (Fluorescein) was used as tracer to test the hydraulic connection between the Danube River and the Ach Spring in southern Germany [*Knop,* 1878]. In 1883, the French physician des Carriéres successfully proved the source of a typhus epidemic in the city of Auxerre by conducting a tracer experiment with the dye aniline [*des Carrières,* 1883]. First systematic investigations on the suitability of dyes as tracers were conducted even before the turn of the century [*Trillat,* 1899]. Subsequently, the use of dyes as tracers became a common practice in hydrological investigations [*Davis et al.,* 1980*; McLaughlin,* 1982*; Flury and Wai,* 2003].

A classical example of the use of dyes in hydrology is the study of residence times and pathway connectivities in Karst [*Aley,* 1997]. Further applications range from studying dispersion in streams and lakes, to determine sources of water pollution,

and to evaluate sewage systems. In the vadose zone, dyes have been mainly used to visualize flow patterns [*Flury and Wai,* 2003].

Thousands of different dyes are commercially available [*Colour Index,* 2001], but only a few are suitable for hydrological investigations. Many dyes have been studied specifically for their suitability as hydrological tracers, and recommendations were made on "best" dye tracers [*Corey,* 1968*; Smart and Laidlaw,* 1977*; Smettem and Trudgill,* 1983*; Flury and Flühler,* 1995]. Depending on the specific applications, different chemical characteristics of a dye may be desirable. For instance, for visualization of water flow in soils, a dye should be clearly visible and trace the water movement accurately. In this particular case, the dye will preferably be blue, red, green, or fluorescent to contrast distinctly from the soil background. The accurate tracing of the water movement demands that the dye does not sorb too strongly to subsurface materials. This poses limitations on the chemical characteristics of a dye.

Here, we summarize tracer characteristics and the applications of dye tracers in surface and subsurface hydrology. We then discuss the limitations and potential problems in using dyes for tracing water flow and solute movement. Selection of an appropriate dye is critical for the success of a tracing study. We present a case study on the application of quantitative structure-activity relationships (QSAR) for screening, selecting, and designing optimal dye tracers for a specific use.

2.3 Tracer Characteristics of Dyes

Dye tracers, particularly fluorescent dyes, are often preferred over several other types of tracing materials because of their unique characteristics. Many dyes (a) can be readily detected at concentration as low as a few micrograms per liter, (b) can be quantified with simple and readily available analytical equipment, (c) are nontoxic at low concentrations, and (d) are inexpensive and commercially available in large quantity [*Aley,* 1997*; Flury and Flühler,* 1995*; Field,* 2002b]. In addition, due to their coloring properties, dyes allow to visualize flow pathways in the subsurface. Many dye tracing studies conducted in the past ten years have clearly demonstrated that flow patterns in the subsurface are often highly irregular; an example of a non-uniform infiltration front in a sandy soil is shown in Figure 2.1.

Despite these desirable characteristics, there are important drawbacks in using dye tracers. Dye tracers are not conservative tracers, i.e., they sorb to subsurface media and do not necessarily move at the same speed as the water to be traced. The sorption behavior of dyes is influenced by the properties of the subsurface materials and the chemistry of the aqueous phase [*Corey,* 1968*; Flury and Flühler,* 1995*; Reynolds,* 1966*; Kasnavia et al.,* 1999*; German-Heins and Flury,* 2000]. Some dyes degrade when they are exposed to sunlight, e.g., Uranine [*Smart and Laidlaw,* 1977*; Feuerstein and Selleck,* 1963*; Viriot and André,* 1989], and some can be degraded by microorganisms. Consequently, dye tracers may behave differently under different natural environments. Thus, the suitability of dye tracers should be tested before they are used in hydrological

studies.

An "ideal" water tracer is a substance that (a) has conservative behavior (i.e., does not sorbed to solid media, is resistant to degradation, and stable in different chemical environments), (b) does not occur naturally in high concentrations in the system to be investigated, (c) is inexpensive, (d) is easy to apply, sample, and analyze, and (e) is non-toxic to humans, animals, and plants [*Flury and Wai,* 2003]. These requirements are difficult to meet for a single chemical. Different types of dyes have been proposed as best suitable water tracers, and these dyes are discussed below.

2.4 Surface Water, Groundwater, and Vadose Zone Tracers

Fluorescent dyes are frequently used in surface and groundwater applications, and to some degree also in vadose zone hydrology. Certain dyes, such as Rhodamine WT and Uranine, are used for surface water, groundwater, as well as vadose zone applications, while others, such as Brilliant Blue FCF, are exclusively used as vadose zone tracers. Many of the common dye tracers (Table 3.1) belong to the chemical class of the xanthene dyes. Structures of commonly used dyes are shown in Figure 2.2.

Dye tracers have been used in measuring flow velocity, travel time, and dispersion in rivers and streams [*Church,* 1974*; Cox et al.,* 2003]. Among the dyes commonly used as surface water tracers (Table 3.1), the most frequent one is Rhodamine WT

[*Cox et al.,* 2003*; Kratzer and Biagtan,* 1998*; Imes and Fredrick,* 2002*; Gooseff et al.,* 2003]. Uranine has been recognized as a good hydrological tracer, but its susceptibility to photochemical decay [*Feuerstein and Selleck,* 1963] is of concern in tracing surface water.

Dye tracers have also been used to study groundwater flow velocity, flow direction, hydraulic connections, and aquifer characteristics [*Davis et al.,* 1980*; McLaughlin,* 1982]. Uranine and Rhodamine WT are the two most commonly used tracers in groundwater studies (Table 3.1). However, these two dyes should not be used as co-tracers because Rhodamine WT degrades to carboxylic fluorescein, which may confound tracer quantification [*Field,* 2002b]. Rhodamine WT is highly water soluble, easily visible and detectable, photochemically more stable than Uranine, and has moderate tendency for sorption [*Field,* 2002b]. Commercially available tracer-grade Rhodamine WT contains two isomers (Figure 2.2) which have different sorption properties [*Sutton et al.,* 2001]. The para isomer of Rhodamine WT sorbs less to different aquifer materials than does the meta isomer [*Sutton et al.,* 2001*; Vasudevan et al.,* 2001]. Consequently the two isomers travel with different velocities in subsurface media, leading to chromatographic separation [*Sutton et al.,* 2001]. In groundwater tracer studies, as in surface water tracing, dye tracers can be easily detected or quantified in water samples using fluorometers or spectrophotometers. Methods and software for designing and analyzing tracer tests are available [*Field,* 2002b*; Field,* 2002a*; Field,* 2003a*; Field,* 2003b].

In the vadose zone, dyes are mainly used to delineate water flow patterns. Flow pathways in soils, sediments, and fractured rock have been visualized using dye tracers [*Bouma et al.,* 1977*; Germann et al.,* 1984*; Flury et al.,* 1994*; Hu et al.,* 2002*; Nobles et al.,* 2004]. Many dyes have been tested in search for an optimal vadose zone dye tracer and different dyes have been recommended [*Flury and Wai,* 2003]. Most commonly used vadose zone tracers are listed in Table 3.1. Brilliant Blue FCF has gained acceptance as a good dye tracer for visualization of flow patterns [*Flury and Flühler,* 1995*; Nobles et al.,* 2004] and solute transport in the vadose zone [*Vanderborght et al.,* 2002*; Öhrström et al.,* 2004*; Zinn et al.,* 2004]. In the vadose zone, dye tracer analysis is not as simple as in surface water or groundwater tracer studies, particularly if tracer concentrations are to be determined. Image analysis or fiber-optic spectroscopy can be used to measure tracer distributions in soil profiles [*Forrer et al.,* 2000*; Aeby et al.,* 2001].

2.5 Limitations in Using Dyes as Tracers

Most dyes are organic molecules and their interactions with other materials in the subsurface are influenced by environmental conditions. Generally, dye tracers sorb to solid surfaces and the degree of sorption depends on surface properties and solution chemistry. Solubility, photochemical decay, absorption spectra, and fluorescence of dyes are often affected by environmental conditions, such as temperature, sunlight, acidity, and alkalinity. Thus, not only properties of the dyes but also of the environment in which

dyes are to be applied often limit the use of dyes as tracers.

Sorption of dyes to subsurface media is one of the major limitations for using dyes to trace water flow pathways. Sorption causes dyes to move with a slower velocity than water. Some dyes are used to mimic the movement of certain chemicals rather than the flow of water. For instance, Rhodamine WT was used to mimic the movement of atrazine [*Kanwar et al.,* 1997].

Dyes selected as hydrological tracers often contain functional groups, such as carboxylic and sulfonic acids, which contribute to high water solubility and decrease sorption [*Corey,* 1968*; Reife and Freeman,* 1996]; however, the functional groups cause dyes to have pH dependent properties. The properties of mineral surfaces may also change with pH, i.e., negatively charged surfaces may become neutral or positively charged as pH decreases, and sorption of anionic dyes may increase. Therefore, the sorption of dyes should be tested before dyes are applied as tracers.

Fluorescence of dyes may change under different environmental conditions. For instance, fluorescence intensity of Rhodamine B increases with decreasing temperature [*Feuerstein and Selleck,* 1963]. The presence of electron donating ions, such as chlorine, bromine and iodine, in water samples as well as changes in solution pH can cause fluorescence quenching [*Smart and Laidlaw,* 1977*; Church,* 1974].

2.6 Selection of Dye Tracers for Specific Uses

2.6.1 QSAR as an Alternative to Experimental Screening

Screening is a basic step for selection of the most suitable dye tracers for specific uses, but experimental screening of thousands of commercially available dyes is not practical. An efficient technique (accurate, simple, fast, and inexpensive) is necessary to find the most suitable dye tracer for a specific investigation. A promising screening technique is the use of Quantitative Structure-Activity Relationships (QSAR).

The QSAR relate the molecular structure of a chemical to its activity. While this technique has been used extensively in pharmacology, it has also been applied to estimate environmental fate and risk of organic chemicals [*Sabljić,* 1989b*; Nendza,* 1998*; Sabljić,* 2001*; Worrall,* 2001]. The QSAR models are based on calculated molecular descriptors and selected measured data that describe the property to be predicted. A statistical model then allows to predict the properties of structurally similar chemicals which have not yet been experimentally tested.

2.6.2 QSAR Case Study Using Triarylmethane Dyes

We illustrate the use of QSAR for dye tracer screening using the example of the triarylmethane dyes. These dyes are often used as food dyes, and because they are highly water soluble, they have preferable characteristics as dye tracers [*Flury and Wai,* 2003]. Brilliant Blue FCF, one member of this dye class, is commonly used as

vadose zone tracer. Other members, however, may be even better suited as dye tracers. We developed a QSAR model with triarylmethane dyes to predict their soil sorption characteristics. Four triarylmethane dyes were selected as training set: Brilliant Blue FCF (C.I. Food Blue 2), FD&C Green No. 3 (C.I. Food Green 3), ORCOacid Blue A 150% (C.I. Acid Blue 7), and ORCOacid Fast Green B (C.I. Acid Green 9). These four dyes share the same molecular kernel but differ in numbers, types, and positions of functional groups (Figure 2.3a–d).

We experimentally measured soil sorption parameters of the four dyes and used QSAR to relate these parameters to the structural properties of the dyes. Soil sorption was determined by batch sorption experiments similar to the ones described in German-Heins and Flury [*German-Heins and Flury,* 2000]. A sandy soil (Vantage, WA), pH 8, and 0.01 M $CaCl_2$ solution were used for the sorption experiments. A Langmuir sorption isotherm was fitted to the experimental data to obtain the two adsorption parameters, the Langmuir coefficient K_L and the maximum adsorption A_m (Table 2.2), using a normal nonlinear least squares method [*Schulthess and Dey,* 1996]. The Langmuir isotherm describes the relation between sorbed (C_a) and aqueous concentrations (C_s) at equilibrium as [*Schulthess and Dey,* 1996]:

$$C_a = \frac{A_m K_L C_s}{1 + K_L C_s}\,. \tag{2.1}$$

Structural properties (molecular descriptors) of the dyes were calculated using the MDL QSAR (version 2.1, 2002, MDL Information System, Inc., San Leandro, CA). The MDL QSAR program converts molecular structures to structural properties, such

as molecular connectivity indices (MCIs), molecular volume, and surface area. Stepwise linear regression analyses were applied to select the descriptors that are well correlated to the experimental parameters [*Sekusak and Sabjlić,* 1992*; Hall et al.,* 2002]. The statistical significance was assumed at $P \leq 0.05$.

The cross validation technique was used to test the predictability of the models. Randomization tests were performed to check the probability that correlation occurred by chance. The models that achieved the best quality of statistics were selected for estimation of each sorption parameter. The two QSAR models, one for estimation of K_L and another for estimation of A_m, were established as follows:

1. Langmuir coefficient (K_L) model:

$$K_L = -54.47({}^9\chi_p) + 183.75 \tag{2.2}$$

where K_L has units of L/mmol and ${}^9\chi_p$ is the 9^{th}-order simple path molecular connectivity index.

2. Maximum adsorption (A_m) model:

$$A_m = -45.72({}^9\chi_p^v) + 35.88 \tag{2.3}$$

where A_m has units of mmol/kg and ${}^9\chi_p^v$ is the 9^{th}-order valence path molecular connectivity index.

2.6.3 Prediction of Soil Sorption Using QSAR Models

Approximately 70 hypothetical molecules were created based on the structure of Brilliant Blue FCF and their sorption parameters were estimated using the QSAR models

(Equations 4.12 and 4.13). These molecules all shared the same molecular kernel as Brilliant Blue FCF but were different in number and position of SO_3 groups. The effects of different numbers and positions of SO_3 groups on soil sorption parameters, i.e., K_L and A_m values, of the new compounds were examined.

The QSAR modeling indicates that the more SO_3 groups attached to the molecular kernel, the smaller will be the soil sorption: both K_L and A_m values decreased with the increasing number of SO_3 groups (Figure 2.4). Negative K_L and A_m values were calculated by the models. Negative values are only possible in case of negative sorption, i. e., ion exclusion. The predicted values should be considered as relative, rather than absolute, measures for comparing the sorption of the chemicals.

The effects of the positions of the SO_3 groups at the molecular kernel was examined using QSAR modeling. Three sets of hypothetical molecules were created, which contained one, two, or three SO_3 groups attached at different positions at the benzene rings of the triarylmethane kernel. Set 1, which contained one SO_3 group, consisted of six molecules; Set 2 (two SO_3 groups) consisted of 22 molecules; and Set 3 (three SO_3 groups) consisted of 31 molecules. The range of the predicted K_L and A_m values is listed in Table 2.2. The large variation in K_L and A_m values within each group of chemicals showed that the sorption parameters were strongly influenced by the positions of the functional groups.

Many of the dyes in Sets 2 and 3 had lower K_L and A_m values than the four test dyes. The hypothetical dyes with four to six SO_3 groups attached to the triarylmethane

kernel (Figure 2.3e,f), had considerably smaller K_L and A_m values than the test dyes. These hypothetical dyes are likely better conservative tracers than any of the test dyes.

The K_L and A_m values of C.I. Food Green 3 were lower than those of C.I. Food Blue 2 (Brilliant Blue FCF). Between these two readily available dyes, C.I. Food Green 3 may be a better tracer than Brilliant Blue FCF for hydrological investigations in the vadose zone.

2.7 Summary

Dye tracers are frequently used in hydrological investigations. Although dyes have unique tracer characteristics, some limitations and problems are associated with using dyes as hydrological tracers. Most dyes sorb to subsurface media, so that tracer characteristics of dyes should be tested under the specific conditions under which dye tracing is to be conducted.

An accurate and cost-effective screening technique is necessary for selection of optimal dye tracers. Quantitative structure-activity relationships (QSAR) offer a powerful tool for screening of a large number dyes in a short time. We conducted a QSAR case study using triarylmethane dyes. The results of the QSAR modeling indicate that many hypothetical triarylmethane dyes have considerably lower sorption characteristics than the triarylmethane dyes currently used as tracers, and likely are good tracer candidates.

2.8 Tables and Figures

Table 2.1: Dyes commonly used as hydrological tracers.

Commercial Name	C.I. Nr.	C.I. Name	Chemical Class	Fluorescence	Maximum excitation (nm)[a]	Maximum emission (nm)[a]	Major uses
Brilliant Blue FCF	42090	Food Blue 2	Triarylmethane	No	None	630[b]	Vadose zone
Rhodamine WT	none	Acid Red 388	Xanthene	Yes	558[c]	583[c]	Surface water, groundwater, vadose zone
Sulforhodamine B	45100	Acid Red 52	Xanthene	Yes	560	584	Groundwater, vadose zone
Rhodamine B	45170	Basic Violet 10	Xanthene	Yes	555	582	Surface water, groundwater, vadose zone
Sulforhodamine G	45220	Acid Red 50	Xanthene	Yes	535	555	Groundwater
Uranine (Fluorescein)	45350	Acid Yellow 73	Xanthene	Yes	492	513	Groundwater, vadose zone
Eosine	45380	Acid Red 87	Xanthene	Yes	515	535	Groundwater, vadose zone
Methylene Blue	52015	Basic Blue 9	Thiazine	No	None	668[d]	Vadose zone
Lissamine Yellow FF	56205	Acid Yellow 7	Aminoketone	Yes	422	512	Groundwater, vadose zone
Pyranine	59040	Solvent Green 7	Anthraquinone	Yes	460	512	Groundwater

[a]Source: Field [*Field,* 2003a].

[b]Our own data.

[c]Sutton et al. [*Sutton et al.,* 2001] reported the excitation maximum for both the para and meta isomers as 555 nm, and the emmision maximum as 585 nm for the para isomer and 588 nm for the meta isomer.

[d]Source: Merck [*Merck,* 1996].

Table 2.2: Comparison of Langmuir coefficient (K_L) and maximum adsorption (A_m) for test and hypothetical triarylmethane dyes.

Triarylmethane dyes	C.I. Nr.	Number of SO_3 groups	Langmuir coefficient K_L (L/mmol)	Maximum adsorption A_m (mmol/kg)
Test triarylmethane dyes			Experimental	
C. I. Food Blue 2	42053	3	5.29	0.42
C. I. Acid Blue 7	42080	2	10.1	2.99
C. I. Food Green 3	42090	3	3.94	0.30
C. I. Acid Green 9	42100	2	16.5	4.40
Hypothetical triarylmethane dyes			Predicted	
Dye set 1	none	1	20.9 to 37.8	5.8 to 11.2
Dye set 2	none	2	8.1 to 31.5	2.0 to 8.7
Dye set 3	none	3	−8.5 to 14.7	−2.9 to 4.1

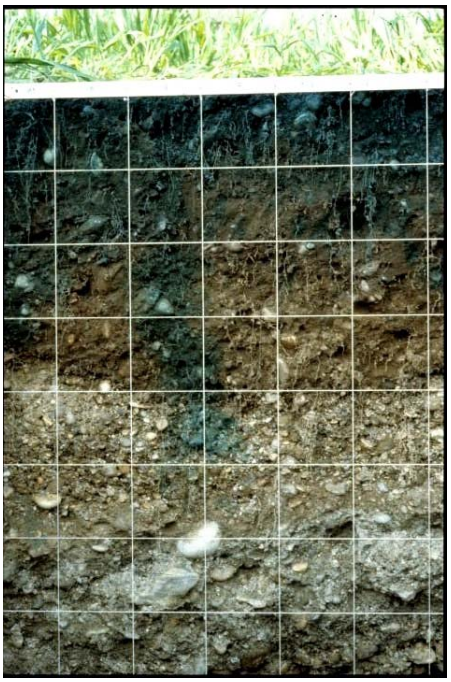

Figure 2.1: Visualization of flow patterns in soils using a dye tracer (Brilliant Blue FCF). Grid size is 10 cm. `(Note: This is a color figure)`

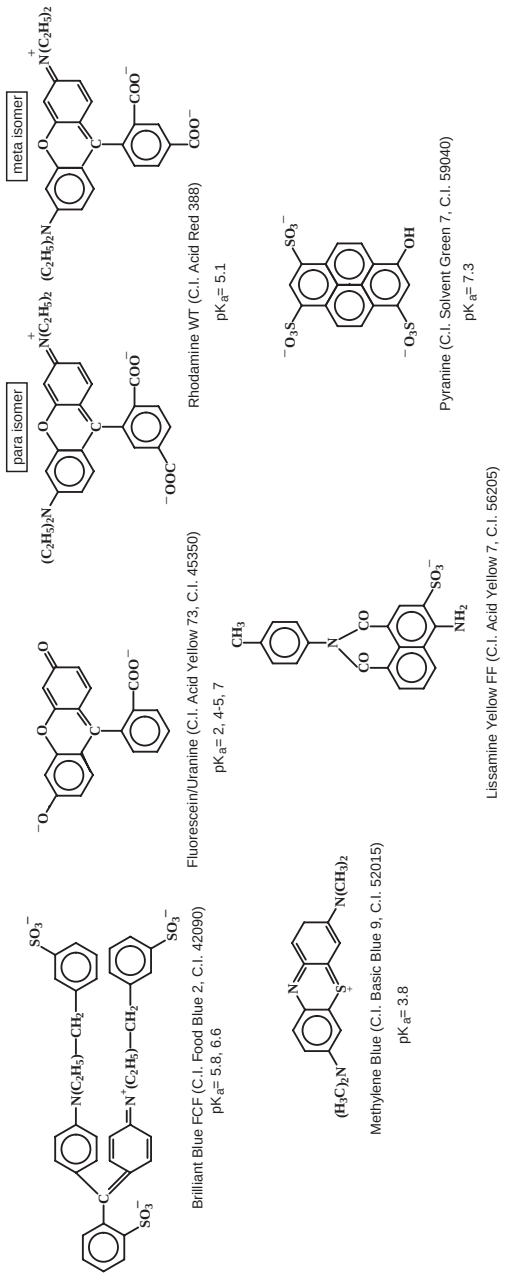

Figure 2.2: Structure of selected dye tracers. Dyes are shown in dissociated form. (Sources of the pK_a values are given in ref. (Flury and Wai, 2003)).

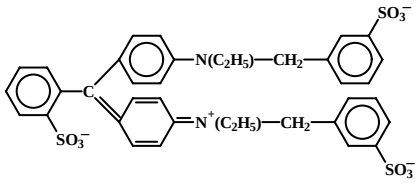

(a) Brilliant Blue FCF (C. I. Food Blue 2)

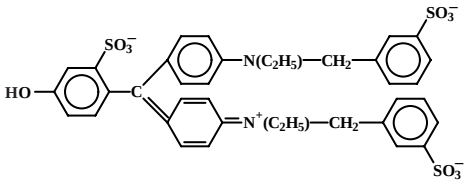

(b) FD&C Green No. 3 (C. I. Food Green 3)

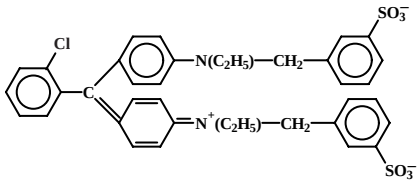

(c) ORCOacid Fast Green B (C. I. Acid Green 9)

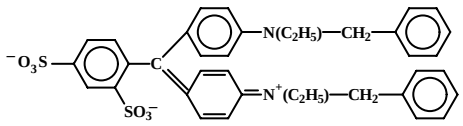

(d) ORCOacid Blue A 150% (C. I. Acid Blue 7)

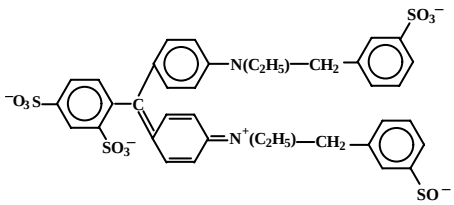

(e) Hypothetical triarylmethane dye

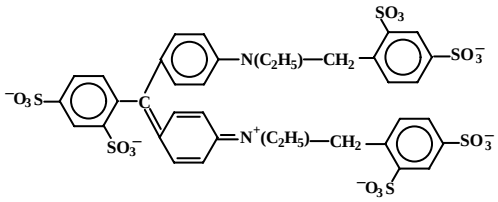

(f) Hypothetical triarylmethane dye

Figure 2.3: Test triarylmethane dyes used to develop the QSAR model (a–d) and hypothetical structure of potential dye tracers (e–f). Dyes are shown in their anionic forms.

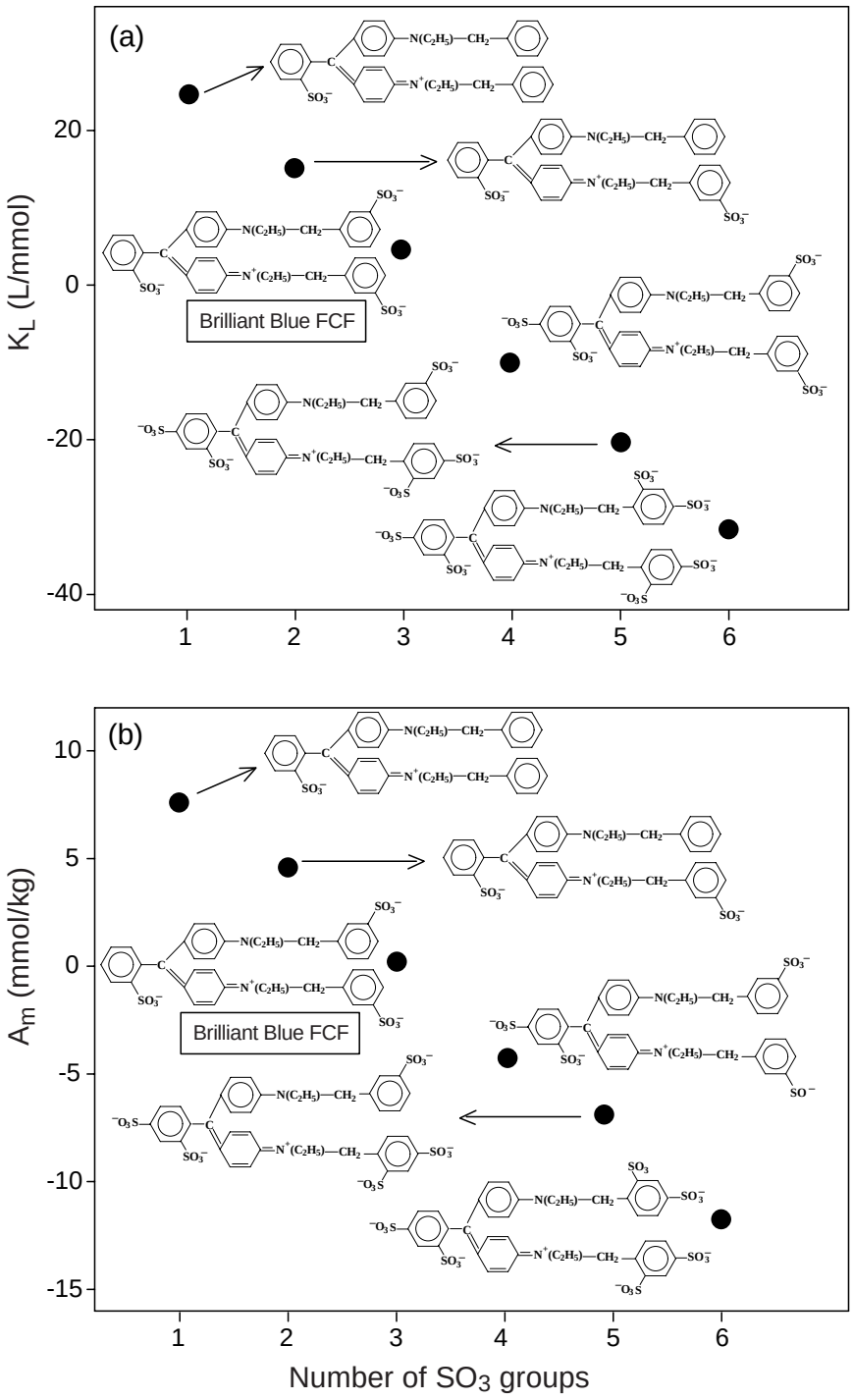

Figure 2.4: Changes in (a) Langmuir coefficient, K_L, and (b) adsorption maximum, A_m, as a function of the number of SO_3 groups on the molecular kernel of triarylmethane dyes.

Chapter 3

Sorption of Four Triarylmethane Dyes in a Sandy Soil determined by Batch and Column Experiments

3.1 Abstract

Dye tracers are important hydrological tracers. Only a few commercially available dyes have been systematically evaluated for their suitability as hydrological tracers. Sorption is one of the limiting factors for the suitability of a dye tracer. In this study we examined the sorption of four dyes to a sandy soil using batch and column techniques. Adsorption isotherms were determined at pH $\approx$ 8.0 in 10 mmol/L $CaCl_2$ background solutions. Batch sorption experiments were conducted using dye concen-

A modified version of this chapter has been submitted for publication: Jarai Mon, Markus Flury, and James. B. Harsh, Sorption of Four Triarylmethane Dyes in a Sandy Soil determined by Batch and Column Experiments, Geoderma (in review).

trations ranging from 0.0001 to 2.9 mmol/L. Sorption isotherms were analyzed with the Langmuir equation. Column experiments were conducted under water saturated conditions using four triarylmethane dyes—C.I. Food Blue 2 (Brilliant Blue FCF), C.I. Food Green 3, C.I. Acid Blue 7, and C.I. Acid Green 9. Adsorption isotherms calculated from column breakthrough data did not show good agreement with those of batch studies. Compared with the batch data, column data tended to over-estimate sorption of the dyes at small dye concentrations: however, batch and column experiments revealed the same relative differences in sorption among the dyes. The four dyes showed two different sorption behaviors: C.I. Food Green 3 and C.I. Food Blue 2 sorbed considerably less than C.I. Acid Green 9 and Acid Blue 7. The former two dyes contain three sulfonic acid groups while the latter only contain two sulfonic acid groups. C.I. Food Green 3 is likely be a good hydrological tracer, as is C.I. Food Blue 2, which is frequently used as a vadose zone tracer.

Key words: dye tracers, sorption, vadose zone, column isotherms, batch isotherms, Langmuir.

3.2 Introduction

Dyes are popular hydrological tracers, both for the saturated as well as the unsaturated zone [*Davis et al.,* 1980*; Flury and Wai,* 2003]. Many different dyes were used or tested as hydrological tracers, but there is little agreement on the most suitable dye tracer [*McLaughlin,* 1982]. Some dyes recommended for soil water tracing are Erio

Floxine 2G (C.I. 18050) [*Corey,* 1968], Pyranine (C.I. 59040) [*Reynolds,* 1966], Lissamine Yellow FF (C.I. 56205) [*Smettem and Trudgill,* 1983], and Brilliant Blue FCF (C.I. 42090) [*Steenhuis et al.,* 1990*; Flury and Flühler,* 1995]. A dye tracer optimal for a specific purpose may not be useful for another purpose. For instance, a tracer useful to determine flow velocity in Karst may not be a good vadose zone tracer, or vice versa.

Thousands of dyes are commercially available [*Colour Index,* 2001], and many may be potentially useful as hydrological tracers: however, only a few of these have been tested and used as hydrological tracers. Sorption to subsurface materials is one of the major factors that limits the application of dyes as hydrological tracers [*Shiau et al.,* 1993*; Flury and Flühler,* 1995*; Ketelsen and Meyer-Windel,* 1999]. To evaluate the suitability of dye tracers, a major component is the determination of sorption parameters.

Currently, one of the most commonly used dye tracers for studying water flow in the vadose zone is Brilliant Blue FCF [*Flury and Wai,* 2003]. Brilliant Blue FCF is a member of the class of triarylmethane dyes, and has been intensively investigated as a hydrological tracer [*Flury and Flühler,* 1995*; Ketelsen and Meyer-Windel,* 1999]. It is likely that other triarylmethane dyes are useful tracers as well. The class of the triarylmethane dyes contains a series of dyes with similar structure as Brilliant Blue FCF; however, no systematic investigations have been conducted on the suitability of these dyes as tracers.

Sorption of dyes to soil material is commonly determined with batch experiments; however, the batch method has certain shortcomings: (1) soil particles may be broken in smaller pieces during shaking, causing errors in the sorption measurements, (2) batch experiments are usually conducted at much lower solid to solution ratios than what would be representative under field conditions, and (3) batch experiments require filtering or centrifugation to separate the liquid from the solids [*Griffioen et al.*, 1992; *Bürgisser et al.*, 1993].

Column experiments have been proposed as an alternative method for measuring sorption isotherms [*Griffioen et al.*, 1992; *Bürgisser et al.*, 1993; *Igler et al.*, 1998; *Atkinson and Bukowiecki*, 2000]. Column techniques have some advantages over batch techniques: the experimental measurement can be automated, the solid to solution ratio is more similar to natural field conditions, no shaking and centrifugation is required, and the flow-through system represents natural flow conditions more closely [*Griffioen et al.*, 1992; *Bürgisser et al.*, 1993]. *Bürgisser et al.* [1993] demonstrated that the adsorption isotherms of cadmium and methylene blue determined with column experiments showed good agreement with those obtained with batch experiments.

The column technique is promising to determine sorption characteristics of dyes, because it would allow rapid screening of dye sorption behavior under a variety of experimental conditions. If a transparent column were used, the column technique also allows one to visualize the staining capability of a dye. The main objectives of this study were to compare the sorption characteristics of four triarylmethane dyes

and to investigate the suitability of column experiments for measuring the sorption isotherms. Sorption isotherms determined with column experiments were compared with those obtained from batch studies.

3.3 Materials and Methods

3.3.1 Dyes and Porous Medium

We selected four commercially available triarylmethane dyes. The commercial names, Colour Index names (C.I. Name), Colour Index numbers (C.I. Nr), and selected properties of the dyes are listed in Table 3.1. These dyes were commercially available in solid forms and obtained directly from the manufacturers. All four dyes share a common molecular template but contain different types and numbers of functional groups attached at different positions on the molecular template (Figure 3.1). The purpose of selecting these four dyes was to evaluate the effect of functional groups on dye sorption.

A sandy soil, collected from Vantage, Washington, was used as test material for the sorption experiments. This soil was the same as the one used by *German-Heins and Flury* [2000]. The pH of the soil was 7.1, the particle size dominated by sand (about 96% by weight), and the mineralogy consisted mainly of quartz and feldspar. More detailed soil characterization is presented in *German-Heins and Flury* [2000].

3.3.2 Batch Experiments

Standard batch sorption experiments were conducted with the Vantage soil. We used nine dye concentrations ranging from 0.0001 to 2.9 mmol/L (0.1, 1, 10, 50, 100, 200, 500, 1000, 2000 mg/L). This large range of concentration was chosen because tracer dyes in the vadose zone are often applied at concentrations up to 2000 mg/L [*Flury and Flühler,* 1995]. The experimental protocol followed the one described in *German-Heins and Flury* [2000]. Briefly, 10 g of soil were mixed with 60 mL of dye solution (1:6 wt/wt solid/solution ratio) or 20 g of soil were mixed with 20 mL of dye solution (1:1 wt/wt solid/solution ratio). Preliminary tests on the particle density effect showed that the use of two different solid-solution ratios did not have a significant effect on adsorption isotherms (Figure 3.2), which was also confirmed in earlier studies [*German-Heins and Flury,* 2000]. The pH of the batch system was 8.0, adjusted with 0.1 mol/L NaOH, and the background electrolyte concentration was 10 mmol/L $CaCl_2$. The samples were shaken using a reciprocal shaker for 24 hrs at 22°C. The samples were then centrifuged at 48,000 g for 15 minutes, the supernatant decanted, and the dye concentration measured with a spectrophotometer (Hewlett Packard 8425 A Diode array) at the wavelength of maximum absorption of each dye. Experiments were made in triplicates and included a blank system.

Sorption isotherms were constructed by plotting dye concentration in solution versus dye sorbed on the soil. The mass of dye sorbed on the soil was calculated based on mass balance considerations. The experimental sorption isotherms were analyzed

with the Langmuir model [*Langmuir,* 1918*; Schulthess and Dey,* 1996]:

$$C_a = \frac{A_m K_L C_s}{1 + K_L C_s} \tag{3.1}$$

where C_a (mmol/kg) is the sorbed concentration, C_s (mmol/L) is the solution concentration, K_L (L/mmol) is the Langmuir coefficient, and A_m (mmol/kg) is the maximum adsorption. The Langmuir parameters, K_L and A_m, were determined by fitting the data with three different regression methods, i.e., Langmuir linearization (LL), non-linear least squares (NLLS), and normal non-linear least squares (NNLS) [*Schulthess and Dey,* 1996], using the LANGMUIR_1 computer program written by *Schulthess and Dey* [1996].

3.3.3 Column Experiments

Column sorption experiments were conducted under water saturated conditions with the flow direction upward. We used a transparent glass chromatography column with an inner diameter of 1.5 cm and length of 12.2 cm (Omnifit, Cambridge, UK). The end plates of the column consisted of porous polypropylene disks. The column effluent was collected using a fraction collector. The eluent solution consisted of 10 mmol/L $CaCl_2$ adjusted to pH 8. To determine the column Peclet number, the $CaCl_2$ was displaced with equimolar $Ca(NO_3)_2$. Nitrate concentration in the outflow samples was measured with a spectrophotometer (Hewlett Packard 8425 A Diode array). Column Peclet numbers, defined as $\mathrm{Pe} = VL/D$, with V being the pore water velocity, L the length of the column, and D the dispersion coefficient, were obtained by fitting the

standard advection-dispersion equation to the NO_3 breakthrough data [*Fortin et al.,* 1997].

For the dye experiments, dyes at a concentration of about 2.5 to 3 mmol/L were dissolved in 10 mmol/L $CaCl_2$ solution. Because of high degree of impurity in the C.I. Acid Blue 7 dye sample, this dye solution was sequentially filtered using an 11 μm filter paper (Grade 1, Whatman Ltd., UK) and a 0.4 μm membrane filter (Nuclepore Corp., CA). Dyes were introduced into the column as a pulse of two to four pore volumes and then eluted with the background electrolyte solution until dye concentrations in the outflow were close to the background. Eluent was collected with a fraction collector and dye concentrations quantified with spectrophotometry. Selected parameters of the column experiments are summarized in Table 3.2.

If hydrodynamic dispersion is negligible (column Peclet > 50), then one can use column breakthrough data to determine the sorption isotherm of a chemical [*Griffioen et al.,* 1992; *Bürgisser et al.,* 1993]. As shown by *Bürgisser et al.* [1993], the sorption isotherm can be derived from the elution part of the breakthrough curve as:

$$C_a(C_s) = \frac{1}{\rho}\int_0^{C_s}\left[\frac{t(c')}{t_0} - \frac{t_{pulse}}{t_0} - 1\right]dc' \tag{3.2}$$

where C_a (mmol/kg) is the sorbed concentration, C_s (mmol/L) is the concentration of the chemical in the column outflow, t is the travel time from the beginning of the experiment when the dyes are fed into the column, t_{pulse} is the time duration of pulse input, t_0 is the average travel time (length of the column divided by pore water velocity), and ρ is the mass of soil per unit pore volume, given as $\rho = \frac{\rho_s(1-\theta)}{\theta}$, where

ρ_s is the particle density and θ is the porosity of the soil in the column. To integrate equation (3.2), we interpolated the experimental data with a cubic spline [*Press et al.,* 1992] as suggested by *Bürgisser et al.* [1993]. The splines were then integrated using the Romberg integration [*Press et al.,* 1992].

3.4 Results and Discussion

The results of the batch sorption experiments are depicted in Figure 3.3, and the Langmuir isotherm parameters estimated with the different regression methods are listed in Table 3.3. Two of the non-linear least square procedures, the non-linear least square and the normal non-linear least square, yielded the best curve fits, except for C.I. Food Green 3, where all methods gave identical fitting results. The Langmuir linearization method tended to underestimate the sorption affinity, K_L, and to overestimate the maximum adsorption, A_m.

The experimental results of the column experiments are shown in Figure 3.4. The Peclet numbers determined from the NO_3^- breakthrough curves were between 145 ± 0.7 and 151 ± 0.8 (Figure 3.5), suggesting that it is reasonable to ignore the dispersion term in the convection-dispersion equation as needed for calculation of adsorption isotherms. The comparison of the dye breakthrough curves shows that the dye fronts of the C.I. Food Blue 2 and C.I. Food Green 3 were very similar and the dye breakthrough occurred at about 2.5 to 3 pore volumes (Figure 3.4a,b).

The breakthrough of C.I. Acid Blue 7 and C.I. Acid Green 9 occurred between

5 and 6 pore volumes (Figure 3.4c,d). Unlike the other three dyes, the maximum concentration of the C.I. Acid Green 9 in the outflow was only about one half of the input concentration (Figure 3.4d). Both, C.I. Acid Blue 7 and C.I. Acid Green 9 show a pronounced tailing of the desorption front and up to 500 pore volumes had to be eluted before the dye concentration fell below the analytical detection limit. After about 90 pore volumes of throughflow, the flow rate in the C.I. Acid Green 9 column decreased from 0.9 to 0.44 mL/min, suggesting that the dye was clogging up the column. Dye outflow concentrations at that time were near the analytical detection limit, so we do not consider the errors caused by the clogging to have affected the sorption isotherm determination.

The sorption isotherms obtained from the column experiments (Equation 3.2) and those obtained from the batch experiments are compared in Figure 3.6. In general, the adsorption isotherms calculated from column data show the same trends as those from the batch data: greater sorption determined in columns corresponded to greater sorption observed in batch experiments. However, the sorption isotherms obtained from the column experiments do not agree well with those obtained from batch studies (Figure 3.6b,c). The agreement between column and batch isotherms appears to be better at high dye concentrations than at low concentrations (Figure 3.6c). On a logarithmic scale, the isotherms at high concentrations agree fairly well.

The results of both column and batch studies show that C.I. Food Blue 2 and C.I. Food Green 3 were sorbed less than C.I. Acid Blue 7 and C.I. Acid Green 9.

The main difference among these four dyes is the number of sulfonic acid groups in their structures: C.I. Food Blue 2 and C.I. Food Green 3 contain three sulfonic acid groups, while C.I. Acid Blue 7 and C.I. Acid Green 9 contain only two sulfonic acid groups (Figure 3.1). It has been reported that dyes consisting of more sulfonic acid groups tend to sorb less and have a better mobility in soils than dyes with fewer sulfonic acid groups [*Corey,* 1968*; Reife and Freeman,* 1996]. Our results corroborate this observation.

If a transparent column is used, the dye penetration into and elution from the column can be visually observed, and this provides information on how well the dyes can stain the porous material. All the four dyes used here strongly stained the sandy soil and could be clearly visualized by eye. Although a very qualitative measure, these visual observations are very helpful to determine the coloring ability of a dye when used as vadose zone tracer. Such information cannot be obtained from batch experiments.

From all four dyes investigated, C.I. Food Green 3 sorbed the least. Both C.I. Food Green 3 and C.I. Food Blue 2 contain three sulfonic acid groups, but C.I. Food Green 3 contains, in addition, a hydroxyl group. This additional hydroxyl group likely causes increased water solubility. From all four dyes tested, both C.I. Food Green 3 and C.I. Food Blue 2 seem to be good hydrological tracers, and C.I. Food Green 3 seems to be the best tracer. At high concentrations ($\approx$g/L), the hue of C.I. Food Green 3 is very similar to that of C.I. Food Blue 2, and the staining power of the two dyes is very similar as well.

3.5 Conclusions

The column technique is a useful method to screen dyes as hydrological tracers. Although sorption isotherms obtained from the column technique did not agree well with batch isotherms, the relative sorption of different dyes can be accurately assessed. The column technique is faster, and thus allows a more efficient screening of dyes. In addition, the column technique allows assessment of the coloring ability of dyes in porous media, and may also represent natural conditions more closely than the batch technique.

The triarylmethane dyes tested in this study showed that the more SO_3 groups attached to the molecule template, the less was the sorption. Besides C.I. Food Blue 2, C.I. Food Green 3 was found to be a potentially useful tracer candidate. This dye is a certified food due in the U.S. and therefore suitable as a hydrological tracer from a toxicological point of view as well.

3.6 Tables and Figures

Table 3.1: Dyes used in this study and selected properties of the dyes.

Common Name	C.I. Name	C.I. Nr.	Hue	Mol. wt. (g/mol)	Solubility[a] (g/L)	Maximum absorption (nm)	Absorptivity (L/g-cm)	Manufacturer
FD&C Green 3	C. I. Food Green 3	42053	Bluish Green	808	200	630	164	Pylam Products Co., Tempe, AZ
FD&C Blue 1, Brilliant Blue FCF	C. I. Food Blue 2	42090	Bright Greenish-Blue	792	200	626	156	Pylam Products Co., Tempe, AZ
ORCOacid Blue 150% A	C. I. Acid Blue 7	42080	Bright Greenish-Blue	690	Very Soluble	638	n/a	ORCO, East Providence, RI
ORCOacid Fast Green B	C. I. Acid Green 9	42100	Bright Bluish-Green	724	Very Soluble	636	n/a	ORCO, East Providence, RI

[a] Water solubility at 25°C.

Table 3.2: Selected parameters for the column experiments.

Parameter	Unit	Value
Length of column, L	cm	12.2
Bulk density	g/cm^3	1.52–1.54
Water content	cm^3/cm^3	0.42–0.43
Column pore volume	mL	9.1–9.3
Flow rate, Q	mL/min	0.9–1.1
Water flux, J_w	cm/min	0.5–0.6
Pore water velocity, V	cm/min	1.20–1.42
Hydrodynamic dispersion, D	cm^2/min	0.10–0.11
Column Peclet number, Pe $= VL/D$	–	145–151
Dye pulse length in pore volumes	–	3–4
Duration of experiments in pore volumes	–	137–461

Table 3.3: Estimated Langmuir coefficient, K_L, and maximum adsorption, A_m, for the test dyes.

Dye	C.I. Nr.	Langmuir coefficient K_L (L/mmol)			Maximum adsorption A_m (mmol/kg)			Correlation Coefficient[d] η^{*2}		
		NLLS[a]	NNLS[b]	LL[c]	NLLS[a]	NNLS[b]	LL[c]	NLLS[a]	NNLS[b]	LL[c]
C. I. Food Blue 2	42053	5.7	5.29	1.86	0.41	0.42	0.50	0.95	0.95	0.91
C. I. Acid Blue 7	42080	10.5	10.6	7.58	2.95	2.99	3.19	0.98	0.98	0.92
C. I. Food Green 3	42090	3.9	3.94	4.34	0.30	0.30	0.29	0.98	0.98	0.98
C. I. Acid Green 9	42100	17.0	16.5	9.99	4.36	4.40	5.73	0.99	0.99	0.99

[a]NLLS = Non-linear least squares.

[b]NNLS = Normal non-linear least squares.

[c]LL = Langmuir linearization.

[d]This coefficient assumes that a normal squared minimum is the best goodness-of-fit (Schulthess and Dey, 1996).

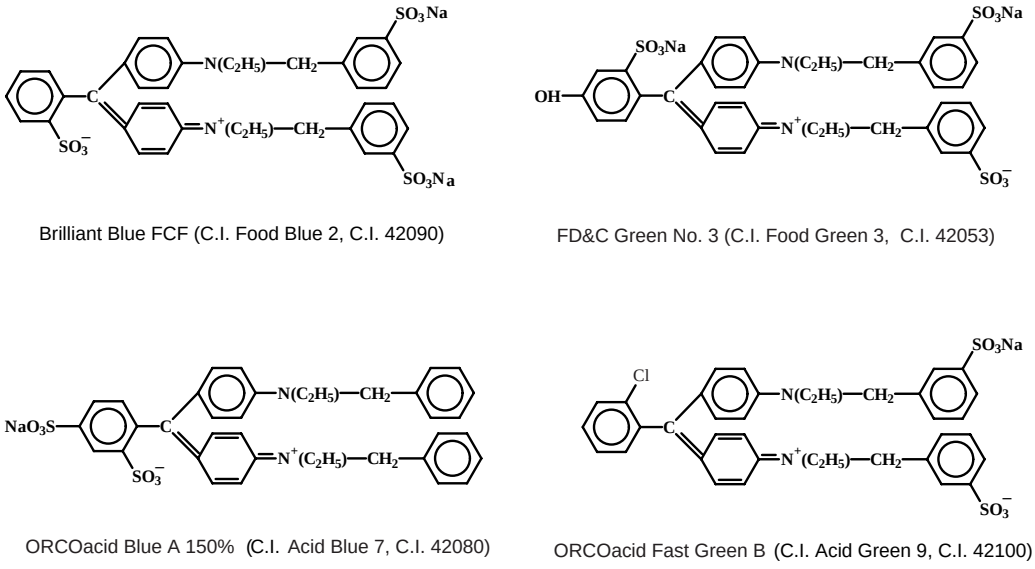

Figure 3.1: Molecular structures of the four triarylmethane dyes used in this study.

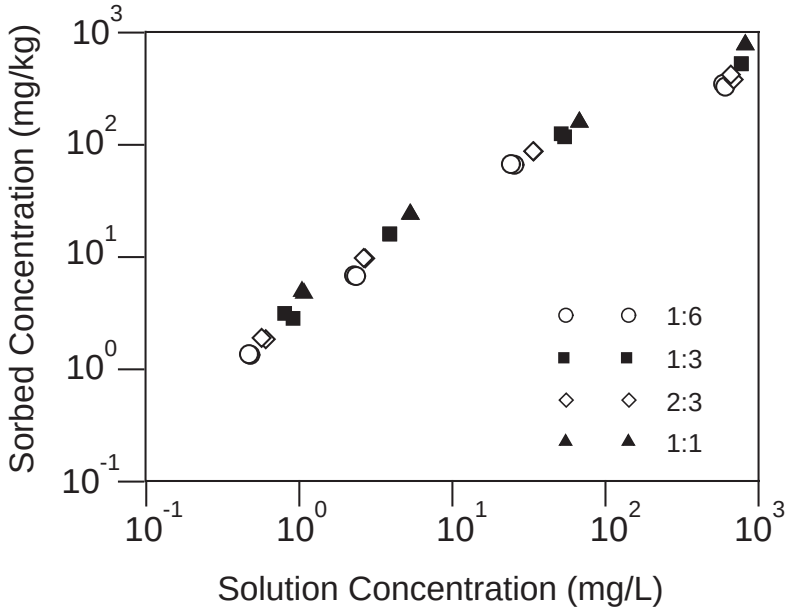

Figure 3.2: Effect of solid to solution ratio on the adsorption isotherm of Brillant Blue FCF (C.I. Food Blue 2). The ratios are solid to solution in the units of g:ml.

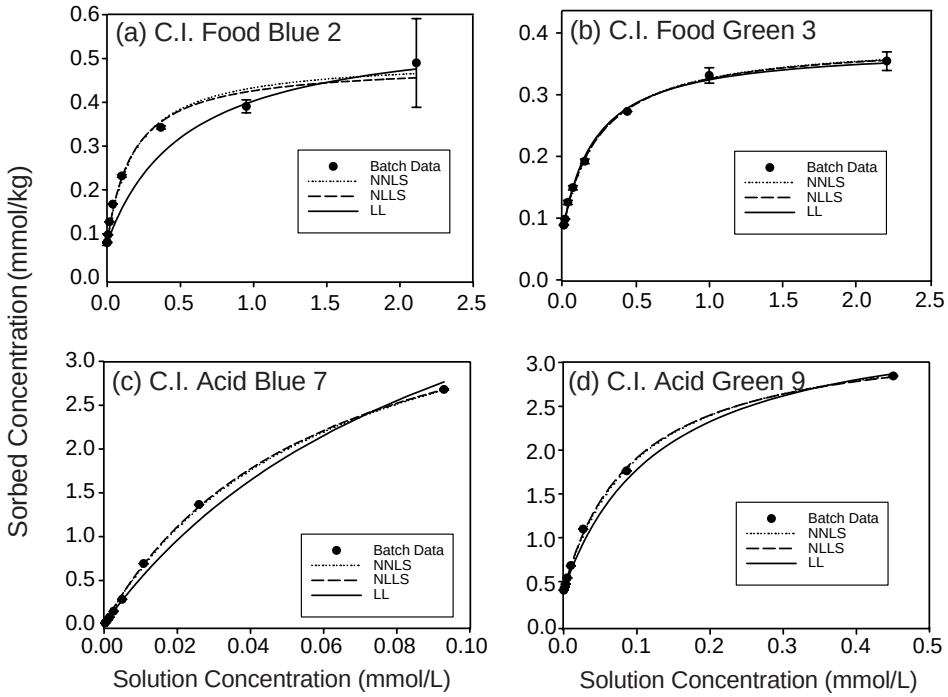

Figure 3.3: Adsorption isotherms of (a) C.I. Food Blue 2, (b) C.I. Food Green 3, (c) C.I. Acid Blue 7, and (d) C.I. Acid Green 9 determined by batch experiments. Symbols represent experimental batch data and error bars are ± one standard deviation. The lines are Langmuir isotherms fitted to the data using different regression methods (NLLS = Non-linear least squares, NNLS = Normal non-linear least squares, LL = Langmuir linearization).

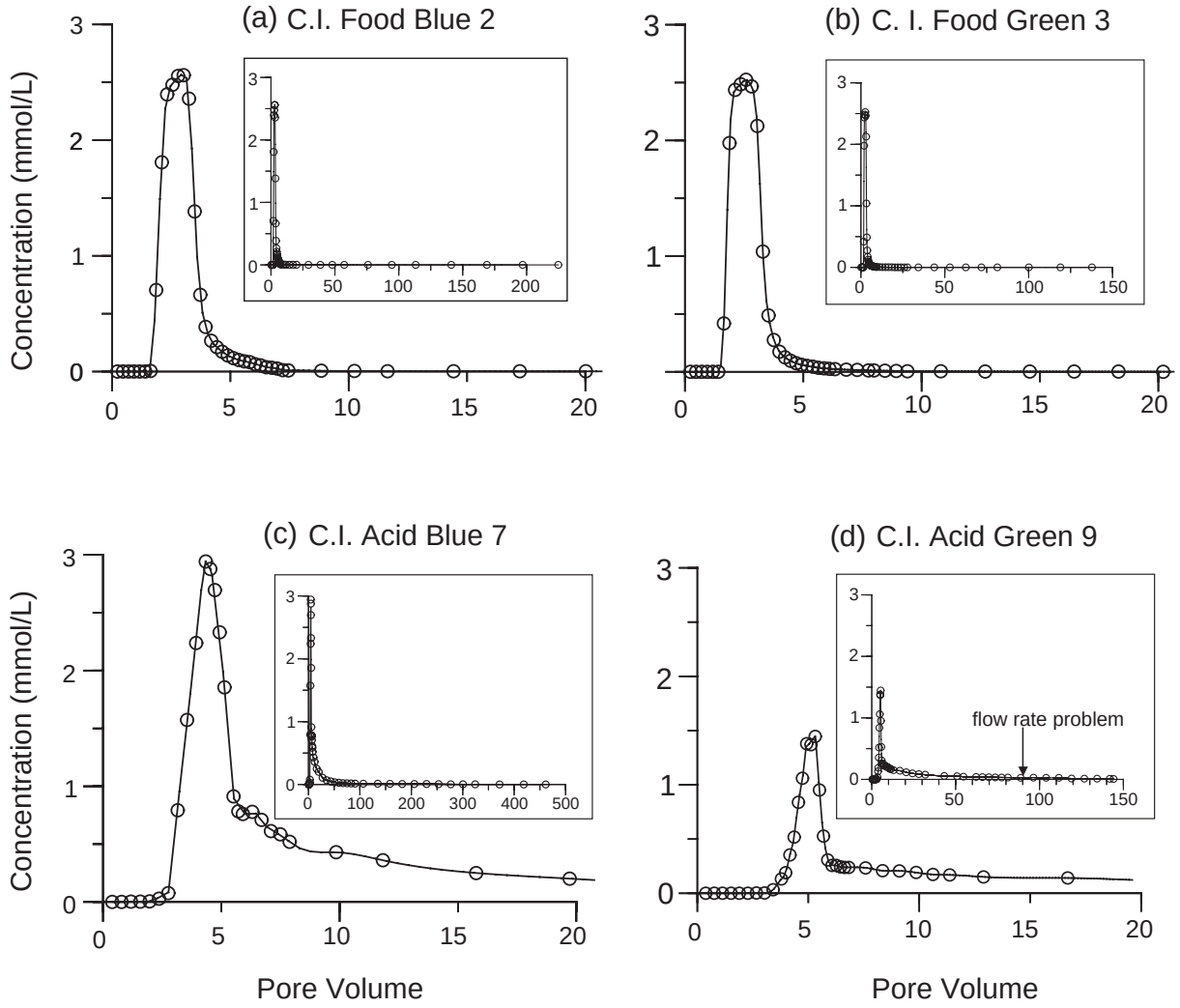

Figure 3.4: Column breakthrough curves of (a) C.I. Food Blue 2, (b) C.I. Food Green 3, (c) C.I. Acid Blue 7, and (d) C.I. Acid Green 9. Symbols represent experimental data and the solid lines are spline interpolations. The insets show the breakthrough curves for the entire duration of the experiment.

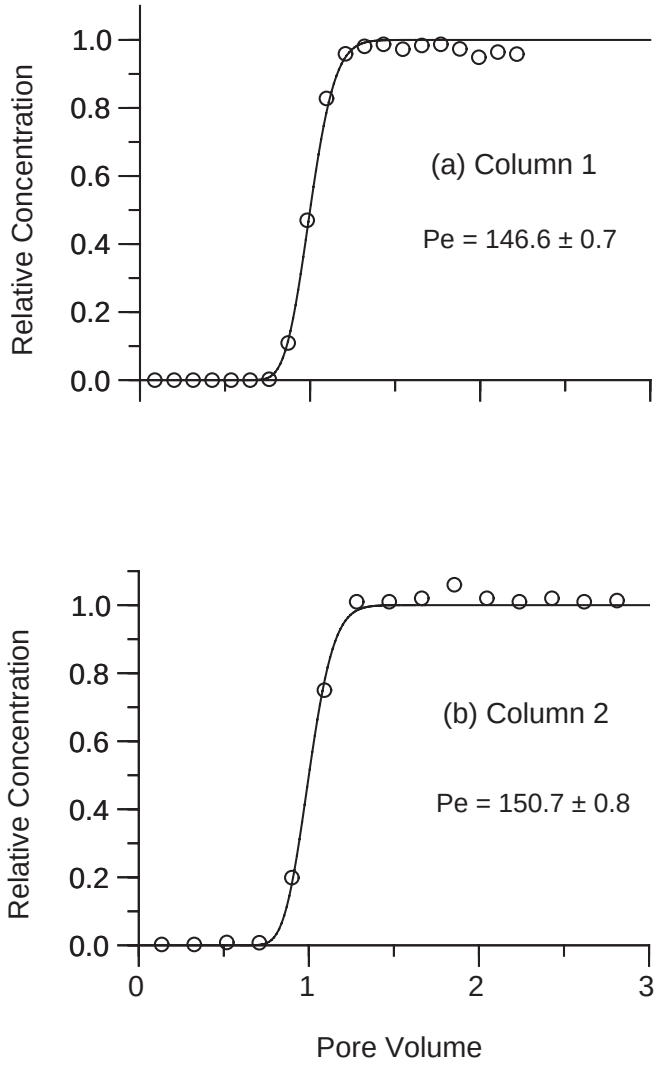

Figure 3.5: Nitrate breakthrough curves for columns 1 and 2. Calcium nitrate was used as a conservative tracer to determine the hydrodynamics of the columns.

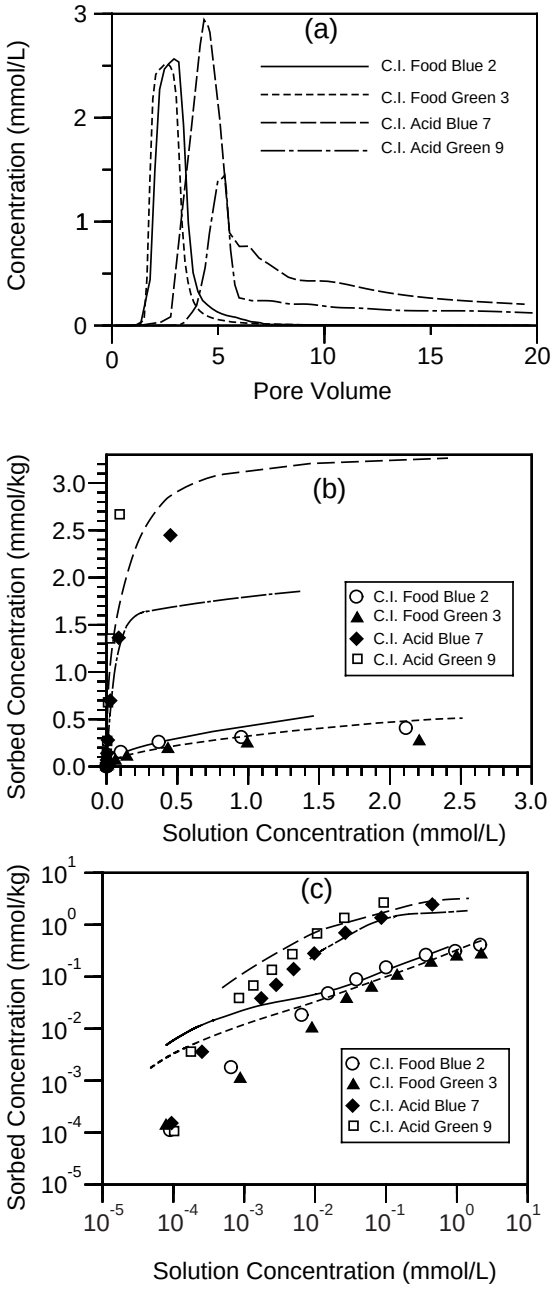

Figure 3.6: Comparison of breakthrough curves and adsorption isotherms of the dyes used in this study. (a) Column breakthrough curves (spline interpolations), (b) adsorption isotherms (linear scale), and (c) adsorption isotherms (log-log scale). Symbols represent batch data and lines are column data.

Chapter 4

Quantitative Structure-Activity Relationships (QSAR) for Screening of Dye Tracers

4.1 Abstract

Dyes are important hydrological tracers. Many different dyes have been proposed as optimal tracers, but none of these dyes can be considered an ideal water tracer. Some dyes are toxic and most sorb to subsurface materials. The objective of this study was to find the molecular structure of an optimal water tracer. We used QSAR to screen a large number of hypothetical molecules, belonging to the class of triarylmethane dyes, in regard to their sorption characteristics to a sandy soil. The QSAR model was

A modified version of this chapter has been submitted for publication: Jarai Mon, Markus Flury, and James. B. Harsh, Quantitative Structure-Activity Relationships (QSAR) for Screening of Dye Tracers, Journal of Hydrology (in review).

based on experimental sorption data obtained from four triarylmethane dyes: Brilliant Blue FCF (C.I. 42090), FD&C Green No. 3 (C.I. 42053), ORCOacid Blue A 150% (C.I. 42080), and ORCOacid Fast Green B (C.I. 42100). Sorption characteristics of the dyes were expressed with the Langmuir isotherm. Our premise was that dye sorption can be minimized by attachment of sulfonic acid (SO_3) groups to the triarylmethane template. About 70 hypothetical dyes were created and QSAR were used to estimate their sorption characteristics. The results indicated that both the position and the number of SO_3 groups affected dye sorption. The more SO_3 groups were attached to the molecule template, the smaller was the sorption. An optimal hydrological water tracer contains four to six SO_3 groups.

Keywords: dyes, hydrological tracers, water tracing, QSAR, sorption

4.2 Introduction

Dye tracers are frequently used in hydrology to measure groundwater flow velocity, identify flow directions, hydraulic connections, and the pattern of water movement [*Drew,* 1968*; Smart and Laidlaw,* 1977*; Davis et al.,* 1980*; McLaughlin,* 1982*; Flury and Wai,* 2003]. An ideal dye to trace the movement of water should move conservatively, i.e., without interacting with the solid phase and without decaying during the time period of the tracer test. By and large, however, dyes react with subsurface media, and the fate and behavior of dyes in the subsurface depend on the environmental conditions, i.e., property of the media and solution chemistry [*Smart and Laidlaw,*

1977; *Flury and Flühler,* 1995; *German-Heins and Flury,* 2000]. A good dye tracer under one environmental condition may not perform as well under a different environment. Therefore, dye tracers should be evaluated for their suitability in specific applications.

Thousands of dyes are commercially available [*Colour Index,* 2001]. Because experimental screening of a large number dyes in searching for a good tracer for specific environmental condition is not feasible, alternative methods for screening are needed. Quantitative structure-activity relationships (QSAR) offer the possibility for screening a large number of chemicals in a short time and with low cost. QSAR establish a statistical relationship between biological activity or environmental behavior of the chemicals of interest and their structural properties [*Sabljić,* 1989b; *Hansch and Fujita,* 1995]. Using QSAR, we can obtain an approximation of the activity of a chemical from its molecular structure only.

Comment: QSAR have been employed in several areas such as agrochemical, pharmaceutical, and environmental studies. In environmental science, the application of QSAR is mostly for describing the toxicity of a certain chemicals and for the assessment of environmental contamination [*Nendza,* 1998]. Thereby, the objective of QSAR is often to find a mathematical model that can be used for predictions of the activity of chemicals of interest [*Sabljić,* 1989b]. QSAR models are usually derived from a group of compounds whose activities are known and whose structures are similar to those of compounds to be investigated [*Hall et al.,* 2002]. Such models often break down in

attempting to predict the activities of a group of compounds that are not structurally related or are from different chemical classes [*Gerstl and Helling,* 1987]. A successful QSAR model will adequately predict the activity of compounds from their respective chemical structures. The QSAR approach is a powerful tool for estimation of the activity of a large number of similar compounds without time consuming experimental measurements. However, it is not implied that experimental measurements could be replaced by model estimations. In looking for the best dye tracers, QSAR model predictions should be used as basic information for finding preferred candidates that are then to be tested experimentally. In addition, QSAR should be used for designing the best possible chemicals, which possess the most desirable tracer characteristics. ■

QSAR have been successfully applied to predict soil sorption coefficients of non-polar and non-ionizable organic compounds such as many pesticides [*Gerstl and Helling,* 1987*; Pussemier et al.,* 1989]. Sorption of organic chemicals in soils or sediments is usually measured by sorption coefficients. QSAR models with the first-order molecular connectivity index have been used to estimate soil sorption coefficients of non-polar organic chemicals [*Sabljić,* 1989a*; Sabljić,* 1989b*; Meylan et al.,* 1992*; Sabljić,* 2001]. However, the first-order molecular connectivity model was insufficient in predicting sorption coefficients of polar organic compounds [*Sabljić,* 1989b*; Sekusak and Sabjlić,* 1992]. *Meylan et al.* [1992] suggested that sorption coefficients of some polar organic compounds could be successfully predicted with a model that includes molecular con-

nectivity indices (MCIs) and polarity correction factors. *Sekusak and Sabjlić* [1992] reported that a QSAR model consisting of the second-order MCI and a descriptor representing the polar part of a molecule was able to describe the log K_{oc} of amides, while the first-order MCI alone failed. High-order MCIs are possible descriptors to identify pesticides susceptible to leaching [*Worrall,* 2001].

Higher-order MCIs might have a better correlation with sorption of organic compounds than lower-order MCIs. Sorption coefficients normalized by organic carbon content (log K_{oc} or log K_{om}) have been used in several QSAR models [*Pussemier et al.,* 1989*; Sabljić,* 1989a*; Sabljić,* 1989b*; Meylan et al.,* 1992*; Sabljić,* 2001]. Soil sorption of ionizable, hydrophobic organic chemicals could be estimated using a QSAR model which included the octanol/water partition coefficient, organic carbon content, and correction factors for acids and bases [*Bintein and Devillers,* 1994]. The K_{oc}, however, is not an appropriate parameter for describing sorption of ionizable, polar molecules, such as organic dye tracers. Sorption of ionizable organic compounds in soils or sediments depends on the concentration of chemicals, solution pH, ionic strength, and medium properties [*Schwarzenbach et al.,* 2003]. Obtaining a soil sorption QSAR model that accounts for differences in solution chemistry and media properties may be impossible. Moreover, sorption models derived from a specific chemical class under specific environmental conditions would not be valid for general use. QSAR models are specific to chemicals and their interactions with the targeted environment [*Nendza,* 1998].

Dyes are grouped into classes based on their chemical structures or their methods of application. A number of hydrological tracers are from the class of triarylmethane dyes [*Flury and Wai,* 2003]. This class includes hundreds of dyes that are mostly red, violet, blue, or green in colors and is one of the largest dye groups [*Colour Index,* 1971]. The class includes Brilliant Blue FCF (C.I. Food Blue 2), which is a well known vadose zone tracer, but may also contain dyes that are better tracers than Brilliant Blue FCF. In addition, new and better dye tracers could be designed by structural modification of existing tracers.

Dyes that contain more sulfonic acid groups are generally less sorbed to soils than those with fewer SO_3 groups [*Corey,* 1968]. Testing the adsorption of dyes and selected intermediates to activated carbon, Reife and Freeman (1996) found that chemicals that contain more sulfonic acid groups in their molecular structures were less sorbed. These results suggest that as more sulfonic acid groups are attached to the molecular template, dyes become more water-soluble and more readily move with the water. Not only the number but also the positions of SO_3 groups in the structures may influence the sorption of dyes. At neutral pH, orthanilic acid (one sulfonic acid group attached at the *ortho* position on aniline) sorbed much more strongly to activated carbon than that of metanilic acid (one sulfonic acid group attached at the *meta* position) [*Reife and Freeman,* 1996]. Similarly, the para isomer of Rhodamine WT exhibits less sorption to aquifer materials than does its meta isomer [*Vasudevan et al.,* 2001].

The goal of this study was to identify the structure of a dye best suited for tracing

water flow in porous media. We based our selection of dyes on the class of triarylmethane dyes. The specific objective was to examine the sorption properties of dyes consisting of the same molecular template as Brilliant Blue FCF but with different numbers and positions of sulfonic acid groups. Four commercially available triarylmethane dyes were used to develop a QSAR model that allowed us to predict the sorption characteristics of hypothetical dyes with similar molecular structure.

4.3 Theory

QSAR development requires three basic elements: (1) an activity or property data set, measured experimentally, (2) molecular descriptors, which are the quantitative descriptions of structural properties, and (3) statistical techniques to establish the relationship between molecular descriptors and activities. QSAR analysis consists of statistical modeling, and consequently QSAR results are associated with some uncertainty and the predictive power of a QSAR model is related not only to the quality of the input data but also the power of the statistics [*Hall et al.,* 2002].

Comment: The major assumption in QASR model development is that all the activities of chemicals are influenced by electronic, hydrophobic, and steric effects [*Hansch and Fujita,* 1995*; Hansch and Leo,* 1995*; Kier and Hall,* 1986]. Further, QSAR formulation assumes that similar changes in structural properties have similar effects on the activity of chemicals [*Hansch and Leo,* 1995]. Thereby, the effect of

structural changes on the activity of a compound can be extrapolated from a similar system [*Hansch and Leo,* 1995]. This important idea was developed and proved by L. P. Hammett around 1935 [*Hansch and Leo,* 1995]. Based on these principles, QSAR have been developed for describing properties/activity of hundreds of chemicals as well as for prediction of toxic effects, fate and environmental behaviors of potentially hazardous chemicals [*Nendza,* 1998]. For any applications, QSAR procedure includes six basic steps (Figure 4.1). ■

The first step in a QSAR study is the selection of a group of compounds for which experimental data are available. This group of compounds, the training set, should cover the whole range of compounds whose activities/properties are to be modeled [*Hall et al.,* 2002]. The QSAR analysis is further based on the calculation of appropriate molecular descriptors. Many different descriptors are available, but only few of them might be used as independent variables in a QSAR model. Appropriate descriptors are selected from previous knowledge of interaction processes or by statistical techniques, i.e., by choosing descriptors that are highly correlated to the experimental parameters of interest.

One group of molecular descriptors, the MCIs, have been successfully used in QSAR to describe sorption of some hydrophobic chemicals in soils [*Sabljić,* 2001]. The indices quantify the structure of a molecule by coding the electrons present in the whole molecule [*Kier and Hall,* 1999] and carry much structural information including in-

termolecular accessibility [*Kier and Hall,* 2000]. There are two basic types of MCIs: simple MCIs and valence MCIs, which can be calculated as [*Kier and Hall,* 1986*; Hall and Kier,* 2001]:

$$^1\chi = \sum(\delta_i\delta_j)^{-0.5} \tag{4.1}$$

and

$$^1\chi^v = \sum(\delta_i^v\delta_j^v)^{-0.5} \tag{4.2}$$

where $^1\chi$ is the first-order simple MCI; δ_i, δ_j are the counts of sigma electrons in adjacent non-hydrogen atoms i, j; $^1\chi^v$ is the first-order valence MCI; and $\delta_i^v\delta_j^v$ are the counts of all valence electrons in adjacent non-hydrogen atoms i, j. The lower MCIs (zeroth- to second-order) encode global or bulk properties, such as molecular size, and the higher-order MCIs (> second-order) encode local structural properties, e.g., para substitutions [*Hall and Kier,* 2001*; Sabljić,* 2001].

Comment: The selection of compounds for a training set is one of the major processes in QSAR studies. A training set is a group of compounds from which experimental data to be used in model development will be obtained. The training set should cover the whole range of compounds whose activities/properties are to be modeled [*Hall et al.,* 2002]. The training set could be a homologous, homogeneous, or heterogeneous data set [*Hall et al.,* 2002]. A homologous data set represents compounds that are the same in chemical type but different in sizes; a homogeneous data set is a group of compounds that are significantly related to one another or that share

a major common core. A group of compounds that do not have any similarity in structures or compounds of multiple chemical types is known as a heterogeneous data set. In general, a training set should include compounds in which their structures are similar to the compounds whose activities are of interest.

The second step in QSAR development is to obtain experimental data. The accuracy and precision in measuring the activity is a basic requirement in QSAR because the quality of a model depends on the quality of the data set from which it is derived. All the activity of the chemicals in a training set should be obtained by the same experimental procedure [*Hall et al.,* 2002]. Thereby, the variations due to different experimental techniques can be avoided and the quality of the data set is improved. In addition, activity should be quantified in molar terms [*Kier and Hall,* 1986*; Hall et al.,* 2002], so that compounds of different molecular weight can be compared on the same scale.

The third step required in the QSAR analysis is to specify and calculate the appropriate molecular descriptors. Many descriptors have been defined for use in different types of QSAR. In general, molecular descriptors can be organized as the following [*Katritzky,* University of Florida, Gainesville, FL, 2002]:

1. Constitutional descriptors, e.g., molecular weight, numbers of atoms, bonds.

2. Topological descriptors, e.g., Kier and Hall indices or molecular connectivity indices, Wiener indices.

3. Geometric descriptors, e.g., principal moments of inertia, molecular volume.

4. Electrostatic descriptors, e.g., partial charges, polarity indices

5. Quantum-chemical descriptors, e.g., dipole moment, thermodynamic properties.

Appropriate descriptors can be selected from previous knowledge of interaction processes or by statistical technique, *i.e.*, by choosing descriptors that are highly correlated to the experimental parameters of interest. Regardless of the selection method, a set of descriptors included in a model should have its own physical meanings [*Sabljić,* 2001].

Molecular connectivity indices (MCIs), topological descriptors, are the most often used descriptors in soil sorption coefficient QSARs [*Sabljić,* 2001]. Molecular connectivity indices were developed by L. B. Kier and L. H. Hall, using the principle of the Randić branching index [*Kier and Hall,* 1986*; Randic,* 1992*; Hall and Kier*, 2001]. The indices quantify the structure of a molecule by coding the electrons present in a whole molecule [*Kier and Hall,* 1999] and carry rich structural information including intermolecular accessibility [*Kier and Hall,* 2000]. The simple MCIs are based on the number of sigma electrons in non-hydrogen atoms and the valence MICs are calculated from the number of total valence electrons in non-hydrogen atoms [*Kier and Hall,* 1986*; Hall and Kier*, 2001]. The MCIs of different orders can be obtained based on how a molecular structure is dissected. For instance, the first order MCIs can be obtained if a molecular structure is dissected by each bond that connects two adjacent atoms. The second order MCIs can be obtained if a molecular structure is dissected by two consecutive bonds that connect three adjacent atoms. Depending on the degree

of skeletal branching of a structure, different types of indices such as path, cluster, or chain MCIs can be obtained in both simple and valence MCIs, e.g., simple path MCIs, valence path MCIs [*Kier and Hall,* 1986]. The following formulae [*Kier and Hall,* 1986] describe the calculation of MCIs of different orders.

Simple molecular connectivity index

1. The zero-order simple MCI ($^0\chi$):

$$^0\chi = \sum(\delta)^{-0.5} \tag{4.3}$$

where δ = count of sigma electrons in all non-hydrogen atoms.

2. The first-order simple MCI ($^1\chi$):

$$^1\chi = \sum(\delta_i\delta_j)^{-0.5} \tag{4.4}$$

where δ_i, δ_j = count of sigma electrons in adjacent non-hydrogen atoms i, j.

3. The second-order simple MCI ($^2\chi$):

$$^2\chi = \sum(\delta_i\delta_j\delta_k)^{-0.5} \tag{4.5}$$

where $\delta_i, \delta_j, \delta_k$ = count of sigma electrons in adjacent non-hydrogen atoms i, j, k.

4. The third-order simple MCI ($^3\chi$):

$$^3\chi = \sum(\delta_i\delta_j\delta_k\delta_l)^{-0.5} \tag{4.6}$$

where $\delta_i\delta_j\delta_k\delta_l$ = count of sigma electrons of adjacent non-hydrogen atoms i, j, k, l.

Valence molecular connectivity index

1. The zero-order valence MCI ($^0\chi^v$):

$$^0\chi^v = \sum(\delta^v)^{-0.5} \tag{4.7}$$

where:

$\delta^v = (z^v) - (h)$

z^v = count of all valence electrons in each non-hydrogen atom

h = count of hydrogen atoms

2. The first-order valence MCI ($^1\chi^v$):

$$^1\chi^v = \sum(\delta_i^v \delta_j^v)^{-0.5} \tag{4.8}$$

where $\delta_i^v \delta_j^v$ = count of all valence electrons in adjacent non-hydrogen atoms i, j.

3. The second-order valence MCI ($^2\chi^v$):

$$^2\chi^v = \sum(\delta_i^v \delta_j^v \delta_k^v)^{-0.5} \tag{4.9}$$

where $\delta_i^v \delta_j^v \delta_k^v$ = count of all valence electrons in adjacent non-hydrogen atoms i, j, k.

4. The third-order valence MCI ($^3\chi^v$):

$$^3\chi^v = \sum(\delta_i^v \delta_j^v \delta_k^v \delta_l^v)^{-0.5} \tag{4.10}$$

where $\delta_i^v \delta_j^v \delta_k^v \delta_l^v$ = count of all valence electrons in adjacent non-hydrogen atoms i, j, k, l.

Higher order MCIs, i.e, $4^{th}, 5^{th}, \cdots, n^{th}$, can be calculated using the analogy of the first, second, and third order MCIs. Usually, MCIs are highly correlated to one another [*Hall et al.,* 2002], and totally uncorrelated independent variables are uncommon in QSAR studies [*Kier and Hall,* 1986]. Correlation matrices should be checked to see if a variable is highly correlated to others and those highly inter-correlated variables should not be included in modeling.

The maximum number of independent variables to be included in a model depends on the number of experimental observations. To achieve a sufficient degree of freedom, one should consider one variable per five experimental observations [*Nendza,* 1998]. Generally, the ratios of experimental observations to variables (descriptors) should be 5 to 10 [*Kier and Hall,* 1986]. One should not overfit a model just to gain a large r^2 because it would include experimental errors in the regression [*Sabljić,* 1989b]. Other statistical parameters, i.e., correlation coefficients (r), standard errors of estimation (s), F values, covariances, and residuals should be checked for the quality of statistics [*Sabljić,* 1989b]. However, good regression statistics might be obtained by chance, and thus the probability of chance correlation should also be tested, i.e. by performing randomization tests [*Hall et al.,* 2002].

A QSAR model must be tested for its stability in predicting the activity of other compounds that are not in the training set. *Hall et al.* [2002] explained that validation of a model can be done in two ways: internal or cross validation and external validation. The cross validation technique is also known as leave-one-out (LOO) be-

cause the procedure omits one of the observations from the original data set and then regenerates a new regression. External validation requires activity data that have not been included in building the model. The activities of the new set of compounds are estimated using the model, and the predicted are compared with the measured values to indicate predictive power the model. The external validation method is more rigorous than the LOO but is not applicable for small data sets. The multiple correlation coefficients in model validations are usually denoted as Q^2 to differentiate them from correlation coefficients in model establishments (r^2).

A successful model is useful for prediction of activity of similar compounds that have not been tested or synthesized. Analysis of descriptors of the model might provide a structural property that influences the activity. Consequently, model interpretations might lead us to identify the possible mechanism(s) involved in the activity being investigated. However, QSAR are specific to the class of chemicals used in developing the models and are valid only under specified conditions. In addition, QSARs are derived from activity data, which are subject to experimental error. In some cases, experimental data used in establishing a model might not cover the whole activity field of the chemical class. As a result, errors can be introduced into QSARs. Therefore, the correlation stated in a model might not represent the actual condition. Rules and limitations of the approach with regard to the specific purpose of applications should be carefully considered in employing QSAR. ■

4.4 Materials and Methods

4.4.1 QSAR Model Development

The class of triarylmethanes includes a number of dyes that are often used as hydrological tracers [*Flury and Wai,* 2003]. Four members of this class, Brilliant Blue FCF (C.I. Food Blue 2, C.I. 42090), FD&C Green No. 3 (C.I. Food Green 3, C.I. 42053), ORCOacid Blue A 150% (C.I. Acid Blue 7, C.I. 42080), and ORCOacid Fast Green B (C.I. Acid Green 9, C.I. 42100), were selected as a training set for QSAR model development. These dyes share the same molecular template but differ in the number and position of functional groups (Figure 4.2).

Sorption properties of these dyes to a sandy soil were determined with laboratory batch experiments. We followed an experimental protocol similar to the one described in *German-Heins and Flury* [2000]. Briefly, dye solutions with concentrations ranging from 0.0001 to 2.9 mM were equilibrated with a Vantage sand (95.7% sand, 2.5% silt, and 1.8% clay by weight) at 20 to 22°C. Equilibrium dye concentrations in solution were measured spectrophotometrically. The pH of the batch system was maintained at 8.0 to 8.5 using 0.01 M NaOH or HCl, and the background ionic strength was 0.1 M $CaCl_2$.

Comment: The following frames include interactive cartoon clips of the three dimensional structures of the test dyes: (a) C.I. Food Blue 2, (b) C.I. Food Green 3, (c) C.I. Acid Blue 7, and (d)C.I. Acid Green 9. The frames can be activated by using

QuickTime or Windows Media Player.

(a) 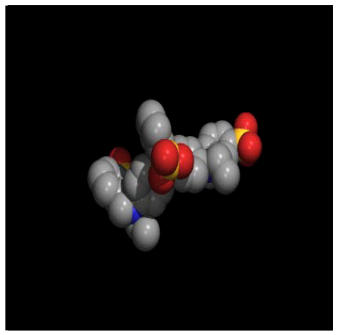 (b) 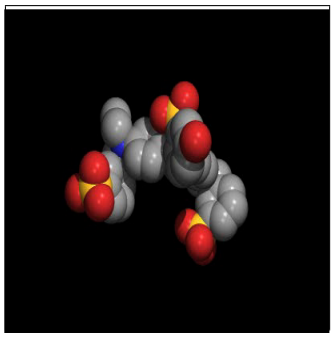

(c) 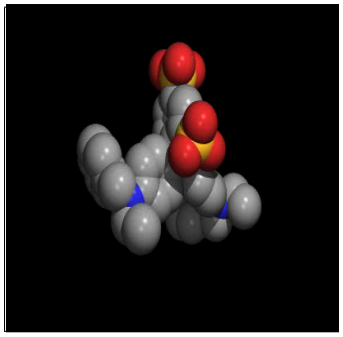 (d) 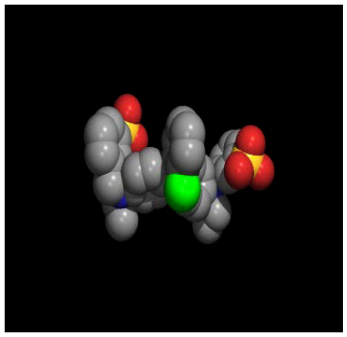

In black and white printout, the atoms in light gray color are the oxygen of SO_3 groups and dark colors are the carbon. Sulfur and nigtrogen atoms in the molecules are covered among oxygen and carbon atoms.

In activated fames, dark spheres are carbon atoms, reds are oxygen, sulfur atoms are in orange and nitrogen atoms are in purple.

■

The experimental data were analyzed with the Langmuir sorption isotherm [*Lang-*

muir, 1918*; Schulthess and Dey,* 1996]:

$$C_a = \frac{A_m K_L C_s}{1 + K_L C_s} \tag{4.11}$$

where C_a is the sorbed dye concentration, A_m is maximum adsorption capacity of the medium, K_L is the Langmuir coefficient, and C_s is aqueous dye concentration at equilibrium. We used the normal nonlinear least squares regression method as described in *Schulthess and Dey* [1996] to estimate the sorption parameters K_L and A_m. This method considers that not only dependent variables but also independent variables are subjected to errors. We chose the two sorption parameters, K_L and A_m, as experimental data (activity) for the QSAR development.

Structural properties (molecular descriptors) to develop the QSAR model were calculated using MDL QSAR (version 2.1, 2002, MDL Information System Inc., San Leandro, CA). MDL QSAR provides nearly 200 molecular descriptors including simple and valence MCIs up to the tenth order. The molecular structure data files were created using the ISIS/Draw program (version 2.4, 2001, MDL Information System Inc., San Leandro, CA). Default bond length, bond angle, and functional groups provided in the program template were used in creating the structure graphs. The training set contained zwitterions—molecules in which both positive and negative charges are present. As MDL QSAR does not recognize that structural type, a positive charge and a negative charge were manually assigned to the respective atoms in each molecule. This charge contributes to the electronegativity of the molecules.

The most appropriate descriptors to be included in the QSAR model were chosen

by statistical considerations. Stepwise linear regression analyses were applied to determine which descriptors were well correlated to the experimental parameters [*Hall et al.,* 2002]. Cross validation was used for validation of the model, and randomization tests were performed to check the probability that the descriptors included in a model were selected by chance [*Hall et al.,* 2002]. The MDL QSAR program carried out 100 randomizations of the activity values for each compound and then calculated multiple r^2 and the mean r^2 for all regressions. Only the model that achieved the best quality of statistics was selected for estimation of each sorption parameter. Thus, two QSAR models were established, one for estimation of the Langmuir coefficient and another for estimation of the maximum adsorption.

4.4.2 Molecular Structures of Potential Dye Tracers

Our premise was that SO_3 groups are the key components in designing an optimal water tracer. By attaching different numbers of SO_3 groups at different positions on the molecular template of the triarylmethane dyes used in the training set, we obtained many hypothetical molecules. Specifically, one or two SO_3 groups were attached to the benzene rings and the SO_3 group(s) attached on each ring were moved one position at a time. We followed the rule for the substitution of meta-directing deactivators in attaching the SO_3 on each benzene ring [*McMurry,* 1996]. Different molecules were identified by the position of the SO_3 groups. These positions were numbered as shown in Figure 4.3. Each SO_3 group was identified by the number of the benzene ring and by

the position (number in parenthesis) where the group is attached to that benzene ring. For example, a molecule is named as 1(2) if the SO_3 group is attached to ring number 1 and position number 2 on that ring. Similarly, a molecule named 1(2)2(3) indicates that two SO_3 groups are attached to the molecule; one group is at ring number 1 and position number 2, and another is attached at ring 2 and position 3. If two SO_3 groups are attached to the same benzene ring, the notation is abbreviated, e.g., the molecule named 1(24) contains two SO_3 groups at ring number 1 at positions 2 and 4.

We systematically varied number and positions of SO_3 groups. Four different sets of molecules were generated. The first set contained six molecules with different numbers of SO_3 groups: 1, 2, 3, ... , 6 SO_3 groups on each molecule, respectively. The second set of molecules contained only one SO_3 group attached to the molecular template at six different positions. First, the SO_3 group was attached on benzene ring number 1 at position 2, and then the SO_3 group was moved to position 3, and position 4 in clockwise directions (Figure 4.3). In doing so, three different molecules, 1(2), 1(3), and 1(4), were created. The same procedure was repeated for benzene ring 3, and thus another three molecules, 3(2), 3(3), 3(4), were obtained (Figrue 4.5). Functional groups were not attached at the positions where atom overlap was indicated by the ISIS/Draw program. The same rules were applied in creating the third and the fourth set of molecules. The third set contained two SO_3 groups attached to the template in all 22 possible combinations (Figure 4.6). The fourth set included molecules with three SO_3 groups attached to the molecular templates. A maximum of two SO_3 groups

were attached to a benzene ring in meta-positions. By attaching three SO_3 groups in all the possible combinations, 31 molecules were obtained (Figure 4.7).

4.5 Results and Discussion

4.5.1 Experimental Data and Molecular Descriptors

The adsorption of the selected dyes could be well described by a Langmuir isotherm (Figure 4.8). The sorption parameters estimated by the normal nonlinear least squares are shown in Table 4.1. Selected structural descriptors of the four dyes, calculated with MDL QSAR, are listed in Table 4.2. We only list the zeroth- to the tenth-order MCIs, because these MCIs are some of the most important descriptors for modeling soil sorption coefficients and are relevant to this study.

4.5.2 QSAR Models

The regression analysis produced a number of QSAR models based on the input data and molecular descriptors. However, the results of the stepwise regression suggested that K_L and A_m parameters of the four tested dyes were best correlated to the ninth-order simple path MCI ($^9\chi_p$) and the ninth-order valence path MCI ($^9\chi_p^v$), respectively. These two molecular descriptors yielded the best statistical indicators, such as correlation coefficient (r^2), standard error of estimation (s), F-statistic (F), level of significance (P), predictive correlation coefficient (Q^2), residual sum of squared error

in validation (RSS), and mean correlation coefficients in randomization tests (r_k^2).

The optimal model obtained for the Langmuir coeffcient was:

$$K_L = -54.47\,({}^9\chi_p) + 183.75 \tag{4.12}$$

where K_L is given in L/mmol, ${}^9\chi_p$ is the ninth-order simple path MCI, and the statistical parameters are $r^2 = 0.999, s = 0.114, F = 7384, P = 0.0001, Q^2 = 0.998, RSS = 0.105, r_k^2 = 0.311$. For the maximum adsorption, the optimal model was:

$$A_m = -45.72\,({}^9\chi_p^v) + 35.88 \tag{4.13}$$

where A_m is given in mmol/kg, ${}^9\chi_p^v$ is the ninth-order valence path MCI, and the statistical parameters are $r^2 = 0.996, s = 0.125, F = 779, P = 0.001, Q^2 = 0.991, RSS = 0.114, r_k^2 = 0.357$.

The QSAR models showed excellent agreement between estimated and experimentally measured sorption parameters for the four test dyes. The estimated and the experimental values closely followed a 1:1 line (Figure 4.9). The Q^2 values resulting from the cross-validations were similar to the r^2, which suggests that the models are relatively stable [*Sabljić,* 2001*; Hall et al.,* 2002]. The Q^2 is usually considered as the estimate predictability of the models [*Sabljić,* 2001]. The mean r_k^2 from the randomization tests were relatively small, so that the probability of having a chance correlation between dependent and independent variables is small [*Hall et al.,* 2002]. The models were derived from a small set of compounds but they are specific to a chemical group. Such specific models tend to have a high predictive power in the specific chemical domain [*Sabljić et al.,* 1995].

Soil sorption QSAR reported in the literature were mostly constructed with lower-order MCIs [*Sabljić,* 1989a*; Sekusak and Sabjlić,* 1992*; Sabljić et al.,* 1995*; Hong et al.,* 1997]. Most of those reported models were based on relatively small, non-polar organic molecules. The sixth-order chain MCIs ($^6\chi_{ch}$) were included in a QSAR that described the log K_{oc} of some polar and non-polar organic compounds [*Tao and Lu,* 2000]. *Worrall* [2001] suggested the sixth-order valence path MCI ($^6\chi_p^v$) as a discriminator between herbicides that leach and those that do not leach to groundwater. Higher-order (> second-order) MCIs presumably carry more detailed structural information than the lower-order MCIs [*Hall et al.,* 2002].

Our QSAR model suggests that the sorption coefficient K_L is negatively correlated with $^9\chi_p$. Higher-order simple MCIs, such as $^9\chi_p$, contain information about size, branching patterns, and positions of substituents [*Hall et al.,* 2002]; however, the simple MCIs do not account for types of elements or types of bonds included in a molecule. According to these considerations, the QSAR model offers a generic interpretation that K_L values of the training set were dominated by the molecular size, branching pattern, and positions of substituents. Among the molecules with the same number of SO_3 groups, there seems to be a correlation between the molar volume of the molecules and their K_L values (Table 4.1), but among all the molecules there were no relationships between molar volume or surface area and K_L values (Table 4.1). The number of SO_3 groups, which also represents the amount of negative charge present in the molecules seems to have a major influence on the K_L of the dyes tested.

In our QSAR model, the maximum adsorption A_m was negatively correlated with ${}^9\chi_p^v$. Valence MCIs, such as ${}^9\chi_p^v$, account for all valence electrons in σ, π, and lone pair orbitals of non-hydrogen atoms. The π and lone pair electrons are more active or have a higher potential for intermolecular interactions than σ electrons. Hence, A_m values might be more related to the interactions between the molecules and the soil medium surfaces than to the size or the shape of the molecules.

4.5.3 Estimation of the Activity of Potential Dye Tracers

The QSAR models developed were used to estimate the sorption parameters (K_L and A_m) of the hypothetical dyes. We first discuss the effect of the number of SO_3 groups on the sorption parameters and then the effect of position.

The more SO_3 groups attached to the molecule, the smaller were both the K_L and A_m values (Figure 4.10). The figure shows a selection of dyes with a certain position of the SO_3 groups. If the position of the groups is changed, the K_L and A_m values will change as well, but the general trend observed in Figure 4.10 still remains. For both K_L and A_m, the model estimated negative values for some cases. Those negative K_L and A_m suggest negative sorption, i.e., ion exclusion. The estimated parameters should be considered as relative, rather than absolute, measures for comparing the sorption of the chemicals. The trend observed in our study agrees with previous results that showed that dyes containing more SO_3 groups are less sorbed to solid media than dyes containing less SO_3 groups [*Corey,* 1968*; Reife and Freeman,* 1996].

The position of the SO_3 groups affected the predicted sorption parameters. Figure 4.11 shows molecules containing one SO_3 group attached at different positions at the benzene rings. The smallest K_L and A_m were obtained for the molecule that contains the SO_3 group attached at the *ortho* position of the benzene ring 1, namely molecule 1(2). The K_L and A_m values vary not only with the position of the SO_3 group on each ring, but also with the ring to which the SO_3 group is attached. Molecules with the SO_3 group attached to ring 1 appear to have smaller K_L and A_m than those with the SO_3 group attached to ring 3 (Figure 4.11). The relative change of the sorption parameters as function of position of the SO_3 group was less than the change due to the number of SO_3 groups. This suggests, not surprisingly, that the number of SO_3 groups is the more dominant factor in determining the sorption characteristics.

The sorption parameters of the 22 molecules containing two SO_3 groups at different positions are shown in Figure 4.12. The K_L and A_m values of the molecules again showed differences with the position of the SO_3 groups on each ring as well as with their distribution on different rings in the molecules. Attaching the two SO_3 groups on ring 1 produced smaller K_L and A_m values than attaching them on ring 3, e.g., molecules such as 1(24) or 1(35) showed generally smaller K_L and A_m values than 3(24) or 3(35). Among the molecules whose SO_3 groups were distributed on two different rings, those that contain SO_3 groups on ring 1 and ring 3, e.g., 1(2)3(2) showed smaller K_L and A_m values than those with SO_3 groups on ring 2 and ring 3, e.g., 2(3)3(2). Interestingly, the measured K_L and A_m values of Acid Blue 7, denoted as 1(24) were

among the smallest. In general, K_L and A_m values of molecules with two SO_3 groups attached on ring 1 tend to be smaller, while K_L and A_m values of molecules with two SO_3 groups attached on ring 3 tend to be larger.

By attaching three SO_3 groups to the molecular template, 31 possible molecules were created. QSAR modeling showed that the range of K_L and A_m of the molecules that contain two SO_3 groups attached on ring 1 and one SO_3 group attached on 2 or 3 were not significantly different than K_L and A_m of molecules that contain one SO_3 group attached on each ring (Figure 4.13). The molecules that had the smallest K_L and A_m values contained one SO_3 group attached on ring 1 at an arbitrary position and contained the other two SO_3 groups attached at position 4 (para position) of rings 2 and 3 (e.g., molecules 1(2)2(4)3(4) and 1(3)2(4)3(4), Figure 4.13). There seem to be many hypothetical chemicals whose K_L and A_m values are much smaller than that of C.I. Food Blue 2 and C.I. Food Green 3. C.I. Food Green 3 showed somewhat smaller K_L and A_m values than C.I. Food Blue 2.

Comment: One can visualize structural differences among the molecules that contain the same number of SO_3 groups attached at different positions on the molecular template. The differences in shape may be the reason for the variation of K_L and A_m values among the molecules that contain the same number of SO_3 groups (steric effects). The following are examples of molecules that contain the same numbers of SO_3 groups but have different K_L and A_m values. Each molecule contains three SO_3 groups attached at different positions on a common molecular template.

The frames can be activated by using QuickTime or Windows Media Player.

(a) 1(24)3(4) has much smaller K_L and A_m than (b) 1(3)3(35).

(a) 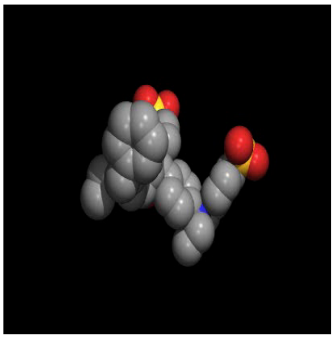

(b) 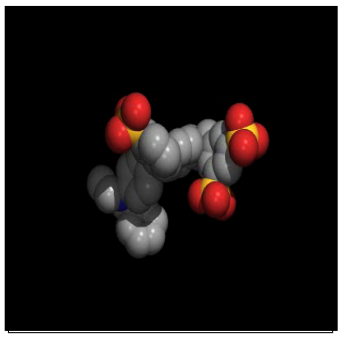

(c) 1(4)2(4)3(4) shows much smaller K_L and A_m than (d) 1(2)2(6)3(2).

(c) 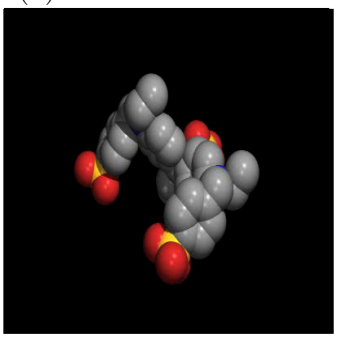

(d) 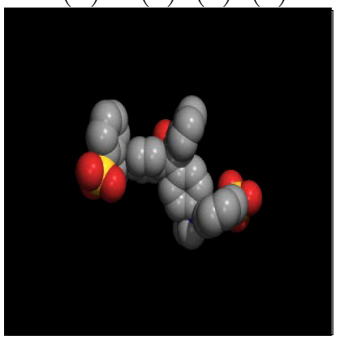

■

In all cases investigated, we observed that the changes in K_L were correlated with the changes in A_m, i.e., molecules having large K_L values tend to have large A_m values (Figures 4.10 to 4.13). When comparing the effect of position of SO_3 groups, the molecules with three SO_3 groups showed the largest variation among their K_L and A_m values. The results indicate that the effect of the position of SO_3 groups on the sorption parameters was more significant when the molecules contained more than one

SO_3 group.

4.5.4 Recommendation for the Design of an Optimal Dye Tracer

We tested the K_L and A_m values of nearly 70 hypothetical triarylmethane compounds using QSAR. Among those 70 compounds, there were many compounds that are possibly better tracers, in terms of their sorption under our test conditions, than the four test dyes. Their K_L and A_m values were considerably smaller than those of Brilliant Blue FCF (C.I. Food Blue 2), which is often used as vadose zone tracer.

The number of the SO_3 groups had a dominant effect on the sorption parameters. The more SO_3 groups attached to the triarylmethane template, the smaller were the sorption parameters. The currently available triarylmethane dyes have a maximum of three SO_3 groups, but hypothetical molecules with more than three SO_3 groups appear to be promising tracer candidates. As more and more SO_3 groups are attached, the molecule becomes larger and the increasing molecular size may lead to increased sorption, counteracting to some degree, the beneficial effect of the addition of SO_3 groups. The hypothetical molecules containing 4, 5, or 6 SO_3 groups, shown in Figure 4.10, are likely promising hydrological tracers.

C.I. Food Green 3, which is a commercially available food dye, sorbed less to Vantage sand than C.I. Food Blue 2. Between these two readily available dyes, Food Green 3 may be a useful alternative tracer for hydrological investigations in the vadose

zone.

4.6 Conclusions

QSAR modeling was used to screen hypothetical dyes for optimal hydrological tracer characteristics. For this study, we considered minimal sorption to soil materials as an optimal tracer characteristic. The QSAR analysis provided relative measures of soil sorption. The results showed that dyes containing more SO_3 groups are less sorbed to soil than dyes containing fewer SO_3 groups. The sorption parameters of the hypothetical compounds vary not only with the position of the SO_3 groups on each benzene ring, but also depend on which benzene rings the SO_3 groups are attached to. Many hypothetical compounds seem to sorb less to soil than the currently known tracer dyes.

4.7 Tables and Figures

Table 4.1: Experimental sorption parameters of the four dyes used as the training set and calculated molecular volumes and surface areas.

Dyes	Number of SO_3 groups	Langmuir coeffcient K_L (L/mmol)	Maximum adsorption A_m (mmol/kg)	Molar volume (Å^3)	Surface area (Å^2)	SO_3 positions
C.I. Acid Blue 7	2	10.06	2.99	415	494	1(24)
C.I. Acid Green 9	2	16.47	4.40	466	546	2(3)3(5)
C.I. Food Blue 2	3	5.29	0.42	490	569	1(2)2(3)3(5)
C.I. Food Green 3	3	3.94	0.30	477	559	1(2)2(3)3(5)

Table 4.2: Molecular connectivity indices (MCIs) for the four test dyes.

MCIs	C.I. Acid Blue 7	C.I. Acid Green 9	C.I. Food Blue 7	C.I. Food Green 3
Simple Path Molecular Connectivity Indices				
${}^{0}\chi$	33.61	34.48	36.98	37.85
${}^{1}\chi$	22.47	22.87	24.08	24.47
${}^{2}\chi$	21.26	21.85	23.85	24.48
${}^{3}\chi_p$	16.56	17.06	17.82	18.16
${}^{4}\chi_p$	13.61	13.83	14.61	14.77
${}^{5}\chi_p$	11.44	11.65	12.25	12.73
χ_p^6	8.03	7.46	8.13	8.31
${}^{7}\chi_p$	5.98	6.01	6.51	6.78
${}^{8}\chi_p$	4.60	4.37	4.52	4.62
${}^{9}\chi_p$	3.19	3.07	3.28	3.30
${}^{10}\chi_p$	2.22	2.09	2.39	2.45
Valence Path Molecular Connectivity Indices				
${}^{0}\chi^v$	27.75	28.80	30.12	30.49
${}^{1}\chi^v$	18.01	18.49	20.03	20.17
${}^{2}\chi^v$	13.76	14.35	15.76	15.94
${}^{3}\chi_p^v$	9.73	10.06	10.91	10.97
${}^{4}\chi_p^v$	6.89	6.94	7.62	7.68
${}^{5}\chi_p^v$	5.17	4.91	5.39	5.48
${}^{6}\chi_p^v$	3.16	2.78	3.16	3.19
${}^{7}\chi_p^v$	1.95	1.91	2.12	2.15
${}^{8}\chi_p^v$	1.24	1.16	1.25	1.25
${}^{9}\chi_p^v$	0.72	0.69	0.78	0.78
${}^{10}\chi_p^v$	0.44	0.40	0.49	0.49

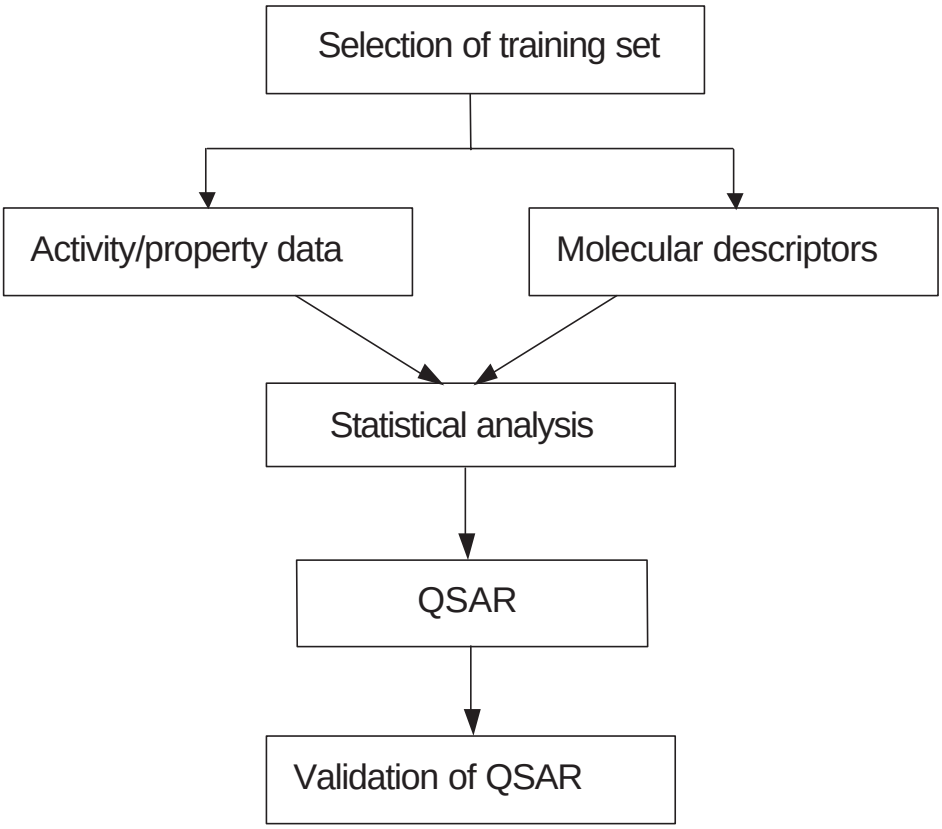

Figure 4.1: Major steps required in development of Quantitative Structure-Activity Relationships. Figure adapted from Nendza (1998).

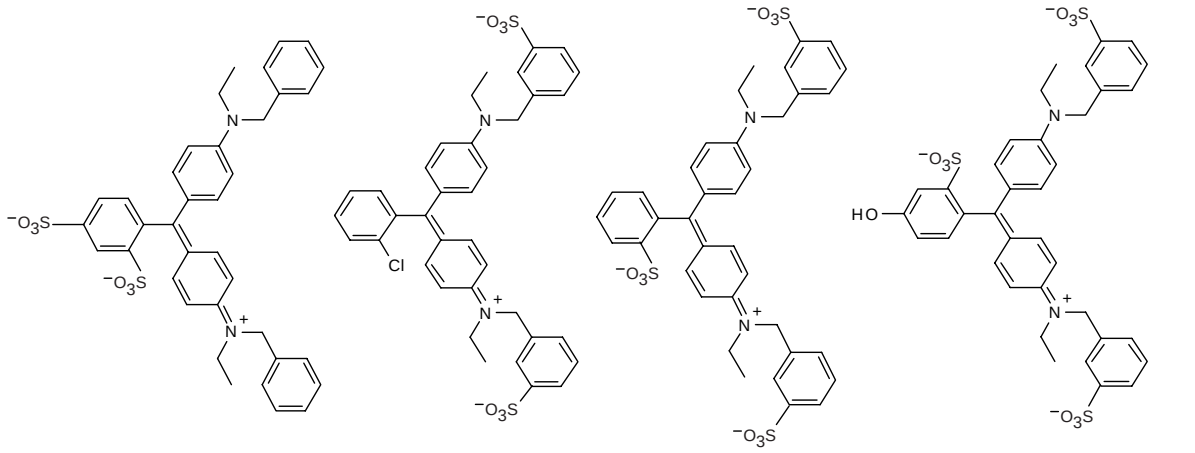

Figure 4.2: Molecular structures of the four triarylmethane dyes used as the training set.

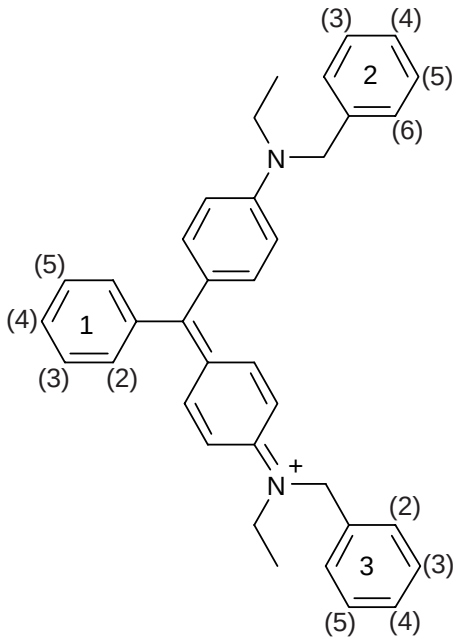

Figure 4.3: Common molecular template shared by the training set and by all hypothetical molecules. Numbers identify the benzene rings and the positions (in parentheses) on each ring. These numbers are used in identifying the molecules with respect to specific positions of their functional groups.

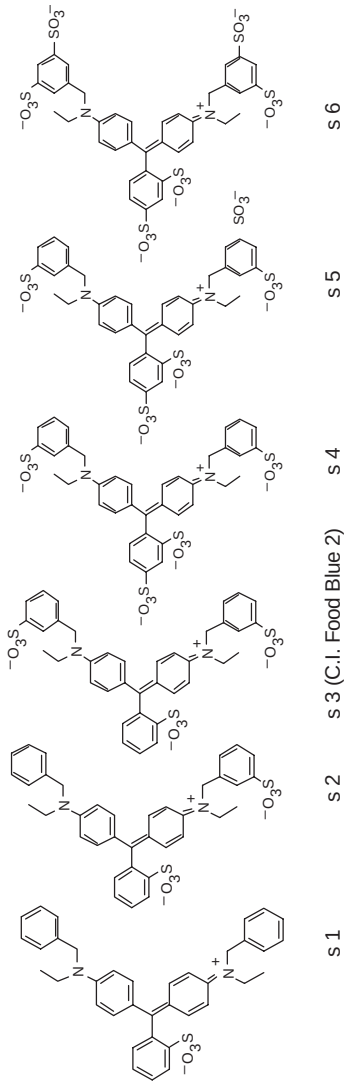

Figure 4.4: Six molecules with different numbers of sulfonic acid groups. Molecules s 1, s 2, s 4, s 5, and s 6 are hypothetical chemicals. Sorption parameters of these chemicals were predicted and compared with that of s 3 (C.I. Food Blue 2) to examine the effect of the number of sulfonic acid groups on sorption of the chemicals.

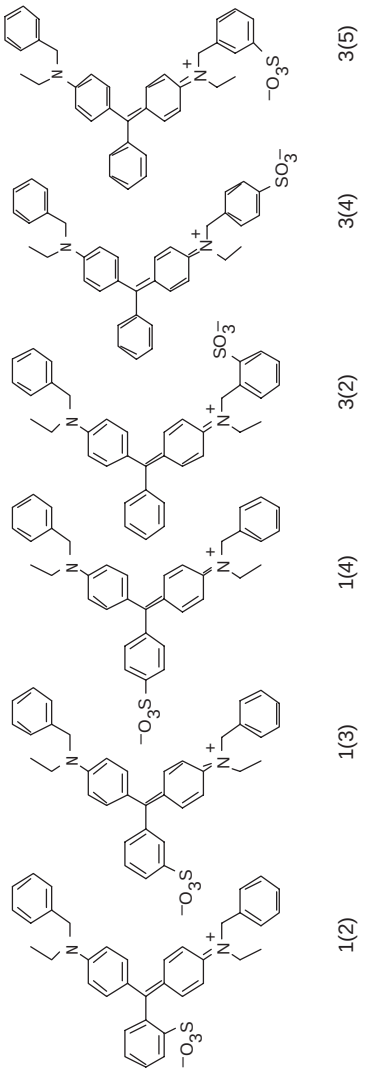

Figure 4.5: Hypothetical molecules containing one sulfonic acid group attached at different positions. The numbers outside the parentheses are designated to benzene rings and the numbers in the parentheses indicate the positions of sulfonic acid groups on each ring, e.g., if a molecule contained one SO_3 group attached to benzene ring 1 at position 2, the molecule is identified as 1(2). (Note: Methods of numbering the rings and the positions are described in Figure 4.3).

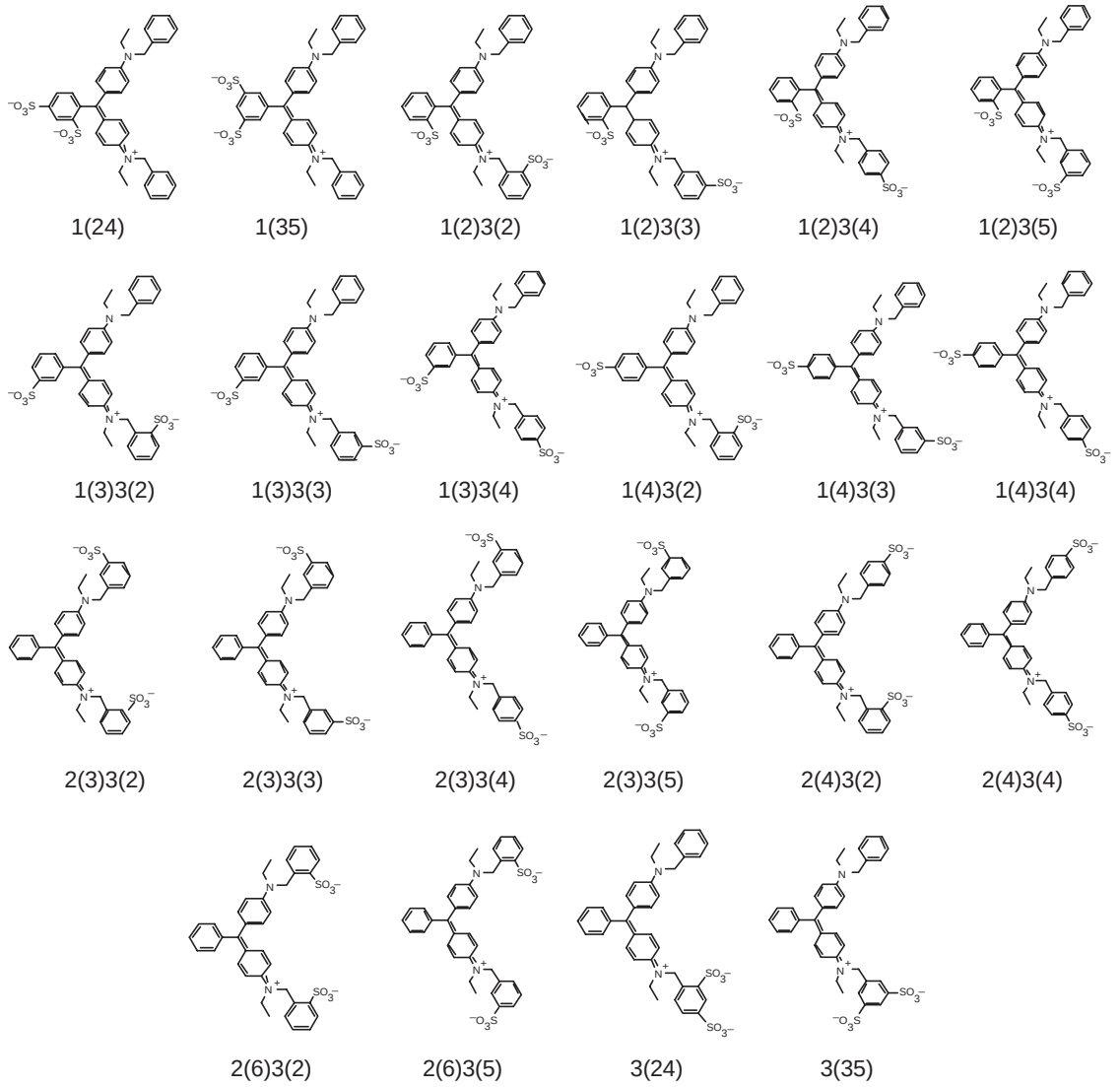

Figure 4.6: Hypothetical molecules containing two sulfonic acid groups. (Note: Methods of numbering the rings and the positions are described in Figure 4.3).

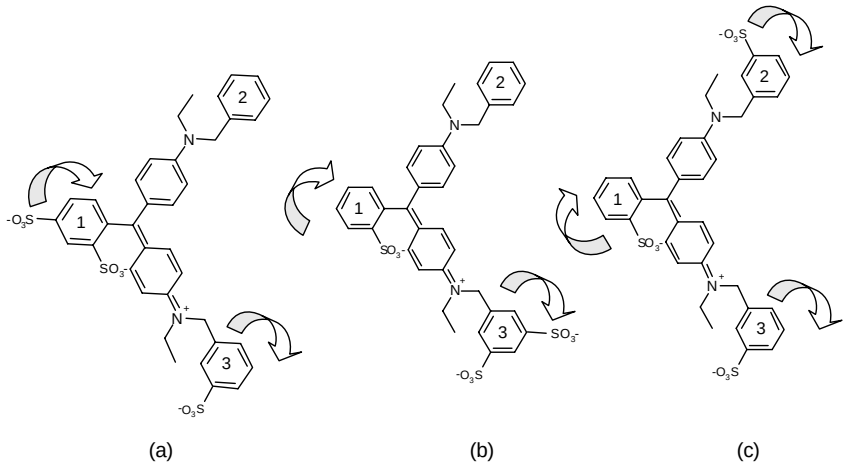

Figure 4.7: Molecules with three SO_3 groups: (a) two SO_3 groups on ring 1 and one SO_3 group on ring 3, (b) one SO_3 group on ring 1 and two SO_3 groups on ring 3, (c) one SO_3 group on rings 1, 2, and 3, each. A total of 31 possible different molecules were obtained by moving each sulfonic acid group one position at a time in clockwise direction as indicated by arrows.

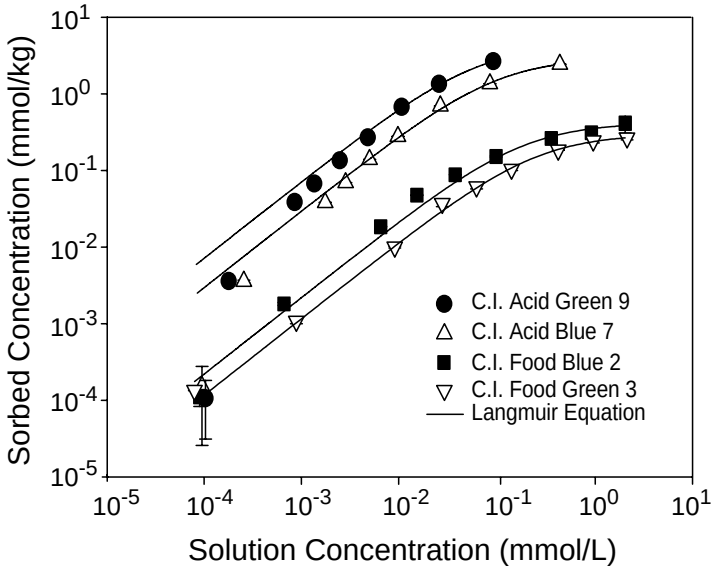

Figure 4.8: Adsorption isotherms of the four test dyes. Symbols are experimental data and lines are fitted Langmuir isotherms. Error bars denote one standard deviation of three replicates. In many cases the error bars are smaller than the symbols.

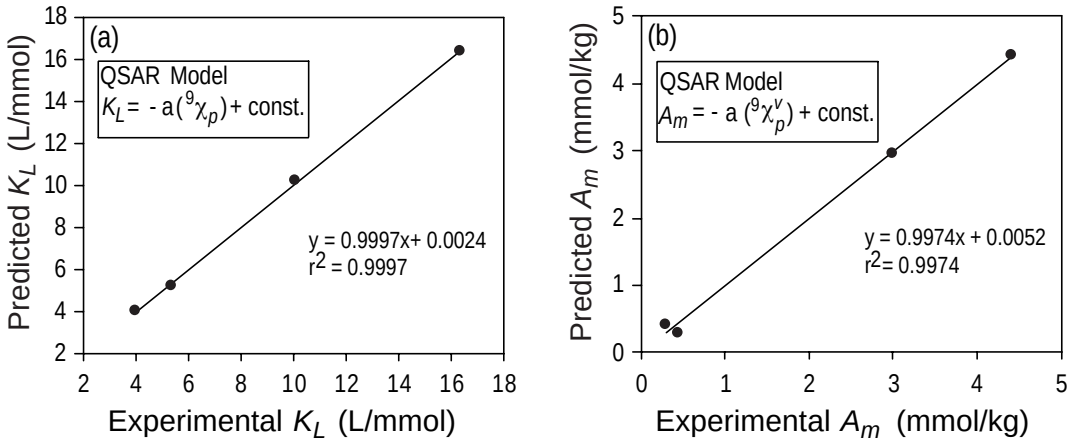

Figure 4.9: Experimental and model predicted (a) Langmuir coefficient, K_L, and (b) adsorption maximum, A_m, of the four dyes used as the training set in the model development.

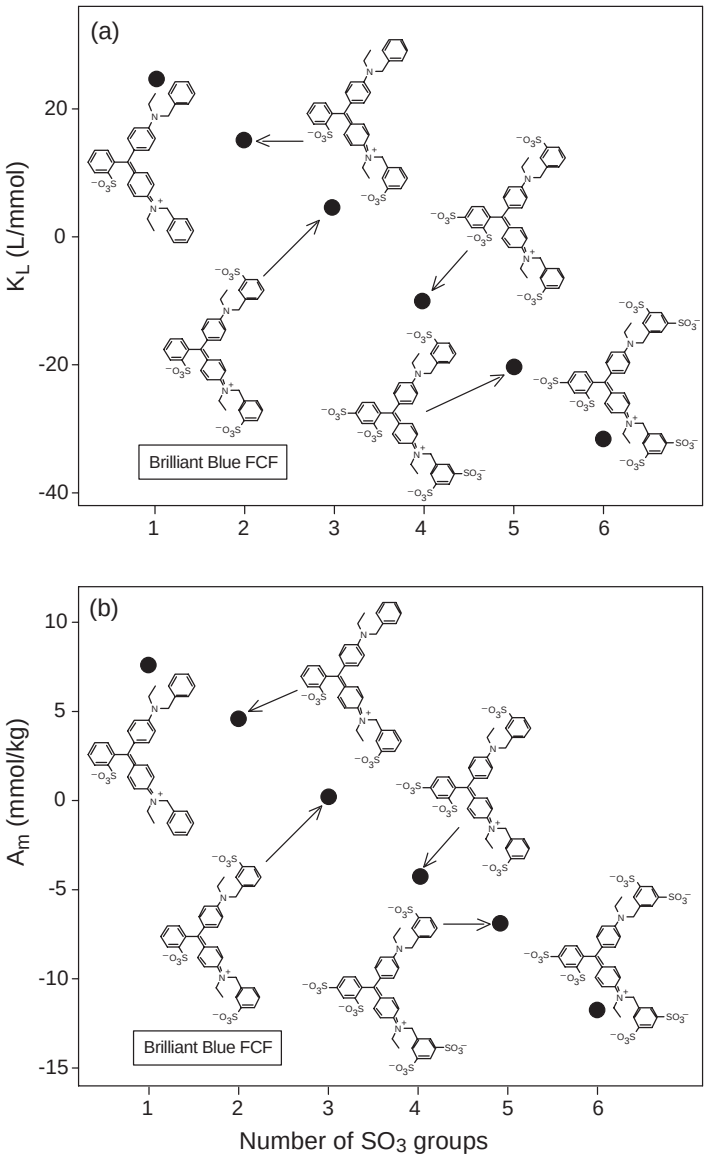

Figure 4.10: Effect of the number of SO_3 groups on (a) Langmuir coefficient, K_L, and (b) adsorption maximum, A_m, of triarylmethane dyes.

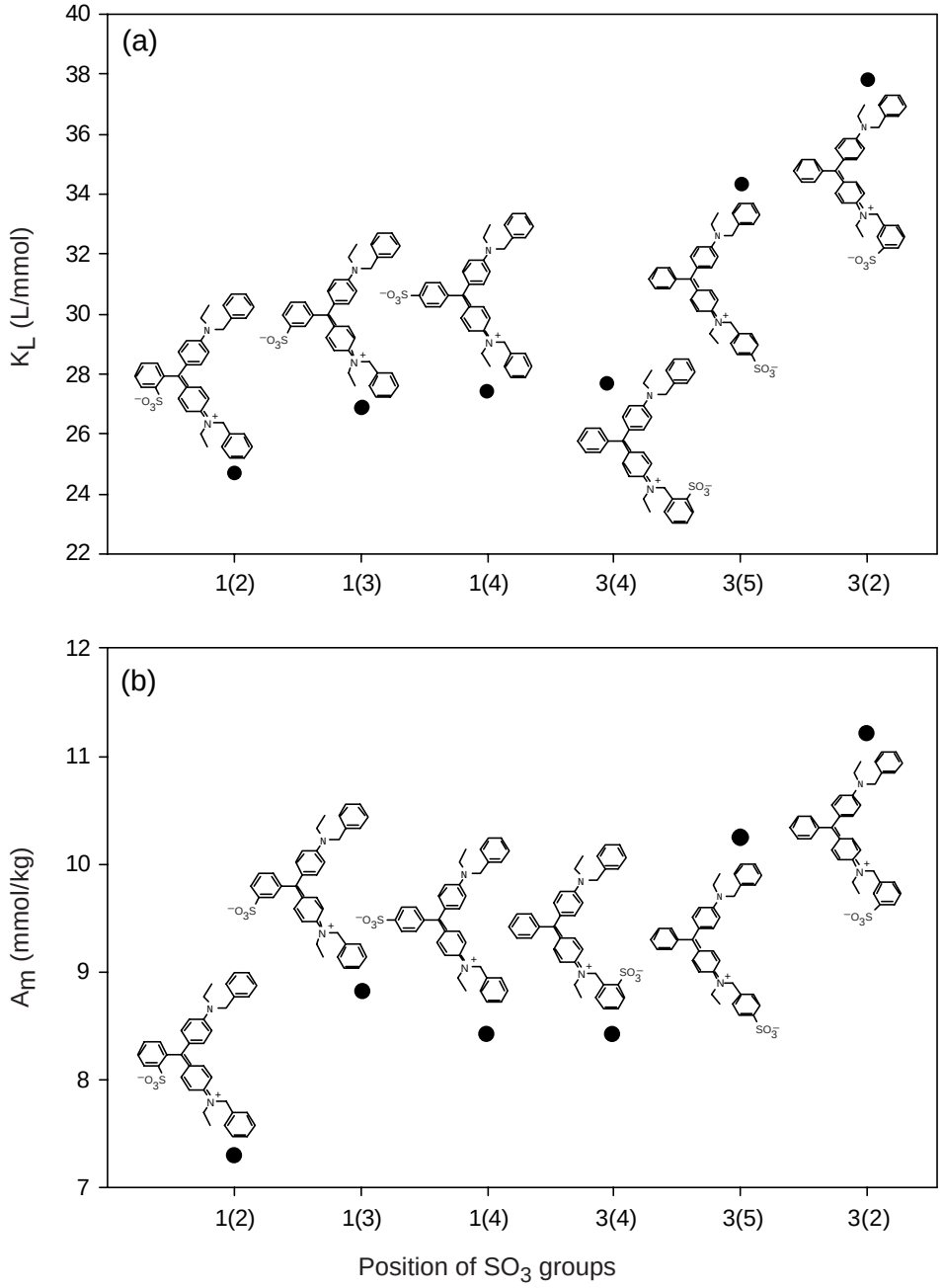

Figure 4.11: Effect of the position of one SO_3 group on (a) Langmuir coefficient, K_L, and (b) adsorption maximum, A_m, of hypothetical triarylmethane dyes.

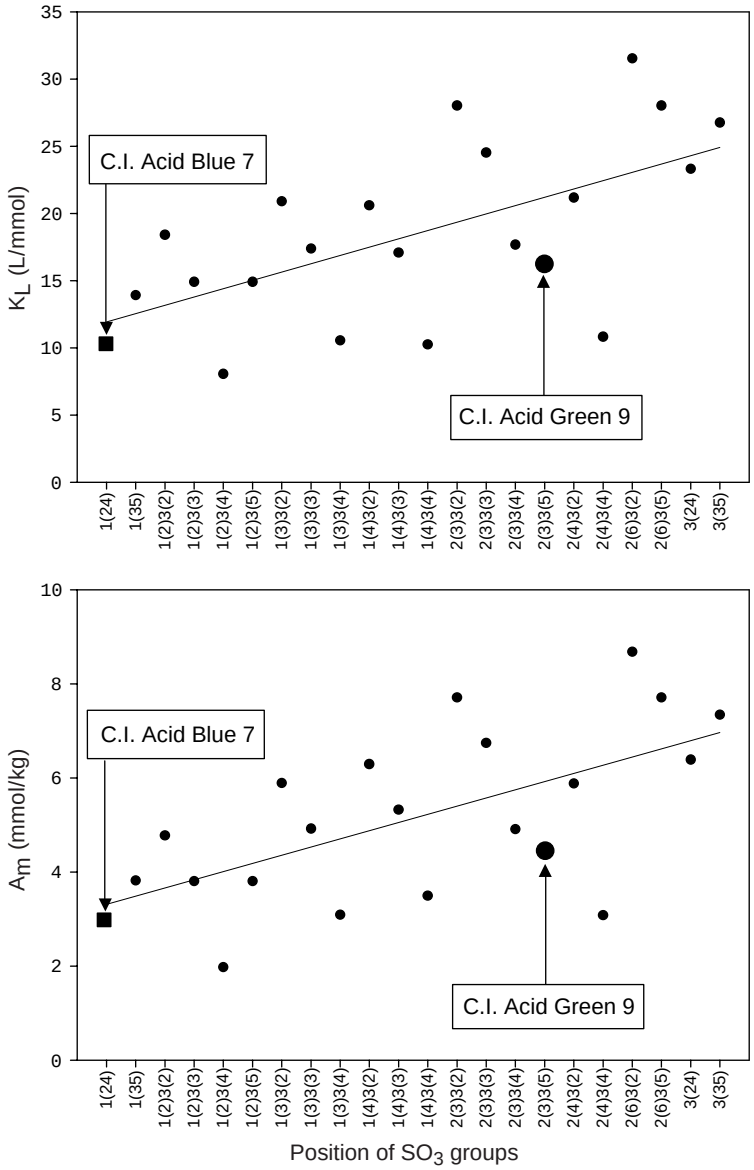

Figure 4.12: Effect of the position of two SO_3 groups on (a) Langmuir coefficient, K_L, and (b) adsorption maximum, A_m, of triarylmethane dyes. The line is a linear regression to indicate the general trend.

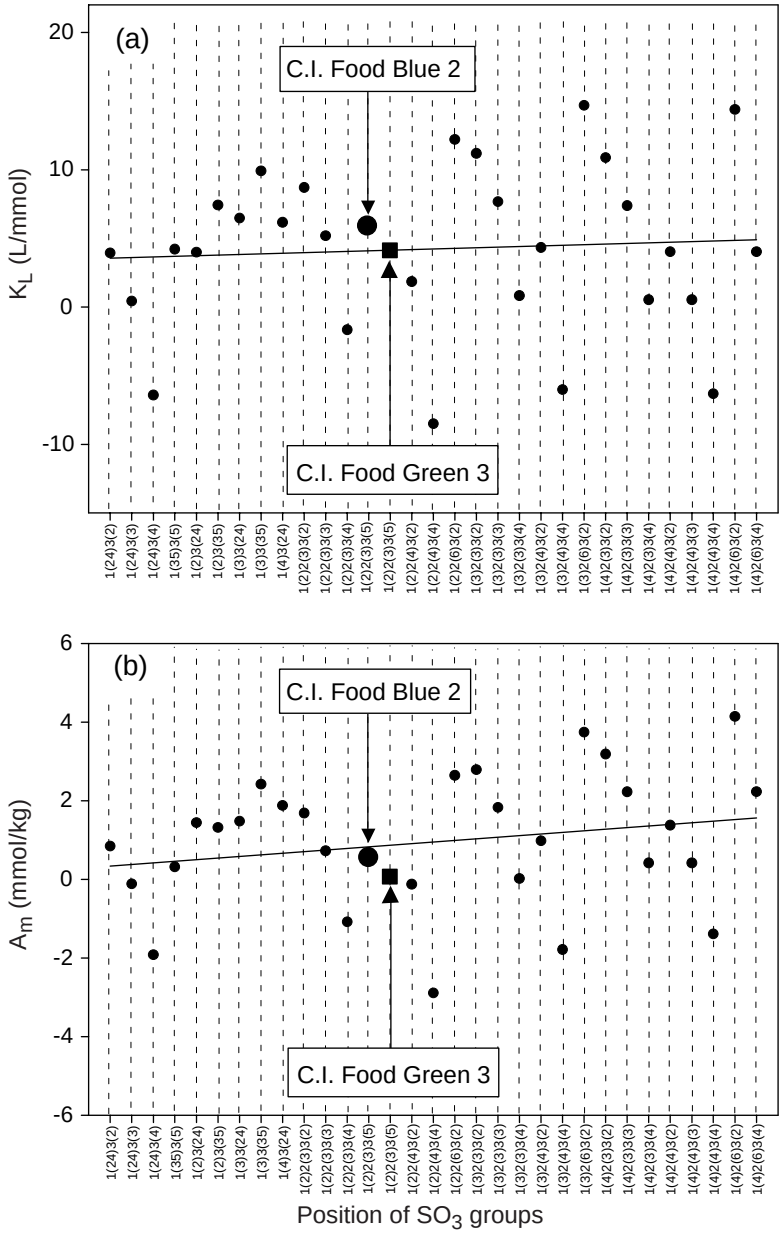

Figure 4.13: Effect of the position of three SO_3 groups on (a) Langmuir coefficient, K_L, and (b) adsorption maximum, A_m, of triarylmethane dyes. The line is a linear regression to indicate the general trend.

Chapter 5

Cesium Incorporation and Desorption in Feldspathoids, Zeolite, and Allophane Formed in Hanford Tank Waste Simulants

5.1 Abstract

At the US Department of Energy's Hanford site, more than one million gallons of high level nuclear waste has leaked from underground storage tanks. The waste consisted of hyperalkaline solutions, which upon contact with the sediments, caused dissolution of silicate minerals and precipitation of secondary aluminosilicate minerals. Cesium, present in the waste solutions, may be incorporated into the structural framework of the precipitates. The objectives of this study were to determine how much Cs is incorporated into the secondary phases, and how much Cs is subsequently released by desorption. A tank leak was mimicked using pure solutions containing Si, Al, Na, Cs, OH, and NO_3. Secondary minerals, identified as feldspathoids (cancrinite, sodalite), zeolite, and allophane, precipitated from these solutions. The minerals were washed

with deionized water, and two sets of ion exchange experiments were conducted. In the first set, Cs was exchanged by Na, K, or Ca using 0.5 M electrolyte solutions for each cation respectively. After 72 hours, the Cs remaining in the minerals was quantified by acid digestion. In the second set, we studied the Cs-Na ion exchange kinetics by using 0.1 M $NaNO_3$ solutions. Cesium concentration in the solution phase was measured as a function of time for a total of 23 days. In zeolite and allophane, most of the incorporated Cs (94–99%) was readily exchangeable with Na or K, whereas Ca was less effective in replacing Cs: only 65–85% of the Cs could be replaced. In cancrinite and sodalite, a large fraction of the incorporated Cs was not easily exchangeable with Na, K, or Ca: only 1–57% of the Cs could be exchanged. The results of the desorption kinetics experiments showed that Cs desorbs quickly from zeolite. Cesium desorption from cancinite, sodalite, and allophane, however, was slow, suggesting that Cs was trapped in cages and channels of these minerals.

Key words: Cesium, ion exchange, desorption, feldspathoids, zeolite, allophane, intra-particle diffusion

5.2 Introduction

At the Hanford site, a former plutonium production complex located in southeastern Washington State, USA, millions of gallons of high-level nuclear waste (HLW) solutions have leaked into the vadose zone. The waste solution are highly alkaline (pH $\approx$ 14), have high ionic strength, high aluminate content, and contain radioactive cesium

(^{137}Cs) in concentrations up to 2×10^{10} Bq/L (0.5 Ci/L = 0.04 mmol/L) [*Serne et al.,* 1998*; McKinley et al.,* 2001]. When the alkaline waste contacts subsurface sediments, minerals such as quartz and phyllosilicates are dissolved and new, secondary minerals precipitate [*Bickmore et al.,* 2001*; Chorover et al.,* 2003*; Liu et al.,* 2003b*; Qafoku et al.,* 2003]. These secondary minerals have been identified as feldspathoids (cancrinite and sodalite), LTA zeolite, and possibly allophane [*Bickmore et al.,* 2001*; Qafoku et al.,* 2003*; Mashal et al.,* 2004*; Zhao et al.,* 2004]. The precipitation of secondary alluminosilicate minerals may affect the mobility of ^{137}Cs in the vadose zone because these minerals are known to have high specific area and cation ion exchange capacity [*Qafoku et al.,* 2003].

Cancrinite, sodalite, and zeolite are porous alluminosilicates that contain cages and channels in their structure frameworks, and the cages and channels contain cations that balance the charge to stablize the mineral structure. Cancrinite contains small ε-cages, which are six-membered rings, and wide channels, consisting of 12-membered rings (Figure 5.1). The wide channels in cancrinite can host both cations and anions, but the ε-cages can only accommodate cations and/or water molecules [*Buhl et al.,* 2000]. Sodalite contains only β-cages, which are made up of six-membered rings, and the shape of β-cages is a truncated octahedron that is often called the sodalite cage [*Bernasconi et al.,* 1999]. The β-cages of natural sodalite contain four sodium ions tetrahedrally associated with a chloride ion at the center of the cages and the sodium ions can be readily exchanged with cations such as Ag and Cu [*Bernasconi et al.,* 1999].

The LTA zeolite structure contains two types of cages, α- and β-cages (Figure 5.1), which can host different cations [*Lee et al.,* 1994].

During precipitation of the secondary minerals, Cs present in the waste solutions, may not only sorb to mineral surfaces but also be incorporated into the mineral structure. *Chorover et al.* [2003] suggested that Cs substitutes for Na and serves as charge-balancing ion during the formation of feldspathoids and zeolite in simulated waste solutions. Cesium and Li can be incorporated into the cages and channels of cancrinite [*Fechtelkord et al.,* 2001] and nitrate has been incorporated in sodalite cages [*Buhl and Löns,* 1996]. If Cs is incorporated into the mineral framework, Cs may not desorb or may desorb only very slowly from the minerals. If the secondary minerals are large and immobile, this may favor Cs immobilization; however, if the minerals are small and mobile, it may lead to enhanced migration of Cs in the subsurface.

In this study, we hypothesized that a fraction of the Cs present in the solutions of Hanford tank waste is incorporated into and sorbed to the secondary feldspathoids, zeolite, and allophane. Upon contact with uncontaminated sediments or pure water, we further hypothesize that the incorporated and sorbed Cs will desorb and diffuse out of the porous mineral structures. Our objectives were (1) to quantify the amount of Cs incorporated into feldspathoids, zeolite, and allophane, (2) to determine the desorption kinetics of Cs from the minerals, and (3) to estimate the effective diffusion coefficients of Cs inside the porous mineral structures.

5.3 Materials and Methods

5.3.1 Mineral Synthesis and Cs Incorporation

We synthesized four minerals in the presence of Cs—Cs-Cancrinite, Cs-sodalite, Cs-LTA zeolite, and Cs-allophane—by mixing 0.175 M Na_2SiO_3, 0.5 M $NaAlO_2$, and 0.05 M $CsNO_3$ or CsOH with different concentrations of NaOH (1, 4, or 8 M). The molar Na to Cs ratios for the different minerals was 277 for cancrinite, 97 for sodalite, 1.9 for LTA zeolite and 2.4 for allophane. Cesium-Cancrinite, Cs-sodalite, and Cs-LTA zeolite were synthesized at 80°C and Cs-allophane at room temperature. The precipitates were washed free of salts and residual Cs using deionized water and centrifugation.

Mineral phases were characterized by X-ray diffraction and electron microscopy. We denote these washed minerals as "water-washed". To quantify the amount of Cs associated with the water-washed minerals, 25 mg of air-dry minerals was digested in 1 M HCl and Cs concentrations were determined with atomic emission spectrometry (AES) (SpectrAA 220, Varian Co., Victoria, Australia). All minerals readily dissolved in 1 M HCl.

5.3.2 Ion Exchange Experiments

We conducted ion exchange experiments with water-washed minerals to determine the fraction of Cs that is exchangeable with Ca, K, or Na. Specifically, 0.4 g of minerals

were equilibrated with 20 mL of 0.5 M Ca, K, or Na electrolyte solution in a 80°C oven for 24 hours. For the first eight hours, the samples were taken out of the oven every two hours and shaken on a reciprocal shaker for 20 minutes. At the end of the 24 hours, the samples were centrifuged and the supernatant was decanted. Fresh 20 mL of electrolyte solution was added, and the same procedure as described above was repeated two additional times. At the end, the minerals were freeze-dried. We denoted these samples as "Ca-, K-, or Na-washed". To determine the amount of Cs remaining in the minerals after ion exchange with Ca, K, or Na, we digested the minerals and determined Cs concentrations as described above. All experiments were replicated three times.

Comment: Mineral synthesis, characterization, and washing the samples with Ca, K, and Na electrolytes were done by Youjun Deng, a postdoctoral scientist in our laboratory. ■

5.3.3 Determination of Cesium Desorption Kinetics

We determined the cesium desorption kinetics from "water-washed" minerals using a batch reactor technique. The kinetic ion exchange experiments were conducted with Na electrolyte solutions only. The experimental setup consisted of a well-stirred reactor containing Cs-bearing minerals and Na electrolyte solutions, where Cs release into the solution phase was monitored as a function of time. Specifically, minerals

(100 mg) were mixed with 200 mL of 0.1 mol/L $NaNO_3$ in polypropylene bottles. The bottles were shaken on a reciprocal shaker at ≈150 rpm. We took an aliquot of 2 to 4 mL of well-stirred suspension at selected time intervals. The sampling started at 2 minutes after the beginning of the experiment and the sampling intervals were doubled thereafter (2, 4, 6, ... , 32786 minutes). The aliquots were filtered with a 0.2 μm Acrodic Syringe filters (Pall Co., Ann Arbor, MI) and were subsequently centrifuged at 12,000 × g for 30 min. Cesium concentration in the supernatant of the aliquots was determined by AES.

These batch reactor experiments were conducted at room temperature (23±2°C) and 50±6°C to examine the effect of temperature on Cs desorption. The high experimental temperature (50°C) was chosen because the temperature of sediments 40 m beneath the Hanford tanks was reported to be 50°C and higher [*Pruess et al.,* 2002*; Liu et al.,* 2003a*; Qafoku et al.,* 2003], and diffusion-limited desorption would occur much faster at 50°C than at 23°C. The 50°C temperature was controlled by a water bath. All experiments were replicated three times.

5.3.4 Determination of Cesium Diffusion Coefficient

The effective diffusion coefficient of Cs in the minerals was estimated from the experimental parameters and measurements using a solution of the radial diffusion equation for diffusion within porous particles. The radial diffusion problem is given as [*Crank,*

1975]:

$$\frac{\partial C}{\partial t} = \frac{D_{\text{eff}}}{Rr^2}\frac{\partial}{\partial r}\left[r^2\frac{\partial C}{\partial r}\right] \tag{5.1}$$

where C (mmol/L) is the concentration of the chemical in the solution, t is the time, D_{eff} is the effective diffusion coefficient, R is the retardation factor, which is given as $R = 1 + \rho\frac{K_d}{\theta}$, where ρ_s is the particle density, K_d is the distribution coefficient, and θ is the porosity of the particles.

Assuming spherical particles of uniform intraparticle porosity, which are initially spiked with Cs and then immersed in a Cs free solution, we can formulate the initial and boundary conditions as follows [*Flury and Gimmi,* 2002]:

$$C(r, t=0) = \begin{cases} C_0 & \text{for } r < b \\ C_i & \text{for } r = b \end{cases} \tag{5.2}$$

$$\left.\frac{\partial C(r, t>0)}{\partial t}\right|_{r=b} = -D_{\text{eff}}\theta\left(\frac{4\pi b^2 k}{V_r}\right)\left.\frac{\partial C(r, t>0)}{\partial t}\right|_{r=b} \tag{5.3}$$

$$\frac{\partial C(r, t>0)}{\partial r} = C_0 \qquad \text{for r} = 0 \tag{5.4}$$

where C_0 is initial Cs concentration inside the particles, C_i is the initial Cs concentration in solution, V is the volume of the reservoir, k is the number of particles, θ is the porosity and b is the radius of the particles.

The analytical solution of the diffusion problem for the Cs concentration outside the particles is given as [*Crank,* 1975*; Flury and Gimmi,* 2002]:

$$\frac{C(r,t) - C_i}{C_0 - Ci} = \frac{1}{\alpha + 1} - \frac{6\alpha b}{r}\sum_{n=1}^{\infty}\frac{\exp(-D_{\text{eff}} q_n^2 \frac{t}{b^2})}{9 + 9\alpha + q_n^2\alpha^2}\frac{\sin(q_n\frac{r}{b})}{\sin(q_n)} \tag{5.5}$$

where α is:

$$\alpha = \frac{3V_r}{4\pi b^3 k\theta R} \tag{5.6}$$

where V is the volume of the reservoir, k is the number of particles, and θ is the porosity; and the q_n are the nonzero roots of

$$\tan q_n = \frac{3q_n}{3 + \alpha q_n^2} \tag{5.7}$$

The D_{eff} of Cs inside the particles was then estimated from experimental parameters using Equation 5.5. The effect of temperature on the diffusion coefficient was theoretically estimated using the Stokes-Einstein relation [*Flury and Gimmi,* 2002]:

$$D(T) = \frac{T\mu(T_0)}{T_0\mu(T)} D(T_0) \tag{5.8}$$

where $D(T)$ and $D(T_0)$ are diffusion coefficients at temperatures T and T_0 (in Kelvin), respectively, and $\mu(T_0)$ and $\mu(T)$ are dynamic viscosities at temperatures T and T_0, respectively. The value of dynamic viscosity at 50°C was obtained from *Lide* [1994], and for 23°C from the Andrade equation using tabulated viscosity values [*Reid et al., 1987, p. 493*].

5.4 Results and Discussion

5.4.1 Mineral Synthesis and Cs Incorporation

The X-ray diffraction patterns of the Cs-cancrinite, Cs-sodalite, and Cs-LTA zeolite synthesized in the presence of Cs are very similar to the ones published by others

[*Wyckoff,* 1968*; Sieger et al.,* 1991*; Buhl et al.,* 2000]. The SEM images of the minerals are shown in Figure 5.2. The cancrinite particles are clustered in form of spherical balls, sodalite appears as lepispherical particles, zeolite shows cube- to sphere-like structures, and the allophane did not show a distinct particle shape (Figure 5.2).

The amount of Cs associated with each type of mineral after water washing is shown in Figure 5.3. The figures show that there were considerable differences in the amount of Cs associated with the minerals after water washing. These differences are related to the Na:Cs ratio used in the mineral synthesis, rather than the ability of the minerals to sorb Cs. At a higher Na:Cs ratio (used for cancrinite and sodalite), less Cs was incorporated in the minerals than at a lower Na:Cs ratio (zeolite and allophane).

5.4.2 Ion Exchange

The results of the ion exchange experiments are shown in Figures 5.3. Figure 5.3a depicts the absolute concentrations, whereas Figure 5.3b shows the concentrations relative to the initial concentrations.

A large portion of Cs sorbed to cancrinite and sodalite remained in the minerals after ion exchange with Na, K, and Ca electrolytes (Figures 5.3). Cesium in sodalite appears to be particulary nonexchangeable with Na, K, or Ca. These results suggest that a fraction of the incorporated cesium is located in the internal cages and channels of the minerals. Cesium sorbed onto external surfaces of the particles should be readily removed by ion exchange with Na, K, or Ca. In both cancrinite and sodalite, Cs

seems to be more exchangeable with K and Ca than with Na. Overall, K was the most effective ion for ion exchange. We attribute this to the low hydration energy of K compared to Na and Ca, so that K can more readily dehydrate and move into the ε- or β-cages of cancrinite and sodalite. The diameters of the hydrated ions are all larger than the apertures of the ε- or β-cages (Table 5.1, figure 5.1); therefore, the ions cannot enter the cages in their hydrated forms, the ions have to be dehydrated in order to exchange with Cs in cages and channels. K has the lowest hydration energy and is therefore the most effective ion in ion exchange for our minerals. Compared to Na, Ca is a more effective for Cs ion exchange in cancrinite (Figure 5.3). This result is difficult to explain because Na should be favored over the Ca based on their hydration energies [*Liu et al.,* 2003b]. It possible that it is more favorable to place a dehydrated, or partially dehydrated, Ca in a cage than two hydrated Na ions.

In contrast to cancrinite and sodalite, most of the Cs in LTA zeolite and allophane was readily exchanged by the three cations (Figure 5.3). It appears that Cs is sorbed at surfaces that are easily accessible to ion exchange. Na and K were more effective than Ca at replacing Cs in both allophane and LTA zeolite. To move into the cages of zeolite, Na, K, and Ca all have to be dehydrated; the hydrated ions have a larger diameter than the aperture of the mineral cages (Table 5.1). The ability of Ca to move into the cages of zeolite is restricted by its large hydrated radii and hydration energy [*Woods and Gunter,* 2001]. Ca has a much larger hydration energy than Na and K (Table 5.1), and can therefore not as readily dehydrate and diffuse into the mineral

cages. Na and K were more competitive than Ca at replacing the Cs in allophane because they have lower hydration energies than Ca (Table 5.1) [*Liu et al.*, 2003b].

5.4.3 Determination of Cesium Desorption Kinetics

The relative amount of Cs desorbed by Na exchange in ion exchange kinetics experiments varied with the minerals. Cancrinite and sodalite released much smaller amounts of Cs than did LTA zeolite or allophane (Figure 5.4). Over the duration of the experiments, less than 32% and 3% of incorporated Cs was desorbed from cancrinite and sodalite, respectively, at 23°C; however, more than 80% of Cs was released from zeolite and allophane (Figure 5.4, Table 5.1). These results were consistent with those of ion exchange experiments, i.e., cesium sorbed to cancrinite and sodalite were resistant to ion exchange, whereas most Cs in allophane and LTA zeolite were exchangeable. The small desorption of Cs from cancrinite and sodalite further indicates that a large portion of cesium is incorporated in the structural framework of the minerals and is not easily accessible for exchanging ions.

The desorption of Cs from cancrinite and sodalite showed an initially fast release of Cs, continued by a slow Cs release (Figure 5.4). The effect of temperature on Cs desorption from cancrinite and sodalite is shown in Figure 5.5. The amount of desorbed Cs increased at a higher temperature. The percentage of Cs released from cancrinite increased from 31% at 23°C to 40% at 50°C(Table 5.2). Similary, Cs released from sodalite increased from 2.7% at 23°C to 6.4% at 50°C. The increase in Cs desorption

with increasing temperature was reported in contaminated Hanford sediments (micaceous minerals) [*Liu et al.,* 2003a]. Nonetheless, the desorption data suggest that a large portion of Cs sorbed to cancrinite or sodalite still remained in the minerals even after desorption at 50°C.

Irreversible sorption of Cs in Hanford sediments has been reported in many studies [*Zachara et al.,* 2002*; Liu et al.,* 2003b*; Steefel et al.,* 2003]. Studies with uncontaminated Hanford sediments at 25°C showed that only 72% of Cs introduced to a sediment column was desorbed by 1 M $NaNO_3$ solution [*Steefel et al.,* 2003]. As suggested by an intraparticle diffusion and two-site cation exchange model, ion exchange with 0.5 mol/L $NaNO_3$ solution at room temperature, resulted in exchange of about only about 40% of Cs sorbed to Hanford sediments [*Liu et al.,* 2003b]. The percentage of desorbed Cs depends on the electrolyte concentration and the density of sorption [*Zachara et al.,* 2002]. Cesium sorption to selective frayed-edge sites and slow diffusion from interlayer sites explain the irreversible behavior of Cs in Hanford sediments [*Zachara et al.,* 2002*; Liu et al.,* 2003b*; Steefel et al.,* 2003].

The LTA zeolite released most of the Cs almost immediately upon contact with Na electrolyte solution and Cs concentration remained constant throughout the experiment (Figure 5.4). It appears that all the exchangeable Cs was quickly released into the solution and the remaining ≈20% (Table 5.2) of sorbed Cs may be fixed inside the mineral particles, at least within the time scale of the experiment. One possible explanation for this behavior is that some of the Cs inside the β-cages is strongly

associated with the framework atoms so that they may be trapped in the cages for a longer time than those in α-cages [*Lee et al.,* 1994].

In allophane, most of the Cs was released at the beginning of the experiment and the concentration in solution reached a plateau within a short time (Figure 5.4). Compared to zeolite, however, the Cs release was not instantaneous. The allophane formed at a high pH is similar to feldspathoids (Youjun Deng, Washington State University, personal communication, November 2004); thus, the Cs-allophane may have a framework structure, and some of the Cs may not be quickly accessible to exchanging cations.

5.4.4 Determination of Cesium Diffusion Coefficient

In solving the radial diffusion problem, we assumed that Cs is evenly distributed inside the minerals. Elemental mapping images after washing of the minerals with Ca revealed that Cs is indeed homogenously distributed inside the minerals. An example of an elemental mapping image is shown in Figure 5.6.

The effective diffusion coefficients, D_{eff}, of Cs in the mineral particles were obtained by fitting Equation 5.5 to experimental data. The parameters that experimentally determined are listed in Table 5.3. The estimated D_{eff} of Cs in cancrinite and sodalite were $\approx 10^{-14}$ m^2/s. The total Cs released during desorption experiments was estimated from the experimental data (Table 5.2), and used as input for the modeling. The modeling results indicate that the diffusion of Cs in cancrinite and sodalite is likely

a solid state diffusion, because the estimated diffusion coefficient (10^{-14} m^2/s) is five orders of magnitude smaller than the Cs diffusion coefficient in solution (2.06×10^{-9} m^2/s, *Flury and Gimmi* [2002]). Considering the apertures of ε- or β-cages, it is possible that Cs diffuses out of the particles as it does through a solid matrix.

The D_{eff} of Cs in cancrinite and sodalite increased with increasing temperature. The D_{eff} for cancrinite and sodalite at 23°C is $\approx 50\%$ smaller than that at 50°C. This result matches well with theoretical approximations. The Stokes-Einstein relation showed that the diffusion coefficient of Cs at 23°C (0.5×10^{-14} m^2/s) is approximately 53.7% of its diffusion coefficient at 50°C (0.93×10^{-14} m^2/s).

The estimated effective diffusion coefficient of Cs in zeolite was $\approx 10^{-9}$ m^2/s (Figures 5.9). The value of D_{eff} indicated that the diffusion of Cs in LTA zeolite is similar to that of free Cs ion diffusion in solution (2.06×10^{-9} m^2/s) [*Flury and Gimmi*, 2002]. This is also reasonable because dehydrated Cs and Na ions can easily move in and out of the α-cages.

The value of D_{eff} of Cs in allophane was estimated to be $\approx 10^{-16}$ m^2/s, which is about two orders of magnitude smaller than solid state diffusion. The diffusion equation under-estimated Cs release into solution. In order to reproduce the slope of the experimental data, a D_{eff} value greater than $\approx 10^{-16}$ m^2/s was not possible. We suspect that the desorption of Cs from allophane may not be a diffusion process, but we have not yet found a good explanation for such a small D_{eff}.

5.5 Conclusions

Cancrinite, sodalite, zeolite, and allophane synthesized in the presence of Cs incorporated Cs in their structure frameworks. Cesium incorporated in the cages of Cs cancrinite and sodalite was not easily exchangeable with Na, K, or Ca. Only a small fraction (1-57%) of Cs in cancrinite and sodalite was exchangeable with Na, K, or Ca, while most Cs (94-99%) associated with LTA Zeolite and allophane was exchangeable with Na or K. Compared to Na and K, Ca was less effective at exchanging with Cs that Cs could replace a smaller fraction of Cs (65-85%) in LTA zeolite and allophane. However, Ca was more effective than Na at replacing Cs in cancrinite and sodalite. Among the ions studied, K was the most effective at replacing Cs in all the four minerals. The results from desorption experiments showed that Cs desorbed quickly from LTA zeolite; however, Cs releases from cancrinite, sodalite, and allophane were relatively slow. Cesium may be located in the cages and channels of these minerals and was not easily accessible for ion exchange.

5.6 Tables and Figures

Table 5.1: The ionic diameter, hydrated diameter, and hydration energies of exchanging ions, the porosity of the minerals and the aperture of mineral cages.

Ion	ionic diameter[a] (nm)	Hydrated diameter[a] (nm)	Hydration energy[b] (kcal/mol)
Na	0.19	0.72	−97
K	0.26	0.66	−79
Cs	0.33	0.66	−66
Ca	0.2	0.83	−373
Mineral	**Cages or channels**	**Aperture diameter[c] (nm)**	**Porosity[c]**
Cacrinite	ε-cages and	≈0.22	0.4
	12-membered rings	0.59	
Sodalite	β-cages	0.22	0.35
Zeolite	α-cages	0.42	0.47
Allophane	na	na	0.3

[a]Nightingale [1959]

[b]Woods and Gunter [2001]

[c]Mumpton [1981]

na = not applicable.

Table 5.2: The amount of Cs incorporated in the minerals studied and Cs remaining in the minerals after diffusion experiments.

Minerals	Cs in water-washed samples (mmol/100g)	Cs remaining after 23 days of diffusion			
		23°C		50°C	
		mmol/100g	%	mmol/100g	%
Cancrinite	9.1±0.03	6.2±0.1	68.4	5.5±0.1	60.2
Sodalite	8.1±0.1	7.9±0.1	97.3	7.6±0.02	93.6
Zeolite	22.1±1.5	3.4±0.1	16.5	na	na
Allophane	18.0±0.2	3.6±0.1	19.1	na	na

na = not applicable.

Table 5.3: Model input parameters needed for Equation 5.5.

Minerals	Diameter b	Porosity[a]	No. of particles k	Volume of solution V_r	K_d (m^3/kg)[b]	
	(μm)	θ		(m^3)	23°C	50°C
Cacrinite	10	0.4	8.2×10^{7}	2.0^{-4}	50.7	42.4
Sodalite	4.0	0.35	1.5×10^{9}	2.0^{-4}	57.8	46.4
Zeolite	1.8	0.47	1.4×10^{10}	2.0^{-4}	36.2	na
Allophane	0.4	0.3	1.3×10^{12}	2.0^{-4}	47.7	na

[a]Mumpton [1981]

[b]Liu et. al., [2003]

na = not applicable.

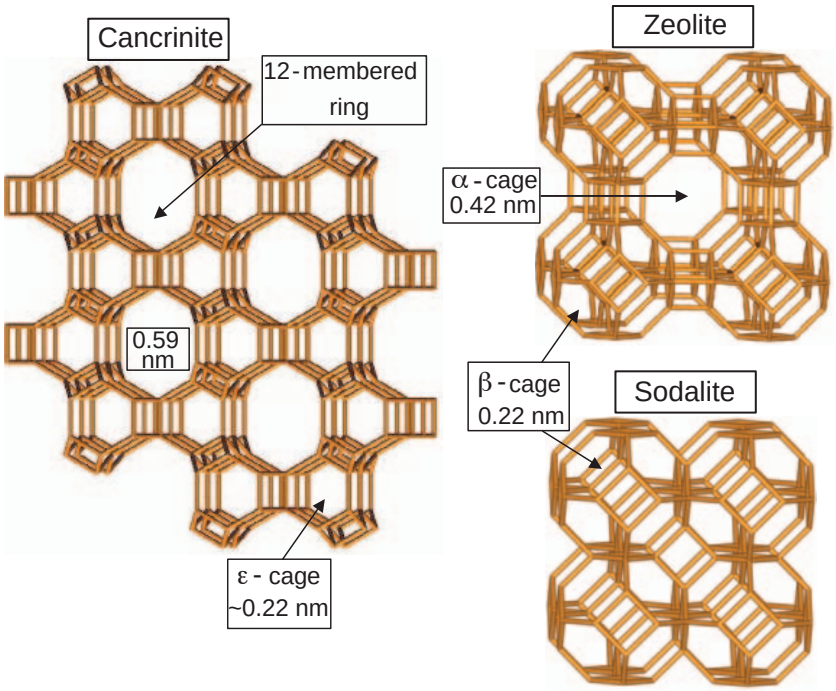

Figure 5.1: The structural frameworks of cancrinite, LTA zeolite, and sodalite. The measurements in nanometers are the aperture diameters of respective cages. Youjun Deng generated these diagrams using Weblab ViewerLite software (Accelrys, San Diego, CA) and structural data published by the International Zeolite Association.

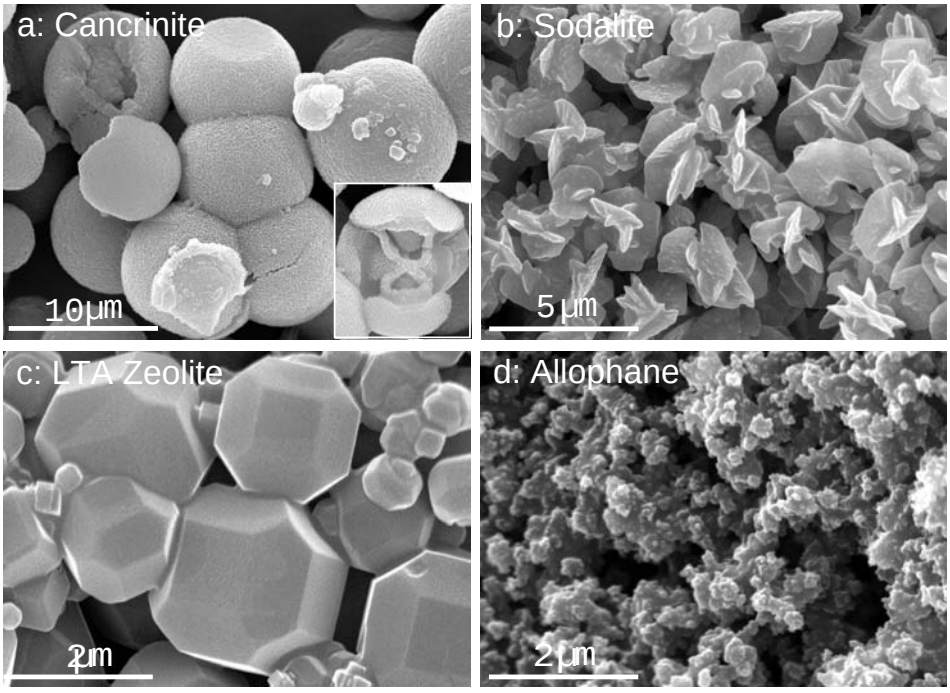

Figure 5.2: Scanning electron microscope images of the four minerals studied. The inset in (a) shows the inside of a ball-shape cancrinite cluster. (These images were taken by Youjun Deng.)

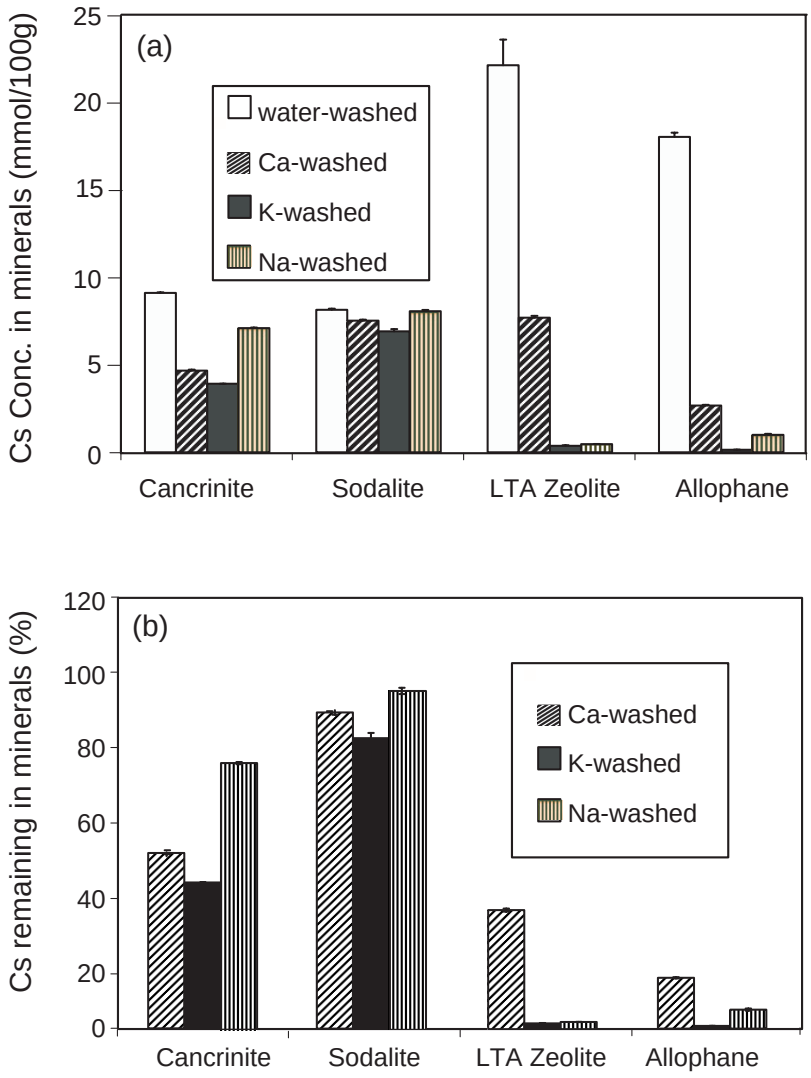

Figure 5.3: Amount of total incorporated Cs in the four minerals (water-washed) and Cs remaining in the minerals after ion exchange with Ca, K, or Na. (a) Cs expressed in absolute concentraion, (b) Cs expressed in relative to water-washed samples. Error bars are ± one standard deviation.

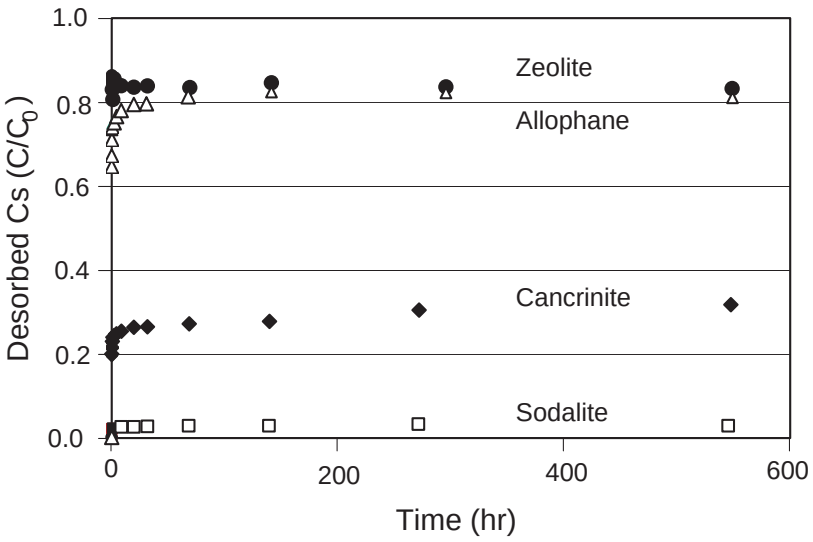

Figure 5.4: Desorption of Cs from the four Cs-incorporated minerals: Cs-cancrinite, Cs-sodalite, Cs-LTA zeolite and Cs-allophane at 23°C.

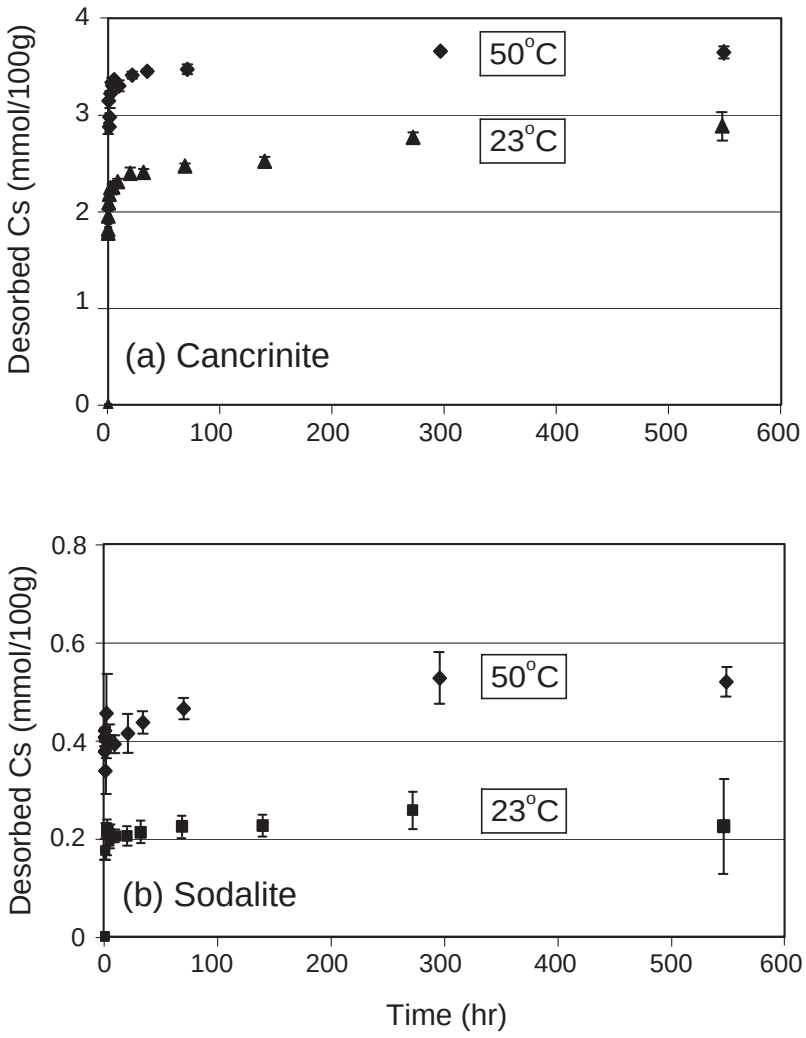

Figure 5.5: The effect of temperature on Cs desorption from Cs-cancrinite and Cs-sodalite. Vertical bars indicate ± one standard deviation.

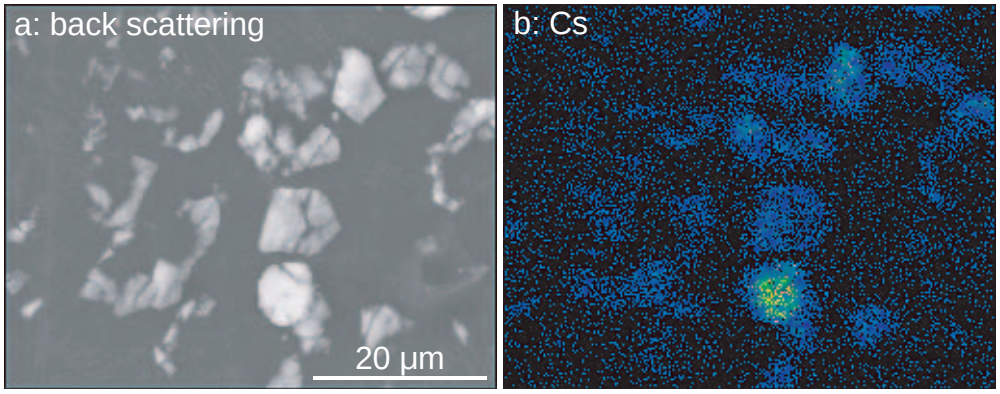

Figure 5.6: Elemental distribution of Cs in Ca-washed cancrinite. (a) Back scattering, showing the position of the minerals, and (b) Location of Cs. (note: Ca-washed cancrinite is a Cs-cancrinite sample that was washed with Ca electrolyte. Images were taken by Youjun Deng. This is a color figure.)

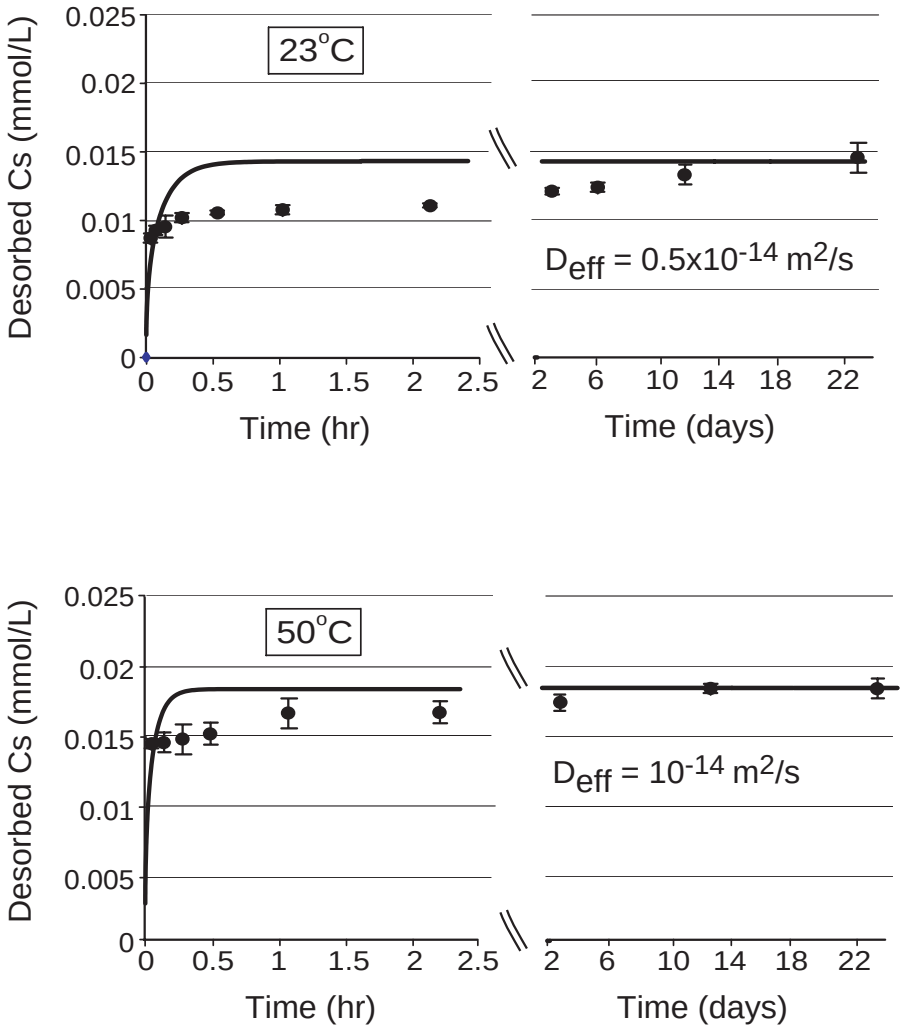

Figure 5.7: Desorption of Cs from Cs-cancrinite at 23°C and 50°C. Symbols represent the experimental data. Vertical bars are ± one standard deviation. Solid lines represent solutions of the radial diffusion problem (Equation 5.5) that show the changes of Cs concentration with time at the respective effective diffusion coefficients.

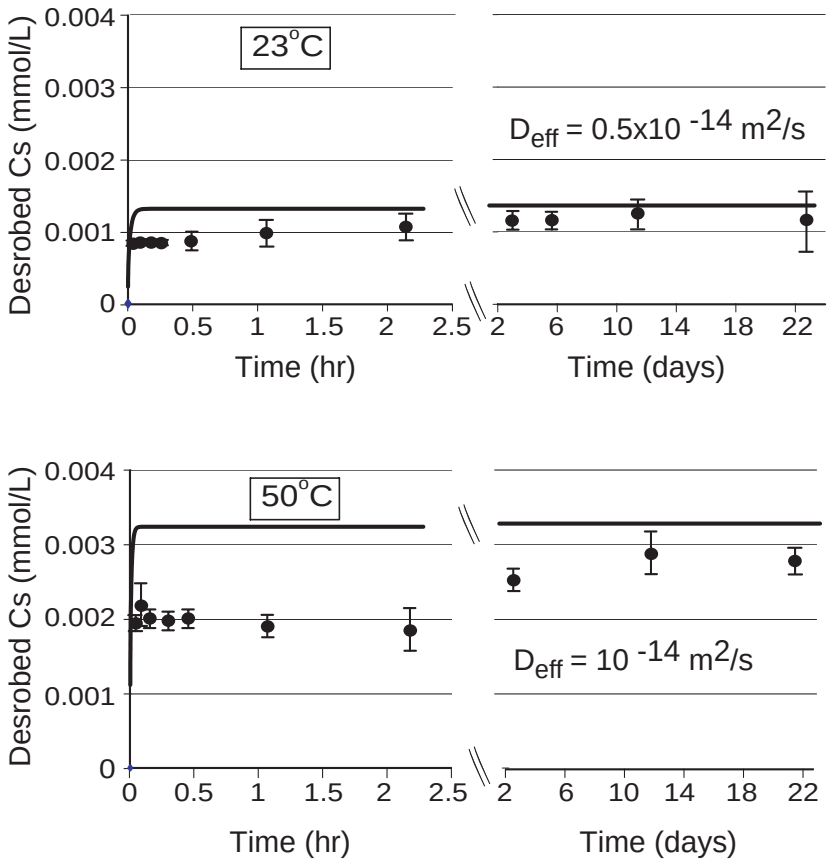

Figure 5.8: Desorption of Cs from Cs-sodalite at 23°C and 50°C. Symbols represent the experimental data. Vertical bars are ± one standard deviation. Solid lines represent solutions of the radial diffusion problem (Equation 5.5) that show the changes of Cs concentration with time at the respective effective diffusion coefficients.

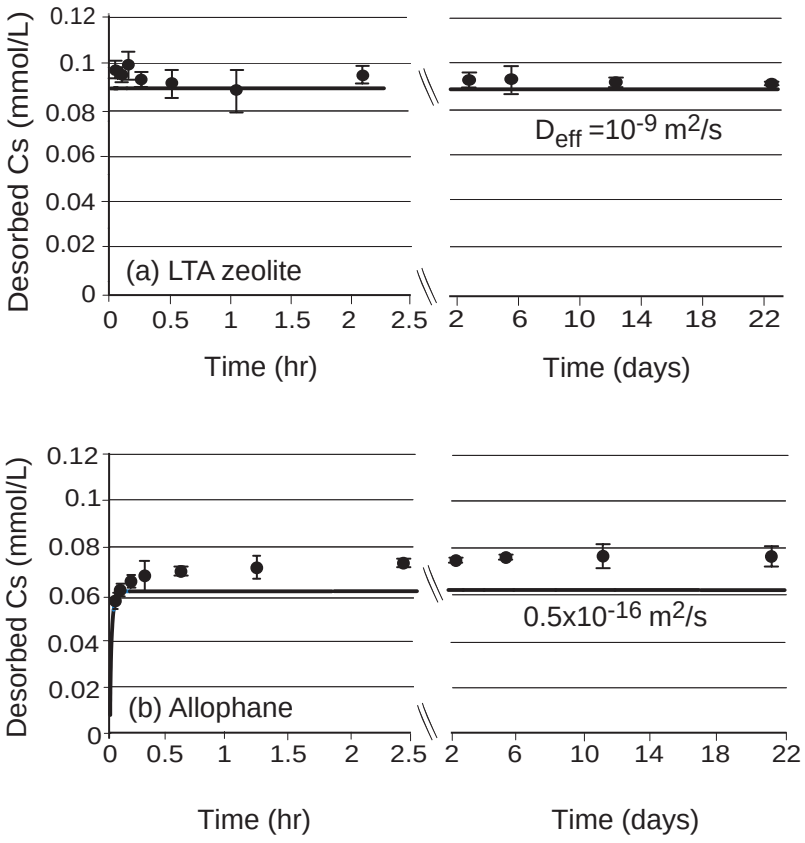

Figure 5.9: Desorption of Cs from (a) Cs-LTA zeolite and (b) Cs-allophane at 23°C. Symbols represent the experimental data. Vertical bars are ± one standard deviation. Solid lines represent solutions of the radial diffusion problem (Equation 5.5) that show the changes of Cs concentration with time at the respective effective diffusion coefficients.

Chapter 6

Summary and Conclusions

This dissertation includes a brief literature review on dye tracer applications in hydrology and reports the results from several laboratory studies that investigated sorption properties of selected organic dyes and their suitability as water tracers, tested screening techniques for a fast and accurate estimation of dye sorption, and investigated the potential redistribution of cesium in contaminated Hanford sediments. The studies include column and batch experiments, breakthrough curve analysis, measurements of sorption isotherms, determination of the amount of Cs incorporation and desorption kinetics in secondary clay minerals—feldspathoids, zeolite, and allophane.

Different types of dyes have been used, studied, and recommended as water tracers. Due to their unique properties, dye tracers are often favored over a variety of other available tracing materials. However, all dye tracers sorb to subsurface materials, and sorption is one of the major limiting factors in using dyes as water tracers.

We studied the sorption of four triarymethane dyes in a sandy soil using column experiments. Among the dyes tested, C.I. Food Green 3 showed the least sorption. The

results from the sorption studies showed that dyes containing three sulfonic acid groups sorbed considerably less than those containing two sulfonic acid groups. Sorption isotherms measured by column technique showed a similar trend with those obtained by batch studies. We suggest that column experiments are valuable for measuring sorption characteristics of dye tracers.

We established QSAR models for estimation of dye sorption parameters. Our QSAR models suggested that sorption parameters are affected not only by the number of SO_3 groups but also by the position of SO_3 groups attached to the molecular template of a dye. We generated hypothetical dyes, which showed much less sorption than C.I. Food Blue 2 (Brilliant Blue FCF), a commonly used vadose zone dye tracer. We concluded that QSAR may offer a powerful tool for screening and designing optimal dye tracers.

We determined the amount of Cs incorporated in cancrinite, sodalite, LTA zeolite and allophane formed in Hanford tank waste simulants and the exchangeability of the incorporated Cs. Our data suggest that a portion of Cs was irreversibly incorporated in the structural frameworks of cancrinite, sodalite, and LTA zeolite. Cesium incorporated in cancrinite and sodalite was not as easily exchangeable as that in LTA zeolite and allophane. Within the duration of our experiments, the irreversible sorbed fractions in cancrinite and sodalite were considerably larger than those in LTA zeolite and allophane.

Bibliography

Aeby, P., U. Schultze, D. Braichotte, M. Bundt, F. Moser-Boroumand, H. Wydler, and H. Flühler, Fluorescence imaging of tracer distributions in soil profiles, *Environ. Sci. Technol.*, *35*, 753–760, 2001.

Aley, T., Dyes don't lie: Practical karst hydrology, in *Karst-Water Environment Symposium Proceedings*, edited by T. Younos, T. J. Burbey, E. H. Kastning, and J. A. Poff, pp. 1–10, Virginial Water Research Center, Roanoke, Virginia, 1997.

Atkinson, T. C., and A. A. Bukowiecki, Sorption of fluorobenzoic acids on peat and kaolinite, in *Tracers and Modelling in Hydrogeology*, vol. IAHS Publ. no. 262, edited by A. Dassargues, pp. 187–194, IAHS, Liège, Belgium, 2000.

Bernasconi, L., E. Fois, and A. Selloni, Cation-anion versus cation-framework interactions in sodalite: First-principles study of model Cu-exchanged sodalite, *J. Chem. Phys.*, *110*, 9048–9055, 1999.

Bickmore, B. R., K. L. Nagy, J. S. Young, and J. W. Drexler, Nitrate-cancrinite precipitation on quartz sand in simulated Hanford tank solutions, *Environ. Sci.*

Technol., *35*, 4481–4486, 2001.

Bintein, S., and J. Devillers, Qsar for organic chemical sorption in soils and sediments, *Chemosphere*, *28*, 1171–1188, 1994.

Bouma, J., A. Jongerius, O. Boersma, A. Jager, and D. Schoonderbeek, The function of different types of macropores during saturated flow through four swelling soil horizons, *Soil Sci. Soc. Am. J.*, *41*, 945–950, 1977.

Buhl, J. C., and J. Löns, Synthesis and crystal structure of nitrate enclathrated sodalite $Na_8[AlSiO_4]_6(NO_3)_2$, *J. Alloys Compounds*, *235*, 41–47, 1996.

Buhl, J. C., F. Stief, M. Fechtelkord, T. M. Gesing, U. Taphorn, and C. Taake, Synthesis, x-ray diffraction and MAS NMR characteristics of nitrate cancrinite $Na_7[AlSiO_4]_6(NO_3)_{1.6}(H_2O)_2$, *J. Alloys Compounds*, *305*, 93–102, 2000.

Bürgisser, C. S., M. Cernik, M. Borkovec, and H. Sticher, Determination of nonlinear adsorption isotherms from column experiments: an alternative to batch studies, *Environ. Sci. Technol.*, *27*, 943–948, 1993.

Chorover, J., S. Choi, M. K. Amistadi, K. G. Karthikeyan, G. Crosson, and K. T. Mueller, Linking cesium and strontium uptake to kaolinite weathering in simulated tank waste leachate, *Environ. Sci. Technol.*, *37*, 2200–2208, 2003.

Church, M., *Electrochemical and Fluorometric Tracer Techniques for Streamflow Measurements*, British Geomorphological Research Group, Technical Bulletin No. 12, Geo Abstracts Ltd., University of East Anglia, Norwich, UK, 1974.

Colour Index *Colour Index*, vol. 4, 3rd ed., The Society of Dyers and Colourists, London, 1971.

Colour Index *Colour Index International Fourth Edition Online*, Society of Dyers and Colourists and the American Association of Textile Chemists and Colorists, http://www.colour-index.org, accessed September 2004, Bradford, England, 2001.

Corey, J. C., Evaluation of dyes for tracing water movement in acid soils, *Soil Sci.*, *106*, 182–187, 1968.

Cox, M. H., G. O. Mendez, C. R. Kratzer, and E. G. Reichard, *Evaluation of Tracer Tests Completed in 1999 and 2000 on the Upper Santa Clara River, Los Angeles and Ventura Counties, California*, vol. Water-Resources Investigations Report 03-4277, U. S. Geological Survey, Sacramento, CA, 2003.

Crank, J., *The Mathematics of Diffusion*, 2nd ed., Clarendon Press, Oxford University Press, Oxford, 1975.

Davis, S. N., G. M. Thompson, H. W. Bentley, and G. Stiles, Ground-water tracers—A short review, *Ground Water*, *18*, 14–23, 1980.

des Carrières, D., Étiologie de l'épidémie typhoïde qui a éclaté a Auxerre en septembre 1882, *Bull. et mém. Soc. méd. des hôpitaux de Paris*, *9, 2d ser*, 277–284, 1883.

Drew, B. P., A review of the available methods for tracing underground waters, *Proc. Br. Speleol. Assoc.*, *6*, 1–19, 1968.

Fechtelkord, M., B. Posnatzki, J.-C. Buhl, C. A. Fyfe, L. Groat, and M. Raudsepp, Characterization of synthetic Cs-Li cancrinite grown in a butanediol-water system: an NMR spectroscopic and Rietveld refinement study, *Am. Mineralogist*, *86*, 881–888, 2001.

Feuerstein, D. L., and R. E. Selleck, Fluorescent tracers for dispersion measurements, *J. Sanit. Eng. Div. Am. Soc. Civ. Eng.*, *89*, 1–21, 1963.

Field, M. S., Efficient hydrologic tracer-test design for tracer-mass estimation and sample-collection frequency, 1. Method development, *Environ. Geology (NY)*, *42*, 827–838, 2002a.

Field, M. S., *The QTRACER2 Program for Tracer Breakthrough Curve Analysis for Tracer Tests in Karstic Aquifers and Other Hydrologic Systems*, vol. EPA/600/R-02/001, Office of Research and Development, U. S. Environmental Protection Agency, Washington D.C., 2002b.

Field, M. S., A review of some tracer-test design for tracer-mass estimation and sample-collection frequency, *Environ. Geology (NY)*, *43*, 867–881, 2003a.

Field, M. S., *Tracer-Test Planning Using the Efficient Hydrologic Tracer-Test Design (EHTD) Program*, Office of Research and Development, U. S. Environmental Protection Agency, EPA/600/R-03/034, Washington D.C., 2003b.

Flury, M., and H. Flühler, Tracer characteristics of Brilliant Blue FCF, *Soil Sci. Soc. Am. J.*, *59*, 22–27, 1995.

Flury, M., and N. N. Wai, Dyes as tracers for vadose zone hydrology, *Rev. Geophys.*, *41*, 1002, doi:10.1029/2001RG000109, 2003.

Flury, M., and T. Gimmi, Solute diffusion, in *Methods of Soil Analysis, Part 4, Physical Methods*, edited by J. H. Dane, and G. C. Topp, pp. 1323–1351, Soil Science Society of America, Madison, WI, 2002.

Flury, M., H. Flühler, W. A. Jury, and J. Leuenberger, Susceptibility of soils to preferential flow of water: A field study, *Water Resour. Res.*, *30*, 1945–1954, 1994.

Forrer, I., A. Papritz, H. Flühler, and D. Luca, Quantifying dye tracers in soil profiles by image processing, *Eur. J. Soil Sci.*, *51*, 313–322, 2000.

Fortin, J., M. Flury, W. A. Jury, and T. Streck, Rate-limited sorption of simazine in saturated soil columns, *J. Contam. Hydrol.*, *25*, 219–234, 1997.

German-Heins, J., and M. Flury, Sorption of Brilliant Blue FCF in soils as affected by pH and ionic strength, *Geoderma*, *97*, 87–101, 2000.

Germann, P. F., W. M. Edwards, and L. B. Owens, Profiles of bromide and increased soil moisture after infiltration into soils with macropores, *Soil Sci. Soc. Am. J.*, *48*, 237–244, 1984.

Gerstl, Z., and C. S. Helling, Evaluation of molecular connectivity as a predictive method for the adsorption of pesticides by soil, *J. Environ. Sci. Health, Part B*, *87*, 55–69, 1987.

Gooseff, M. N., S. M. Wondzell, R. Haggerty, and J. Aderson, Comparing transient storage modeling and residence time distribution (rtd) analysis in geomorphically varied reachs in lookout creek basin, oregon, usa, *Adv. Water Resour.*, *26*, 925–937, 2003.

Griffioen, J., C. A. J. Appelo, and M. van Veldhuizen, Practice of chromatography: Deriving isotherms from elution curves, *Soil Sci. Soc. Am. J.*, *56*, 1429–1437, 1992.

Hall, L. H., and L. B. Kier, Issues in representation of molecular structure: The development of molecular connectivity, *J. of Mol. Graph. Model.*, *20*, 4–18, 2001.

Hall, L. H., L. B. Kier, and L. M. Hall, *The Guide for Development of QSAR with MDL QSAR*, MDL Information System, San Leandro, Califonia., 2002.

Hansch, C., and A. Leo, *Exploring QSAR: Fundamentals and Applications in Chemistry and Biology*, American Chemical Society, Washington, DC., 1995.

Hansch, C., and T. Fujita, Status of qsar at the end of the twentieth century, in *Classical and Three-Dimensional QSAR in Agrochemistry*, vol. Symposium Series 606, edited by C. Hansch, and T. Fujita, pp. –, American Chemical Society, Washington, DC, 1995.

Hassett, J. J., and W. L. Banwart, The sorption of nonpolar organics by soils and sediments, in *Reactions and Movement of Orgaic Chemicals in Soils*, vol. SSSA Special Publication Number 22, edited by B. L. Sawhney, and K. Brown, pp. 31–44, Soil Science Society of America, Madison, WI, 1989.

Hong, H., L. Wang, S. Han, Z. Zhang, and G. Zou, Prediction of soil adsorption coefficient k_{oc} for phenylthio, phenylsulfinyl and phenylsulfonyl acetates, *Chemosphere*, *34*, 827–834, 1997.

Hu, Q., T. J. Kneafsey, R. C. Trautz, and J. S. Y. Wang, Tracer penetration into welded tuff matrix from flowing fractures, *Vadose Zone J.*, *1*, 102–112, 2002.

Igler, B. A., K. U. Totsche, and P. Knabner, Identification of nonlinear sorption isotherms by soil column breakthrough experiments, *Phys. Chem. Earth*, *23*, 215–219, 1998.

Imes, J. L., and B. S. Fredrick, *Using Dye-Tracing and Chemical Analyses to Determine Effects of a Wastewater Drainage to Jam Up Creek on Water Quality of Big Spring, Southeastern Missouri, 2001*, vol. USGS Fact Sheet, fs-103-02 ed., U. S. Geological Survey, Rolla, MO, 2002.

Jr., E. R. N., Phenomenological theory of ion solvation. Effective radii of hydrated ions, *J. Phys. Chem.*, *63*, 1381–1387, 1959.

Kanwar, R. S., J. L. Baker, and P. Singh, Use of chloride and fluorescent dye as tracers in measuring nitrate and atrazine transport through soil profile under laboratory conditions, *J. Environ. Sci. Health, Part A*, *32*, 1907–1919, 1997.

Kasnavia, T., D. Vu, and D. A. Sabatini, Fluorescent dye and media properties affecting sorption and tracer selection, *Ground Water*, *37*, 376–381, 1999.

Katritzky, A. R., *Understanding How Chemical Structure Determines Physical Properties*, http://ark.chem.ufl.edu/pages/Research/QSPR02/QSPR_2002_files/frame.htm, accessed: September 2004, University of Florida, Gainesville, FL, 2002.

Ketelsen, H., and S. Meyer-Windel, Adsorption of Brilliant Blue FCF by soils, *Geoderma*, *90*, 131–145, 1999.

Kier, L. B., and L. H. Hall, *Molecular Connectivity in Structure-Activity Analysis*, John Wiley & Sons, New York, 1986.

Kier, L. B., and L. H. Hall, *Molecular Structure Description: The Electrotopological State*, Academic Press, San Diego, California, 1999.

Kier, L. B., and L. H. Hall, Intermolecular accessibility: The meaning of molecular connectivity, *J. Chem. Inf. Comput. Sci.*, *40*, 792–795, 2000.

Knop, A., Über die hydrographischen Beziehungen zwischen der Donau und der Aachquelle im badischen Oberlande (Schluss), *Neues Jahrb. Mineral. Geol. Paleontol.*, *1878*, 350–363, 1878.

Kratzer, C. R., and R. N. Biagtan, *Determination of Traveltimes in the Lower San Joaquin River Basin, California, from Dye-Tracer Studies during 1994-1995*, vol. Water Resources Investigations Report, 97-4018 ed., U. S. Geological Survey, 1998.

Langmuir, I., The adsorption of gases on plane surfaces of glass, mica and platinum, *J. Am. Chem. Soc.*, *40*, 1361–1403, 1918.

Lee, S. H., G. K. Moon, S. G. Choi, and H. S. Kim, Molecular dynamics simulation studies of zeolite A. 3. Structure and dynamics of Na^+ ions and water molecules in a rigid zeolite A, *J. Phys. Chem.*, *98*, 1561–1569, 1994.

Lide, D. R., *CRC Handbook of Chemistry and Physics*, 75th ed., CRC Press, Boca Raton, 1994.

Liu, C., J. M. Zachara, O. Qafoku, and S. C. Smith, Effect of temperature on Cs^+ sorption and desorption in subsurface sediments at the Hanford site, USA, *Environ. Sci. Technol.*, *37*, 2640–2645, 2003a.

Liu, C., J. M. Zachara, S. C. Smith, J. P. McKinley, and C. C. Ainsworth, Desorption kinetics of radiocesium from subsurface sediments at Hanford Site USA, *Geochim. Cosmochim. Acta*, *67*, 2893–2912, 2003b.

Mashal, K., J. B. Harsh, M. Flury, A. R. Felmy, and H. Zhao, Colloid formation in Hanford sediments reacted with simulated tank waste, *Environ. Sci. Technol.*, *38*, (in press), 2004.

McKinley, J. P., C. J. Zeissler, J. M. Zachara, R. J. Serne, R. M. Lindstrom, H. T. Schaef, and R. D. Orr, Distribution and retention of Cs-137 in sediments at the Hanford Site, Washington, *Environ. Sci. Technol.*, *35*, 3433–3441, 2001.

McLaughlin, M. J., A review on the use of dyes as soil water tracers, *Water SA*, *8*, 196–201, 1982.

McMurry, J., *Organic Chemistry*, Brooks/Cole Publishing Company, Pacific Grove, CA, 1996.

Merck *The Merck Index. An encyclopedia of chemicals, drugs, and biologicals*, twelfth ed., Merck & Co, Inc., Whitehouse Station, N.J., 1996.

Meylan, W., P. H. Howard, and R. S. Boethling, Molecular topology/fragment contribution method for predicting soil sorption coefficients, *Environ. Sci. Technol.*, *26*, 1560–1566, 1992.

Mumpton, F. A., Natural zeolites, in *Mineralogy and Geology of Natural Zeolites*, vol. 4, edited by F. A. Mumpton, pp. 1–17, Mineralogical Society of America, Blacksburg, VA, 1981.

Nendza, M., *Structure Activity Relationships in Environmental Sciences*, Chapman & Hall, London,UK, 1998.

Nobles, M. M., L. P. Wilding, and K. J. McInnes, Pathways of dye tracer movement through structured soils on a macroscopic scale, *Soil Sci.*, *169*, 229–242, 2004.

Öhrström, P., Y. Hamed, M. Persson, and R. Berndtsson, Characterizing unsaturated solute transport by simultaneous use of dye and bromide, *J. Hydrol. (Amsterdam)*, *289*, 23–35, 2004.

Press, W. H., S. A. Teukolsky, W. T. Vetterling, and B. P. Flannery, *Numerical Recipes. The Art of Scientific Computing*, 2nd ed., Cambridge University Press, Cambridge, 1992.

Pruess, K., S. Yabusaki, C. I. Steefel, and P. C. Lichtner, Fluid flow, heat transfer, and solute transport at nuclear waste storage tanks in the Hanford vadose zone, *Vadose Zone J.*, *1*, 68–88, 2002.

Pussemier, L., R. de Borger, P. Cloos, and R. van Bladel, Relation between the molecular structure and the adsorption of arylcarbamate, phenylurea, and anilide pesticides in soil and model organic adsorbents, *Chemosphere*, *18*, 1871–1882, 1989.

Qafoku, N. P., C. C. Ainsworth, J. E. Szecsody, D. L. Bish, J. S. Young, D. E. McCready, and O. S. Qafoku, Alluminum effect on dissolution and preciptation under hyperalkaline conditions: II. Solid phase transformations, *J. Environ. Qual.*, *32*, 2364–2372, 2003.

Randic, M., The connectivity index 25 years after, *J. Mol. Graph. Model.*, *20*, 19–35, 1992.

Reid, R. C., J. M. Prausnitz, and B. E. Poling, *The Properties of Liquids and Gases*, 4th ed., McGraw-Hill, New York, 1987.

Reife, A., and H. S. Freeman, Carbon adsorption of dyes and selected intermediates, in *Environmental Chemistry of Dyes and Pigments*, edited by A. Reife, and H. S. Freeman, pp. 3–31, John Wiley & Sons, New York, 1996.

Reynolds, E. R. C., The percolation of rainwater through soil demonstrated by fluorescent dyes, *J. Soil Sci.*, *17*, 127–132, 1966.

Sabljić, A., On the prediction of soil sorption coefficients of organic pollutants from molecular structures: application of molecular connectivity model, *Environ. Sci. Technol.*, *21*, 358–366, 1989a.

Sabljić, A., Quantitative modeling of soil sorption for xenobiotic chemicals, *Environ. Health Perspect.*, *83*, 179–190, 1989b.

Sabljić, A., Qsar models for estimating properties of persistent organic pollutants required in evaluation of their environmental fate and risk, *Chemosphere*, *43*, 363–375, 2001.

Sabljić, A., H. Güsten, H. Verhaar, and J. Hermens, QSAR modelling of soil sorption. Improvements and systematics of log k_{oc} vs log k_{ow} correlations, *Chemosphere*, *31*, 4489–4514, 1995.

Schulthess, C. P., and D. K. Dey, Estimation of Langmuir constants using linear and nonlinear least squares regression analyses, *Soil Sci. Soc. Am. J.*, *60*, 433–442, 1996.

Schwarzenbach, R. P., P. M. Gschwend, and D. M. Imboden, *Environmental Organic Chemistry*, 2nd ed., John Wiley & Sons, New York, New York, 2003.

Sekusak, S., and A. Sabjlić, Soil sorption and chemical topology, *J. Math. Chem.*, *11*, 271–280, 1992.

Serne, R. J., J. M. Zachara, and D. S. Burke, *Chemical Information on Tank Supernatants, Cs Adsorption from Tank Liquids onto Hanford Sediments, and Field Observations of Cs Migration from Past Tank Leaks*, Pacific Northwest National Laboratory, PNNL-11495/UC-510, Richland, WA, 1998.

Shiau, B., D. A. Sabatini, and J. H. Harwell, Influence of Rhodamine WT properties on sorption and transport in subsurface media, *Ground Water*, *31*, 913–920, 1993.

Sieger, P., M. Wiebcke, J. Felsche, and J. C. Buhl, Orientation disorder of the nitrite anion in the sodalite sodium aluminum silicate nitrate($Na_8[AlSiO_4]_6NO_2)_2$), *Acta Crystallogr., Sect. C: Cryst. Struct. Commun.*, *47*, 498–501, 1991.

Smart, P. L., and I. M. S. Laidlaw, An evaluation of some fluorescent dyes for water tracing, *Water Resour. Res.*, *13*, 15–33, 1977.

Smettem, K. R. J., and S. T. Trudgill, An evaluation of some fluorescent and non-fluorescent dyes in the identification of water transmission routes in soils, *J. Soil Sci.*, *34*, 45–56, 1983.

Steefel, C. I., S. Carroll, P. Zhao, and S. Roberts, Cesium migration in Hanford sediment: a multisite cation exchange model based on laboratory experiments, *J. Contam. Hydrol.*, *67*, 219–246, 2003.

Steenhuis, T. S., W. Staubitz, M. S. Andreini, J. Surface, T. L. Richard, R. Paulsen, N. B. Pickering, J. R. Hagerman, and L. D. Geohring, Preferential movement of pesticides and tracers in agricultural soils, *J. Irrig. Drain. Eng.*, *116*, 50–66, 1990.

Sutton, D. J., Z. J. Kabala, A. Francisco, and D. Vasudevan, Limitation and potential of commercially available Rhodamine WT as a groundwater tracer, *Water Resour. Res.*, *37*, 1641–1656, 2001.

Tao, S., and X. Lu, Estimation of organic carbon normalized sorption coefficient (k_{oc}) for soil by topological indices and polarity factors, *Chemosphere*, *39*, 2019–2034, 2000.

Trillat, M. A., Sur l'emploi des matières colorantes pour la recherche de l'origine des sources et des eaux d'infiltration, *C. R. Hebd. Seances Acad. Sci.*, *128*, 698–702, 1899.

Vanderborght, J., P. Gähwiller, H. Wydler, U. Schultze, and H. Flühler, Imaging fluorescent dye concentrations on soil surfaces: Uncertainty of concentration estimates, *Soil Sci. Soc. Am. J.*, *66*, 760–773, 2002.

Vasudevan, D., R. L. Fimmen, and A. B. Francisco, Tracer-grade Rhodamine WT: Structure of constituent isomers and their sorption behavior, *Environ. Sci. Technol.*, *35*, 4089–4096, 2001.

Viriot, M. L., and J. C. André, Fluorescent dyes: a search for new tracer for hydrology, *Analusis*, *17*, 97–111, 1989.

Woods, R.-M., and M. E. Gunter, Na- and Cs-exchange in a clinoptilolite-rich rock: Analysis of the outgoing cations in solution, *Am. Mineralogist*, *86*, 424–430, 2001.

Worrall, F., A molecular topology approach to predicting pesticide pollution of groundwater, *Environ. Sci. Technol.*, *35*, 2282–2287, 2001.

Wyckoff, R. W. G., *Crystall Structures: Miscellaneous inorganic compounds, silicates, and basic structural information*, vol. 4, 2nd ed., John Wiley and Sons, Inc, New York, 1968.

Zachara, J. M., S. C. Smith, C. Liu, J. P. McKinley, R. J. Serne, and P. L. Gassman, Sorption of Cs^+ to micaceous subsurface sediments from the Hanford Site, USA, *Geochim. Cosmochim. Acta*, *66*, 193–211, 2002.

Zhao, H., Y. Deng, J. B. Harsh, M. Flury, and J. Boyle, Alteration of kaolinite to cancrinite and sodalite by simulated Hanford Tank Wastes and its impact on cesium retention, *Clays Clay Miner.*, *52*, 1–13, 2004.

Zinn, B., L. C. Meigs, C. F. Harvey, R. Haggerty, W. J. Peplinski, and C. F. V. Schwerin, Experimental visualization of solute transport and mass transfer process in two-dimensional conductivity fields with connected regions of high conductivity, *Environ. Sci. Technol.*, *38*, 3916–3926, 2004.